# CHAPTER 5 WING DESIGN

Mohammad Sadraey

Daniel Webster College

# CHAPTER 5

# WING DESIGN

## 5.1. Introduction

In chapter 4, aircraft preliminary design – the second step in design process – was introduced. Three parameters were determined during preliminary design, namely: aircraft maximum takeoff weight ($W_{TO}$); engine power (P), or engine thrust (T); and wing reference area ($S_{ref}$). The third step in the design process is the detail design. During detail design, major aircraft component such as wing, fuselage, horizontal tail, vertical tail, propulsion system, landing gear and control surfaces are designed one-by-one. Each aircraft component is designed as an individual entity at this step, but in later design steps, they were integrated as one system – aircraft- and their interactions are considered.

This chapter focuses on the detail design of the wing. The wing may be considered as the most important component of an aircraft, since a fixed-wing aircraft is not able to fly without it. Since the wing geometry and its features are influencing all other aircraft components, we begin the detail design process by wing design. The primary function of the wing is to generate sufficient lift force or simply lift (L). However, the wing has two other productions, namely drag force or drag (D) and nose-down pitching moment (M). While a wing designer is looking to maximize the lift, the other two (drag and pitching moment) must be minimized. In fact, wing is assumed ad a lifting surface that lift is produced due to the pressure difference between lower and upper surfaces. Aerodynamics textbooks may be studied to refresh your memory about mathematical techniques to calculate the pressure distribution over the wing and how to determine the flow variables.

Basically, the principles and methodologies of "*systems engineering*" are followed in the wing design process. Limiting factors in the wing design approach, originate from design requirements such as performance requirements, stability and control requirements, producibility requirements, operational requirements, cost, and flight safety. Major performance requirements include stall speed, maximum speed, takeoff run, range and endurance. Primary stability and control requirements include lateral-directional static stability, lateral-directional dynamic stability, and aircraft controllability during probable wing stall.

During the wing design process, eighteen parameters must be determined. They are as follows:

1. Wing reference (or planform) area ($S_W$ or $S_{ref}$ or S)
2. Number of the wings
3. Vertical position relative to the fuselage (high, mid, or low wing)
4. Horizontal position relative to the fuselage
5. Cross section (or airfoil)
6. Aspect ratio (AR)
7. Taper ratio ($\lambda$)
8. Tip chord ($C_t$)
9. Root chord ($C_r$)
10. Mean Aerodynamic Chord (MAC or C)
11. Span (b)
12. Twist angle (or washout)  ($\alpha_t$)
13. Sweep angle ($\Lambda$)
14. Dihedral angle ($\Gamma$)
15. Incidence ($i_w$) (or setting angle, $\alpha_{set}$)
16. High lifting devices such as flap
17. Aileron
18. Other wing accessories

Of the above long list, only the first one (i.e. planform area) has been calculated so far (during the preliminary design step). In this chapter, the approach to calculate or select other 17 wing parameters is examined. The aileron design (item 17) is a rich topic in wing design process and has a variety of design requirements, so it will not be discussed in this chapter. Chapter 12 is devoted to the control surfaces design and aileron design technique (as one control surface) will be presented in that chapter. Horizontal wing position relative to the fuselage will be discussed later in chapter 7, when the fuselage and tail have been designed.

Thus, the wing design begins with one known variable (S), and considering all design requirements, other fifteen wing parameters are obtained. The wing must produce sufficient lift while generate minimum drag, and minimum pitching moment. These design goals must be collectively satisfied throughout all flight operations and missions. There are other wing parameters that could be added to this list such as wing tip, winglet, engine installation, faring, vortex generator, and wing structural considerations. Such items will not be examined here in this chapter, but will be discussed in chapter 16 and 17.  Figure 5.1 illustrates the flowchart of wing design. It starts with the known variable (S) and ends with optimization. The details of design steps for each box will be explained later in this chapter.

Select number of wings

Select wing vertical location

Select/Design high lift device

Select/Determine sweep and dihedral angles ($\Lambda$, $\Gamma$)

Select or design wing airfoil section

Determine other wing parameters (AR, $\lambda$, $i_w$, $\alpha_t$)

Calculate Lift, Drag, and Pitching moment

Requirements Satisfied?

No

Yes

*Optimization*

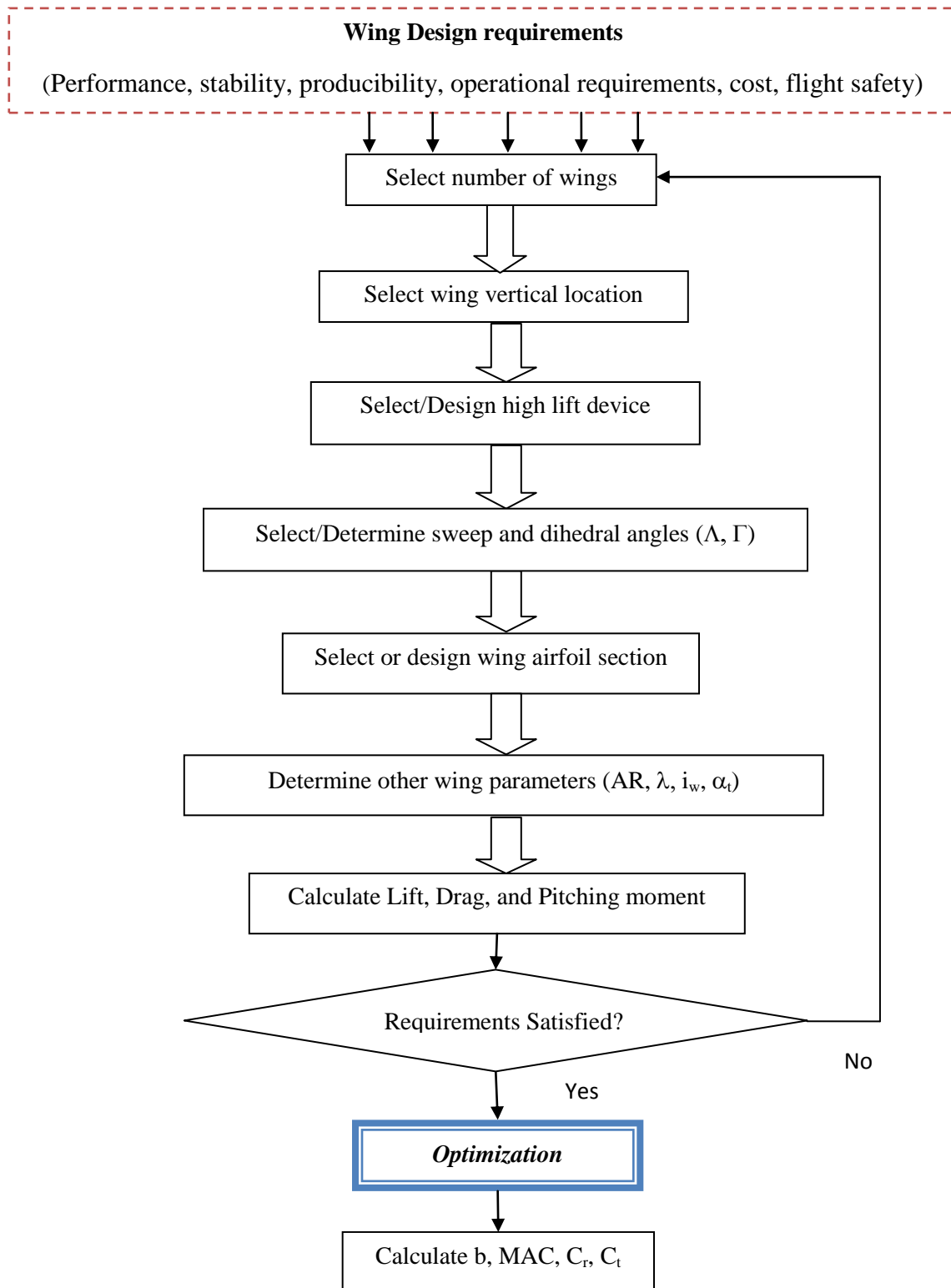Calculate b, MAC, $C_r$, $C_t$

*Figure 5. 1. Wing design procedure*

One of the necessary tools in the wing design process is an aerodynamic technique to calculate wing lift, wing drag, and wing pitching moment. With the progress of the science of aerodynamics, there are variety of techniques and tools to accomplish this time consuming job. Variety of tools and software based on aerodynamics and numerical methods have been developed in the past decades. The CFD[1] Software based on the solution of Navier-Stokes equations, vortex lattice method, thin airfoil theory, and circulation are available in the market. The application of such software –that are expensive and time-consuming – at this early stage of wing design seems un-necessary. Instead, a simple approach, namely Lifting Line Theory is introduced. Using this theory, one can determine those three wing productions (L, D, and M) with an acceptable accuracy.

At the end of this chapter, the practical steps of wing design are introduced. In the middle of the chapter, the practical steps of wing airfoil selection will also be presented. Two fully solved example problems; one about wing airfoil selection, and one in whole wing design are presented in this chapter. It should be emphasized again; as it is discussed in chapter 3; that it is essential to note that the wing design is a box in the iterative process of the aircraft design process. The procedure described in this chapter will be repeated several times until all other aircraft components are in an optimum point. Thus, wing parameters will vary several times until the combinations of all design requirements are met.

## 5.2. Number of Wings

One of the decisions a designer must make is to select the number of wings. The options are:

1. Monoplane (i.e. one wing)
2. Two wings (i.e. biplane)
3. Three wings

The number of wings higher than three is not practical. Figure 5.2 illustrates front view of three aircraft with various configurations.



1. Monoplane,                    2. Biplane,                    3. triwing
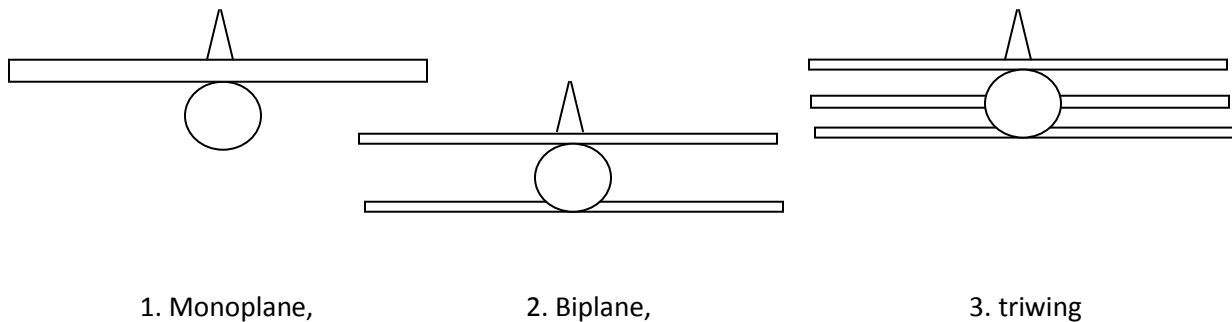
*Figure 5.2.  Three options in number of wings (front view)*

Nowadays, modern aircraft almost all have monoplane. Currently, there are a few aircraft that employ biplane, but no modern aircraft is found to have three wings. In the past, the major

[1] Computational Fluid Dynamics

reason to select more than one wing was the manufacturing technology limitations. A single wing usually has a longer wing span compared with two wings (with the same total area). Old manufacturing technology was not able to structurally support a long wing to stay level and rigid. With the advance in the manufacturing technology and also new aerospace strong materials; such as advanced light aluminum, and composite materials; this reason is not valid anymore. Another reason was the limitations on the aircraft wing span. Hence a way to reduce the wing span is to increase the number of wings.

Thus, a single wing (that includes both left and right sections) is almost the only practical option in conventional modern aircraft. However, a few other design considerations may still force the modern wing designer to lean toward more than one wing. The most significant one is the aircraft controllability requirements. An aircraft with a shorter wing span delivers higher roll control, since it has a smaller mass moment of inertia about x axis. Therefore if you are looking to roll faster; one option is to have more than one wing that leads to a shorter wing span. Several maneuverable aircraft in 1940s and 1950s had biplane and even three wings. On the other hand, the disadvantages of an option other than monoplane include higher weight, lower lift, and pilot visibility limits. The recommendation is to begin with a monoplane, and if the design requirements were not satisfied, resort to higher number of wings.

## 5.3. Wing Vertical Location

One of the wing parameters that could be determined at the early stages of wing design process is the wing vertical location relative to the fuselage centerline. This wing parameter will directly influence the design of other aircraft components including aircraft tail design, landing gear design, and center of gravity. In principle, there are four options for the vertical location of the wing. They are:

1. High wing
2. Mid wing
3. Low wing
4. Parasol wing



*a. High wing*                                   *b. Mid wing*

*c. Low wing*                                   *b. Parasol wing*
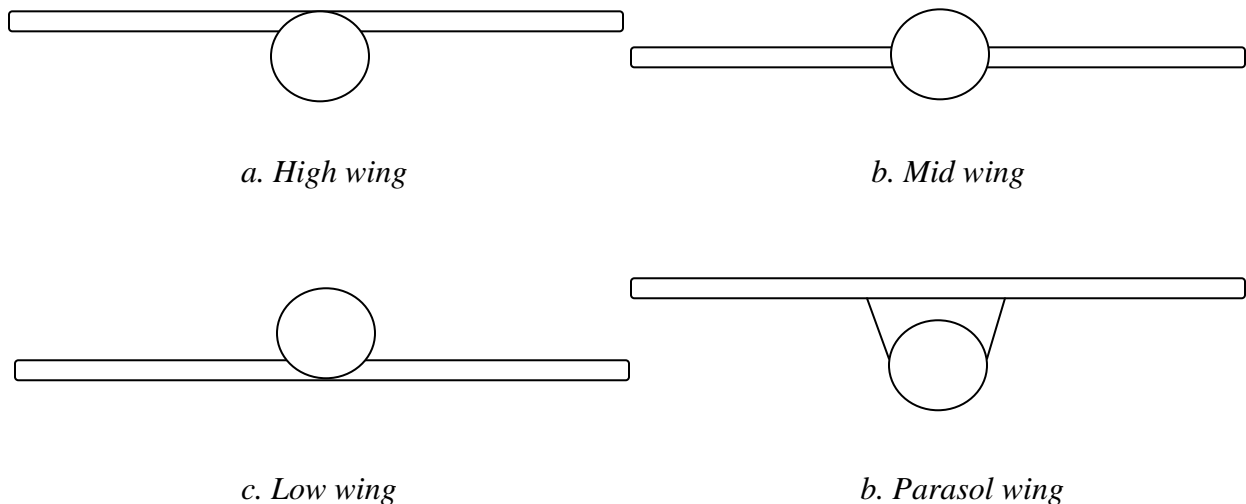
*Figure 5.3. Options in vertical wing positions*

*a. Cargo aircraft C-130 (high wing)*
(Photo courtesy of Tech. Sgt. Howard Blair, U.S. Air Force)



*b. Passenger aircraft Boeing 747 (low wing)*
(Photo courtesy of Philippe Noret – AirTeamimages)



*c. Military aircraft Scorpions (mid wing)*
(Photo courtesy of Photographer's Mate 3rd Class Joshua Karsten, U.S. Navy)



*d. Home-built Pietenpol Air Camper (parasol wing)*
(Photo courtesy of Adrian Pingstone)

*Figure 5.4. Four aircraft with different wing vertical positions*

Figure 5.3 shows the schematics of these four options. In this figure, only the front-views of the aircraft fuselage and wing are shown. In general, cargo aircraft and some GA aircraft have high wing; and most passenger aircraft have low wing. On the other hand, most fighter airplanes and some GA aircraft have mid wing; while hang gliders and most amphibian aircraft have parasol wing. The primary criterion to select the wing location originates from operational requirements, while other requirements such as stability and producibility requirements are the influencing factors in some design cases.

Figure 5.4 illustrates four aircraft in which various wing locations are shown. In this sections, the advantages and disadvantages of each option is examined. The final selection will be made based on the summations of all advantages and disadvantages when incorporated into design requirements. Since each option has a weight relative to the design requirements, the summation of all weights derives the final choice.

### 5.3.1. High Wing
The high wing configuration has several advantages and disadvantages that make it suitable for some flight operations, but unsuitable for other flight missions. In the following section, these advantages and disadvantages are presented.

**a. Advantages**
1. Eases and facilitates the loading and unloading of loads and cargo into and out of cargo aircraft. For instance, truck and other load lifter vehicles can easily move around aircraft and under the wing without anxiety of the hitting and breaking the wing.
2. Facilitates the installation of engine on the wing, since the engine (and propeller) clearance is higher (and safer), compared with low wing configuration.
3. Saves the wing from high temperature exit gasses in a VTOL[2] aircraft. The reason is that the hot gasses are bouncing back when they hit the ground, so they wash the wing afterward. Even with a high wing, this will severely reduce the lift of the wing structure. Thus, the higher the wing is the farther the wing from hot gasses.
4. Facilitates the installation of strut. This is based on the fact that a strut (rod or tube) can handle higher tensile stress compared with the compression stress. In a high wing, struts have to withstand tensile stress, while struts in a low wing must bear the compression stress. Figure 3.5d shows a parasol wing with strut.
5. Item 4 implies that the aircraft structure is heavier when struts are employed.
6. Facilitates the taking off and landing from sea. In a sea-based or an amphibian aircraft, during a take-off operation, water will splash around and will high the aircraft. An engine installed on a high wing will receive less water compared with a low wing. Thus, the possibility of engine shut-off is much less.
7. Facilitates the aircraft control for a hang glider pilot, since the aircraft center of gravity is lower than the wing.
8. High wing will increase the dihedral effect ($C_{l_\beta}$). It makes the aircraft laterally more stable. The reason lies in the higher contribution of the fuselage to the wing dihedral effect ($C_{l_{\beta_W}}$).

---

[2] Vertical Take Off and Landing

9. The wing will produce more lift compared with mid and low wing, since two parts of the wing are attached 9at least on the top part).
10. For the same reason as in item 8, the aircraft will have lower stall speed, since $C_{Lmax}$ will be higher.
11. The pilot has better view in lower-than-horizon. A fighter pilot has a full view under the aircraft.
12. For an engine that is installed under the wing, there is less possibility of sand and debris to enter engine and damage the blades and propellers.
13. There is a lower possibility of human accident to hit the propeller and be pulled to the engine inlet. In few rare accidents, several careless people has died (hit the rotating propeller or pulled into the jet engine inlet).
14. The aerodynamic shape of the fuselage lower section can be smoother.
15. There is more space inside fuselage for cargo, luggage or passenger.
16. The wing drag is producing a nose-down pitching moment, so it is longitudinally stabilizing. This is due to the higher location of wing drag line relative to the aircraft center of gravity ($M_{Dcg} < 0$).

**b. Disadvantages**
1. The aircraft frontal area is more (compared with mid wing). This will increase aircraft drag.
2. The ground effect is lower, compared with low wing. During takeoff and landing operations, the ground will influence the wing pressure distribution. The wing lift will be slightly lower than low wing configuration. This will increase the takeoff run slightly. Thus, high wing configuration is not a right option for STOL[3] aircraft.
3. Landing gear is longer if connected to the wing. This makes the landing gear heavier and requires more space inside the wing for retraction system. This will further make the wing structure heavier.
4. The pilot has less higher-than-horizon view. The wing above the pilot will obscure part of the sky for a fighter pilot.
5. If landing gear is connected to fuselage and there is not sufficient space for retraction system, an extra space must be provided to house landing gear after retraction. This will increase fuselage frontal area and thus will increase aircraft drag.
6. The wing is producing more induced drag (Di), due to higher lift coefficient.
7. The horizontal tail area of an aircraft with a high wing is about 20% larger than the horizontal tail area with a low wing. This is due to more downwash of a high wing on the tail.
8. A high wing is structurally about 20% heavier than low wing.
9. The retraction of the landing gear inside the wing is not usually an option, due to the required high length of landing gear.
10. The aircraft lateral control is weaker compared with mid wing and low wing, since the aircraft has more laterally dynamic stability.

Although, the high wing has more advantages than disadvantages, but all items do not have the same weighing factor. It depends on what design objective is more significant than

---

[3] Short Take Off and Landing

other objectives in the eyes of the customer. The systems engineering approach delivers an approach to determine the best option for a specific aircraft, using a comparison table.

**5.3.2. Low Wing**
In this section, advantages and disadvantages of a low wing configuration will be presented. Since the reasons for several items are similar with the reasons for a high wing configuration, the reasons are not repeated here. In majority of cases, the specifications of low wing are compared with a high wing configuration.

**a. Advantages**

1. The aircraft take off performance is better; compared with a high wing configuration; due to the ground effect.
2. The pilot has a better higher-than-horizon view, since he/she is above the wing.
3. The retraction system inside the wing is an option along with inside the fuselage.
4. Landing gear is shorter if connected to the wing. This makes the landing gear lighter and requires less space inside the wing for retraction system. This will further make the wing structure lighter.
5. In alight GA aircraft, the pilot can walk on the wing in order to get into the cockpit.
6. The aircraft is lighter compared with a low wing structure.
7. Aircraft frontal area is less.
8. The application of wing strut is usually no longer an option for the wing structure.
9. Item 8 implies that the aircraft structure is lighter since no strut is utilized.
10. Due to item 8, the aircraft drag is lower.
11. The wing has less induced drag.
12. It is more attractive to the eyes of a regular viewer.
13. The aircraft has higher lateral control compared with a high wing configuration, since the aircraft has less lateral dynamic stability, due to the fuselage contribution to the wing dihedral effect ($C_{l_{\beta_W}}$).
14. The wing has less downwash on the tail, so the tail is more effectiveness.
15. The tail is lighter; compared with a high wing configuration;.

**b. Disadvantages**
1. The wing generates less lift; compared with a high wing configuration; since the wing has two separate sections.
2. With the same token to item 1, the aircraft will have higher stall speed; compared with a high wing configuration; due to a lower $C_{Lmax}$.
3. Due to item 2, the take-off run is longer.
4. The aircraft has lower airworthiness due to a higher stall speed.
5. Due to item 1, wing is producing less induced drag.
6. The wing has less contribution to the aircraft dihedral effect, thus the aircraft is laterally dynamically less stable.
7. Due to item 4, the aircraft is laterally more controllable, and thus more maneuverable.
8. The aircraft has a lower landing performance, since it needs more landing run.

9.  The pilot has a lower lower-than-horizon view. The wing below the pilot will obscure part of the sky for a fighter pilot.
10. The wing drag is producing a nose-up pitching moment, so a low wing is longitudinally destabilizing. This is due to the lower position of the wing drag line relative to the aircraft center of gravity ($M_{Dcg} > 0$).

Although, the low wing has more advantages than disadvantages, but all items do not have the same weighing factors. It depends on what design objective is more significant than other objectives in the eyes of the customer. The systems engineering approach delivers an approach to determine the best option for a specific aircraft.

### 5.3.3. Mid Wing

In general, the features of a mid wing configuration stands somewhat between the high wing and the low wing configuration. The major difference lies in the necessity to cut the wing spar in two half in order to save the space inside the fuselage. Other than those features that can be easily derived from two previous sections, some new features of a mid wing configuration are as follows:

1.  The aircraft structure is heavier, due to the necessity of reinforcing wing root at the intersection with the fuselage.
2.  The mid wing is more expensive compared with high and low wing configurations.
3.  The mid wing is more attractive compared with two other configurations.
4.  The mid wing is aerodynamically streamliner compared with two other configurations.
5.  The strut is usually not used to reinforce the wing structure.
6.  The pilot can get into the cockpit using the wing as a step in the small GA aircraft.

### 5.3.4. Parasol Wing

This wing configuration is usually employed in hang gliders plus amphibian aircraft. In several areas, the features are similar to a high wing configuration. The reader is referred to above items for more details and the reader is expected to be able to derive conclusion by comparing various configurations. Since the wing is utilizing longer struts, it is heavier and has more drag, compared with a high wing configuration.

| Design objectives | Weight | High wing | Low wing | Mid wing | Parasol wing |
|---|---|---|---|---|---|
| Stability requirements | 20% | | | | |
| Control requirements | 15% | | | | |
| Cost | 10% | | | | |
| Producibility requirements | 10% | | | | |
| Operational requirements | 40% | | | | |
| Other requirements | 5% | | | | |
| Summation | 100% | 93 | 76 | 64 | 68 |

*Table 5.1. A sample table to compare the features of four wing vertical locations*

### 5.3.5. The Selection Process

The best approach to select the wing vertical location is to produce a table (such as table 5.1) consists of weight of each option for various design objectives. The weight of each design objective must be usually designated such that the summation adds up to 100%. A comparison between the summations of points among four options leads the designer to the best configuration. Table 5.1 illustrates a sample table to compare four wing configurations in the wing design process for a cargo aircraft. All elements of this table must be carefully filled with numbers. The last row is the summation of all numbers in each column. In the case of this table, the high wing has gained the highest point (93), so high wing seems to be the best candidate for the sample problem. As it is observed, even the high wing configuration does not fully satisfy all design requirements, but it is an optimum option among four available options. Reference 5 is a rich resource for the procedure of the selection technique.

## 5.4. Airfoil

This section is devoted to the process to determine airfoil section for a wing. It is appropriate to claim that the airfoil section is the second most important wing parameter; after wing planform area. The airfoil section is responsible for the generation of the optimum pressure distribution on the top and bottom surfaces of the wing such that the required lift is created with the lowest aerodynamic cost (i.e. drag and pitching moment). Although every aircraft designer has some basic knowledge of aerodynamics and the basics of airfoils; but to have a uniform starting point, the concept of airfoil and its governing equations will be reviewed. The section begins with a discussion on airfoil selection or airfoil design. Then basics of airfoil, airfoil parameters, and most important factor on airfoil section will be presented. A review of NACA[4] - the forerunner of NASA[5]- airfoils will be presented later, since the focus in this section is on the airfoil selection. The criteria for airfoil selection will be introduced and finally the procedure to select the best airfoil is introduced. The section will be ended with a fully solved example to select an airfoil for a candidate wing.

### 5.4.1. Airfoil Design or Airfoil Selection

The primary function of the wing is to generate lift force. This will be generated by a special wing cross section called airfoil. Wing is a three dimensional component, while the airfoil is two dimensional section. Because of the airfoil section, two other outputs of the airfoil, and consequently the wing, are drag and pitching moment. The wing may have a constant or a non-constant cross-section across the wing. This topic will be discussed in section 5.9.

There are two ways to determine the wing airfoil section:

1. Airfoil design
2. Airfoil selection

The design of the airfoil is a complex and time consuming process and needs expertise in fundamentals of aerodynamics at graduate level. Since the airfoil needs to be verified by testing it in a wind tunnel, it is expensive too. Large aircraft production companies such as Boeing and Airbus have sufficient human expert (aerodynamicists) and budget to design their own airfoil for every aircraft, but small aircraft companies, experimental aircraft producers and homebuilt

---

[4] National Advisory Committee for Aeronautics
[5] National Administration for Aeronautics and Astronautics

manufacturers do not afford to design their airfoils. Instead they select the best airfoils among the current available airfoils that are found in several books or websites.

With the advent of high speed and powerful computers, the design of airfoil is not as hard as thirty years ago. There is currently a couple of aerodynamic software packages (CFD) in the market that can be used to design airfoil for variety of needs. Not only aircraft designers need to design their airfoils, but there other many areas that airfoil needs to be design for their products. The list includes jet engine axial compressor blades, jet engine axial turbine blades, steam power plant axial turbine blades, wind turbine propellers, centrifugal and axial pump impeller blades, turboprop engine propellers, centrifugal and axial compressor impeller blades and large and small fans. The efficiencies of all of these industrial mechanical or aerospace devices rely heavily on the section of their blades; that is "*airfoil*".

If you have enough time, budget and manpower; and decide to design an airfoil for your aircraft, you are referred to the references that are listed at the end of the textbook. But remember the airfoil design is a design project for itself and needs to be integrated into the aircraft design process properly. But if you are a junior aircraft designer with limited resources, you are recommended to select the airfoil from the available airfoil database.

Any aerodynamics textbook introduces several theories to analyze flow around an airfoil. The application of potential-flow theory together with boundary-layer theory to airfoil design and analysis was accomplished many years ago. Since then, potential-flow and boundary layer theories have been steadily improved. With the advent of computers, these theories have been used increasingly to complement wind-tunnel tests. Today, computing costs are so low that a complete potential-flow and boundary-layer analysis of an airfoil costs considerably less than one percent of the equivalent wind-tunnel test. Accordingly, the tendency today is toward more and more commonly applicable computer codes. These codes reduce the amount of required wind-tunnel testing and allow airfoils to be tailored to each specific application.

One of the oldest and most reliable airfoil designers is Richard Eppler (Ref. 1) in Germany. Eppler has developed an airfoil design code that is based on conformal mapping. The Eppler code has been developed over the past 45 years. It combines a conformal-mapping method for the design of airfoils with prescribed velocity-distribution characteristics, a panel method for the analysis of the potential flow about given airfoils, and an integral boundary-layer method. The code contains an option that allows aircraft-oriented boundary-layer developments to be computed, where the Reynolds number and the Mach number vary with aircraft lift coefficient and the local wing chord. In addition, a local twist angle can be input. Aircraft drag polar that includes the induced drag and an aircraft parasite drag can also be computed.

The code will execute on almost any personal computer, workstation, or server, with run times varying accordingly. The most computationally intensive part of the code, the analysis method, takes only a few seconds to run on a PC. The code is written in standard FORTRAN 77 and, therefore, a FORTRAN compiler is required to translate the supplied source code into executable code. A sample input and output case is included. All the graphics routines are contained in a separate, plot-post-processing code that is also supplied. The post-processing code generates an output file that can be sent directly to a printer. The user can adapt the post-processing code to other plotting devices, including the screen.

It is very efficient and has been successfully applied at Reynolds numbers from $3\times10^4$ to $5\times10^7$. A compressibility correction to the velocity distributions, which is valid as long as the local flow is not supersonic, has been incorporated into the code. The code is available, for a fee, in North America exclusively from Mark D. Maughmer[6].

If you are not ready to design your own airfoil, you are recommended to select a proper airfoil from the previously designed and published airfoil sections. Two reliable airfoil resources are NACA and Eppler. The details of Eppler airfoils have been published in Reference 1. NACA airfoils have been published in a book published by Abbott and Von Donehoff (Ref. 2). The book has been published in 1950s, but still reprinted and available in almost every aerospace related library. Both references present the airfoil coordinates plus pressure distribution and a few other graphs such as $C_l$, $C_d$, and $C_m$ for a range angle of attacks. Eppler airfoil names begin with the letter "E" followed by three numbers. More details on NACA airfoils will be presented in Section 5.3.4.

A regular flight operation consists of take off, climb, cruise, turn, maneuver, descent, approach and landing. Basically, the airfoil's optimum function is in cruise, that an aircraft spend much of its flight time in this flight phase. At a cruising flight, lift (L) is equal to aircraft weight (W), and drag (D) is equal to engine thrust (T). Thus the wing must produce sufficient lift coefficient, while drag coefficient must be minimum. Both of these coefficients are mainly coming from airfoil section. Thus two governing equations for a cruising flight are:

$$L = W \Rightarrow \frac{1}{2}\rho V^2 S C_L = mg \tag{5.1}$$

$$D = T \Rightarrow \frac{1}{2}\rho V^2 S C_D = nT_{max} \qquad \text{(jet engine)} \tag{5.2}$$

$$D = T \Rightarrow \frac{1}{2}\rho V^2 S C_D = \frac{n\eta_P P_{max}}{V_C} \qquad \text{(prop-driven engine)} \tag{5.3}$$

The equation 5.2 is for an aircraft with jet engine, but equation 5.3 is for an aircraft with prop-driven engine. The variable "n" ranges between 0.6 to 0.9. It means that only a partial engine throttle is used in a cruising flight and maximum engine power or engine thrust is not employed. The exact value for n will be determined in later design steps. For the airfoil initial design, it is suggested to use 0.75. The maximum engine power or engine thrust is only used during take-off or when cruising with maximum speed. Since a major criterion for airfoil design is to satisfy cruising flight requirements, equations 1 through 3 are used in airfoil design as explained later in this section. In the following section, the wing airfoil selection procedure is described.

---

[6] RR 1, Box 965 Petersburg, PA 16669 USA

### 5.4.2. General Features of an Airfoil

Any section of the wing cut by a plane parallel to the aircraft xz plane is called an airfoil. It is usually looks like a positive cambered section that the thicker part is in front of the airfoil. An airfoil-shaped body moved through the air will vary the static pressure on the top surface and on the bottom surface of the airfoil. A typical airfoil section is shown in figure 5.5, where several geometric parameters are illustrated. If the mean camber line in a straight line, the airfoil is referred to as symmetric airfoil, otherwise it is called cambered airfoil. The camber of airfoil is usually positive. In a positive cambered airfoil, the upper surface static pressure in less than ambient pressure, while the lower surface static pressure is higher than ambient pressure. This is due higher airspeed at upper surface and lower speed at lower surface of the airfoil (see figure 5.6 and 5.7). As the airfoil angle of attack increases, the pressure difference between upper and lower surfaces will be higher (see Ref. 3).
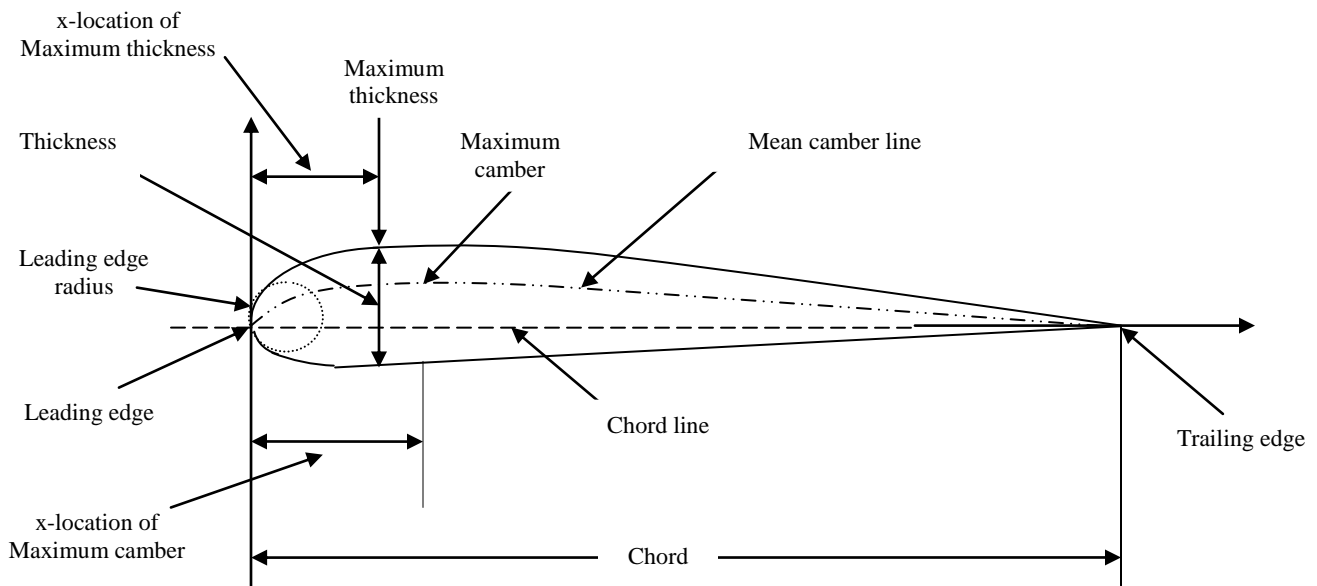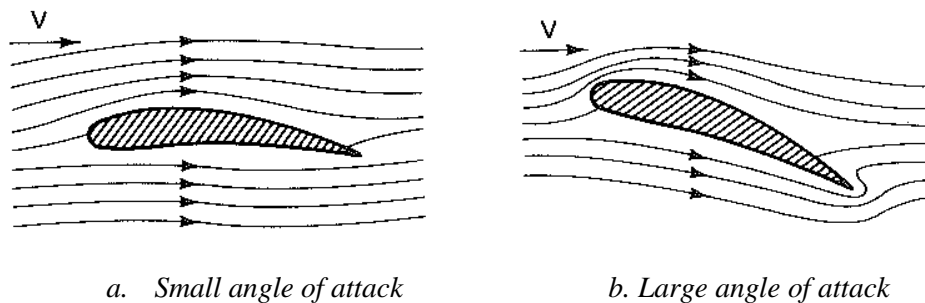
*Figure 5.5. Airfoil geometric parameters*

a.   *Small angle of attack*          b. *Large angle of attack*

*Figure 5.6. Flow around an airfoil*

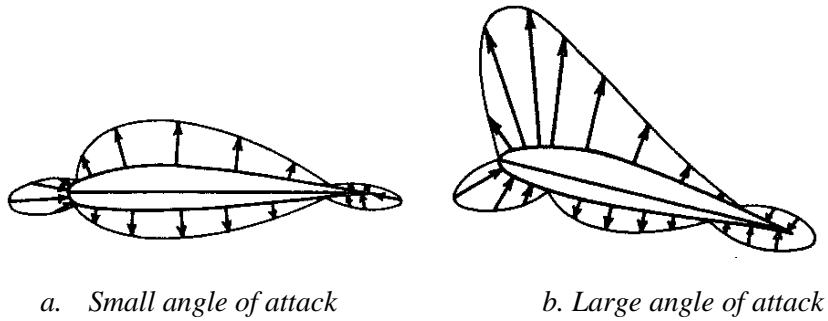a.  *Small angle of attack*                    b. *Large angle of attack*

*Figure 5.7. Pressure distribution around an airfoil*

The force divided by the area is called pressure, so the aerodynamic force generated by an airfoil in a flow field may be calculated by multiplication of total pressure by area. The total pressure is simply determined by integration of pressure over the entire surface. The magnitude, location, and direction of this aerodynamic force are functions of airfoil geometry, angle of attack, flow property, and airspeed relative to the airfoil.
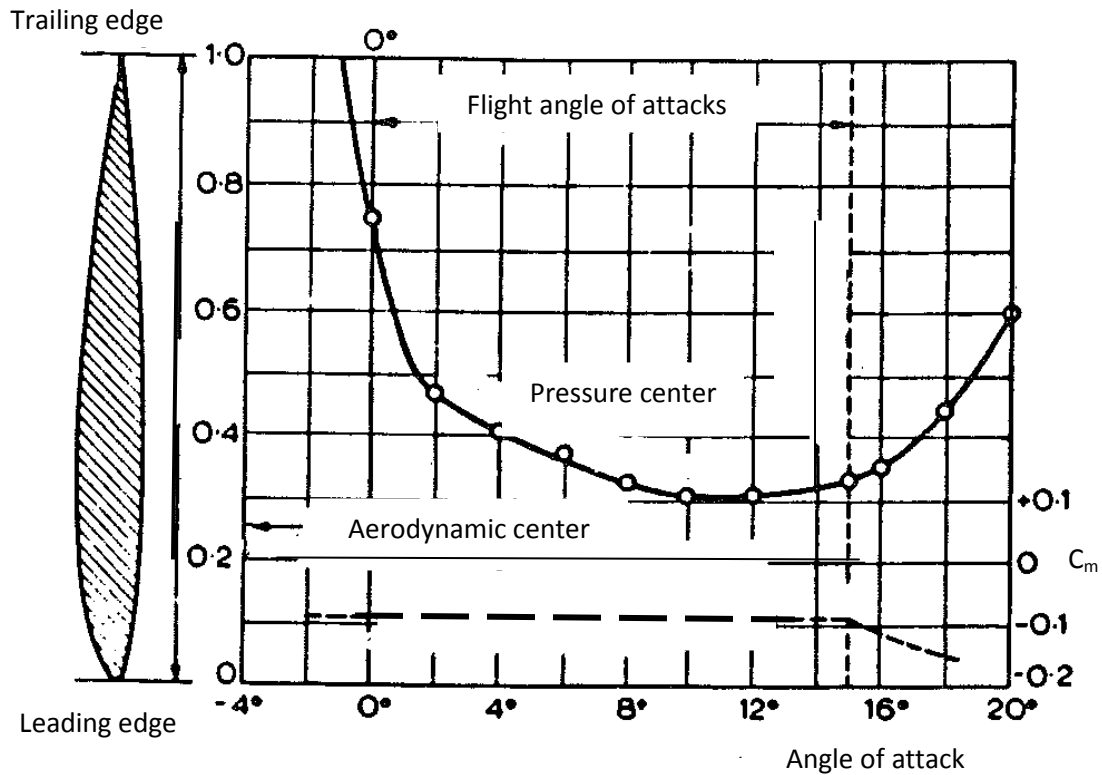


*Figure 5.8. The pressure center movement as a function of angle of attack*

The location of this resultant force out of the integration is called center of pressure (cp). The location of this center depends on aircraft speed plus the airfoil's angle of attack. As the aircraft speed increases, the center of pressure moves aftward (see figure 5.8). At lower speeds, cp location is close to the leading edge and at higher speeds, it moves toward trailing edge. There is a location on the airfoil that has significant features in aircraft stability and control. The aerodynamic center is a useful concept for the study of stability and control. In fact, the force and

moment system on a wing can be completely specified by the lift and drag acting through the aerodynamic center, plus the moment about the aerodynamic center, as sketched in Figure 5.9.

It is convenient to move the location of the resultant force – that is moving along - to the new location; aerodynamic center; that is almost stable. By operation of adding two equal forces – one at the center of pressure, and another one at the aerodynamic center- we can move the location of the resultant force. By doing so, we have to account for that, by introducing an aerodynamic pitching moment (see fig 5.10). This will add a moment to our aerodynamic force. Therefore we can conclude that the pressure and shear stress distributions over a wing produce a pitching moment. This moment can be taken about any arbitrary point (the leading edge, the trailing edge, the quarter chord, etc.). The moment can be visualized as being produced by the resultant lift acting at a particular distance back from the leading edge. As a fraction of the chord, the distance to this point, is known as the center of pressure. However, there exists a particular point about which the moments are independent of angle of attack. This point is defined as the **aerodynamic center** for the wing.
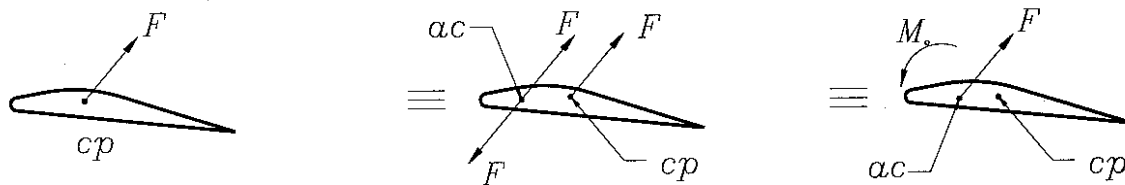


| a. | The force on pressure center | b. Addition of two equal forces | c. Force on aerodynamic center |

*Figure 5.9. The movement of resultant force to aerodynamic center*

The subsonic airfoil theory shows that lift due to angle of attack acts at a point on the airfoil 25% of the chord aft of the leading edge. This location is called the quarter-chord point. The point through which this lift acts is the aerodynamic center (ac). In wind tunnel tests, the ac is usually within 1% or 2% chord of the quarter-chord point until the Mach number increases to within a few percent of the drag divergence Mach number. The aerodynamic center then slowly moves aft as the Mach number is increased further.
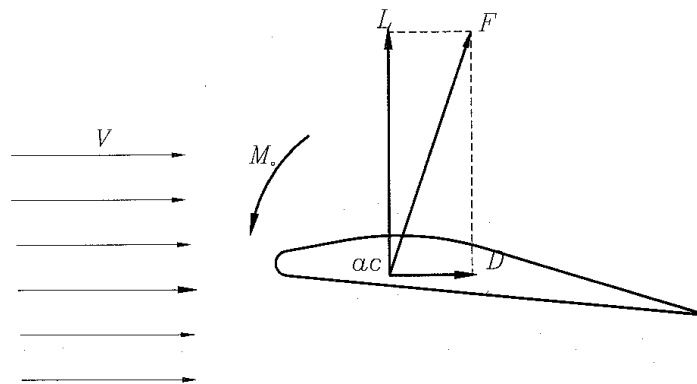


*Figure 5.10. The aerodynamic lift, drag, pitching moment*

Thus, the pressure and shear stress distributions over the airfoil generate an aerodynamic force. However, this resultant force is replaced with two aerodynamic forces and one aerodynamic moment as shown by the vector in Figure 5.10. On the other word, the aerodynamic force can be resolved into two forces, perpendicular (lift) and parallel (drag) to the relative wind. The lift is always defined as the component of the aerodynamic force perpendicular to the relative wind. The drag is always defined as the component of the aerodynamic force parallel to the relative wind.

### 5.4.3. Characteristic Graphs of an Airfoil

In the process of wing airfoil selection, we do not look at airfoil geometry only, or its pressure distribution. Instead, we examine the airfoil operational outputs that are more informative to satisfy design requirements. There are several graphs that illustrate the characteristics of each airfoil when compared to other airfoils in the wing airfoil selection process. These are mainly the variations of non-dimensionalized lift, drag, and pitching moment relative with angle of attack. Two aerodynamic forces and one aerodynamic pitching moment are usually non-dimensionalized[7] by dividing them to appropriate parameters as follows.

$$C_l = \frac{l}{\frac{1}{2}\rho V^2 (C \times 1)} \tag{5.4}$$

$$C_d = \frac{d}{\frac{1}{2}\rho V^2 (C \times 1)} \tag{5.5}$$

$$C_m = \frac{m}{\frac{1}{2}\rho V^2 (C \times 1) \times C} \tag{5.6}$$

where *l*, d, and m are lift, drag, and pitching moment of a two-dimensional airfoil. The area (C x 1) is assumed to be the airfoil chord times the unit span (b = 1).

Thus, we evaluate the performance and characteristics of an airfoil by looking at the following graphs.

1. The variations lift coefficient versus angle of attack
2. The variations pitching moment coefficient versus angle of attack
3. The variations of pitching moment coefficient versus lift coefficient
4. The variations of drag coefficient versus lift coefficient
5. The variations of lift-to-drag ratio versus angle of attack

These graphs have several critical features that are essential to the airfoil selection process. Let's first have a review on these graphs.

---

[7] The technique was first introduced by Edger Buckingham (1867-1940) as Buckingham Π Theorem. The details may be found in most Fluid Mechanics textbook.

1. **The graph of lift coefficient (C$_l$) versus angle of attack ($\alpha$)**

Figure 5.11 shows the typical variations of lift coefficient versus angle of attack for a positive cambered airfoil. Seven significant features of this graph are: stall angle ($\alpha_s$), maximum lift coefficient (C$_{l\max}$), zero lift angle of attack ($\alpha_o$), ideal lift coefficient (C$_{li}$) and angle of attack corresponding to ideal lift coefficient ($\alpha_{Cli}$), lift coefficient at zero angle of attack (C$_{lo}$), and lift curve slope ($C_{l_\alpha}$). These are critical to identify the performance of an airfoil.

   **a.** The stall angle ($\alpha_s$) is the angle of attack at which the airfoil stalls; i.e. the lift coefficient will no longer increase with increasing angle of attack. The maximum lift coefficient that corresponds to stall angle is the maximum angle of attack. The stall angle is directly related to the flight safety, since the aircraft will lose the balance of forces in a cruising flight. It the stall is not controlled properly; the aircraft may enter a spin and eventually crash. In general, the higher the stall angle, the safer is the aircraft, thus a high stall angle is sought in airfoil selection. The typical stall angles for majority of airfoils are between 12 to 16 degrees. This means that the pilot is not allowed to increase the angle of attack more than about 16 degrees. Therefore the airfoil which has the higher stall angle is more desirable.

   **b.** The maximum lift coefficient (C$_{l\max}$) is the maximum capacity of an airfoil to produce non-dimensional lift; i.e. the capacity of an aircraft to lift a load (i.e. aircraft weight). The maximum lift coefficient is usually occurs at the stall angle. The stall speed (V$_s$) is inversely a function of maximum lift coefficient, thus the higher C$_{l\max}$ leads in the lower V$_s$. Thus the higher C$_{l\max}$ results in a safer flight. Therefore, the higher maximum lift coefficient is desired in an airfoil selection process.
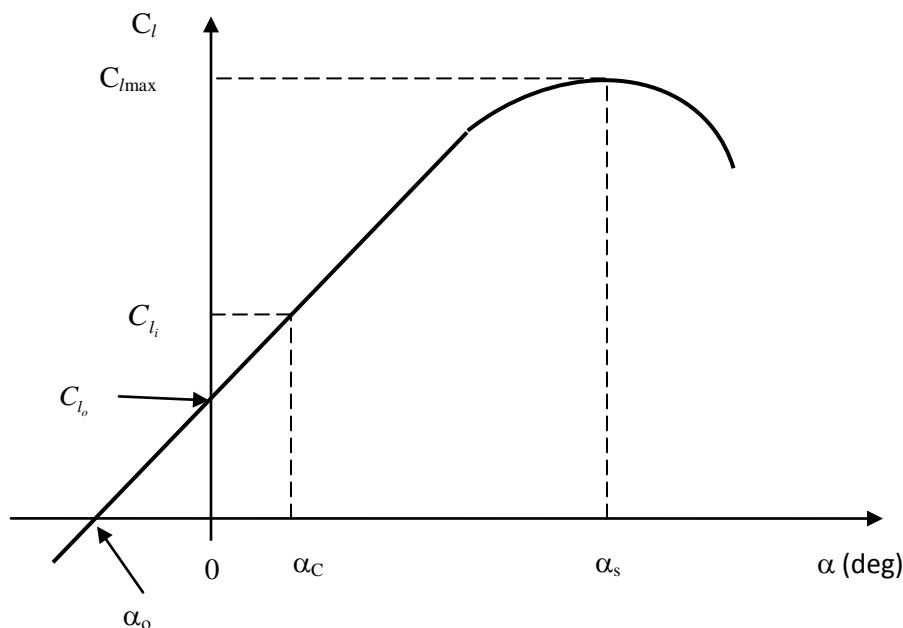


*Figure 5.11. The variations of lift coefficient versus angle of attack*

   **c.** The zero lift angle of attack ($\alpha_o$) is the airfoil angle of attack at which the lift coefficient is zero. A typical number for $\alpha_o$ is around -2 degrees when no high lift

device is employed. However, when a high lift device is employed; such as -40 degrees of flap down; the $\alpha_o$ increases to about -12 degrees. The design objective is to have a higher $\alpha_o$ (more negative), since it leaves the capacity to have more lift at zero angle of attack. This is essential for a cruising flight, since the fuselage center line is aimed to be level (i.e. zero fuselage angle of attack) for variety of flight reasons such as comfort of passengers.

**d.** The ideal lift coefficient ($C_{l_i}$) is the lift coefficient at which the drag coefficient does not vary significantly with the slight variations of angle of attack. The ideal lift coefficient is usually corresponding to the minimum drag coefficient. This is very critical in airfoil selection, since the lower drag coefficient means the lower flight cost. Thus, the design objective is to cruise at flight situation such that the cruise lift coefficient is as close as possible to the ideal lift coefficient. The value of this $C_{l_i}$ will be clear when the graph of variation of drag coefficient versus lift coefficient is discussed. The typical value of ideal lift coefficient for GA aircraft is about 0.1 to 0.4, and for a supersonic aircraft is about 0.01 to 0.05.

**e.** The angle of attack corresponding to ideal lift coefficient ($\alpha_{Cli}$) is self explanatory. The wing setting angle is often selected to be the same as this angle, since it will result in a minimum drag. On the other hand, the minimum drag is corresponding to the minimum engine thrust, which means the minimum flight cost. This will be discussed in more details, when wing setting angle is discussed. The typical value of $\alpha_{Cli}$ is around 2 to 5 degrees. Thus, such an angle will be a optimum candidate for the cruising angle of attack.

**f.** The lift coefficient at zero angle of attack ($C_{l_o}$) is the lift coefficient when angle of attack is zero. From design point of view, the more $C_{l_o}$ is the better, since it implies we can produce a positive lift even at zero angle of attack. Thus, the more $C_{l_o}$ is the better.

**g.** The lift curve slope ($C_{l_\alpha}$) is another important performance feature of an airfoil. The lift curve slope is the slope of variation of lift coefficient with respect to the change in the angle of attack, and its unit is 1/deg or 1/rad. Since the main function of an airfoil is to produce lift, the higher the slope, the better the airfoil. The typical value of lift curve slope of a 2d airfoil is around $2\pi$ (or 6.28) per radian (about 0.1 per degrees). It implies that for each 1 degree of change in the airfoil angle of attack, the lift coefficient will be increased by 0.1. The lift curve slope (1/rad) may be found by the following empirical equation:
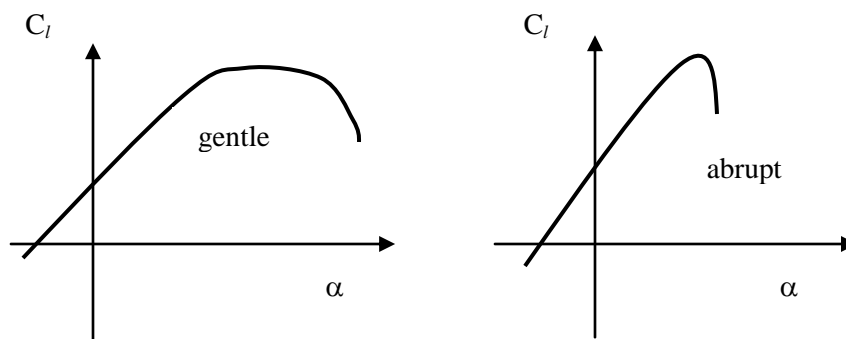
*Figure 5.12. Stall characteristics*

$$C_{l_\alpha} = \frac{dC_l}{d\alpha} = 1.8\pi(1+0.8\frac{t_{max}}{c}) \qquad (5.7)$$

where $t_{max}/c$ is the maximum thickness to chord ratio of the airfoil.

**h.** Another airfoil characteristic is the shape of the lift curve at and beyond the stall angle of attack (stall behavior). An airfoil with a gentle drop in lift after the stall, rather than an abrupt or sharp rapid lift loss, leads to a safer stall from which the pilot can more easily recover (see figure 5.12). Although the sudden airfoil stall behavior does not necessarily imply sudden wing stall behavior, a careful wing design can significantly modify the airfoil tendency to rapid stall. In general, airfoils with thickness or camber, in which the separation is associated with the adverse gradient on the aft portion rather than the nose pressure peak, have a more gradual loss of lift. Unfortunately, the best airfoils in this regard tend to have lower maximum lift coefficient.

As it is observed, there are several parameters to judge about the acceptability of an airfoil. In the next section, the technique to select the best airfoil based on these performance characteristics will be introduced.



*Figure 5.13. The variations of pitching moment coefficient versus angle of attack*
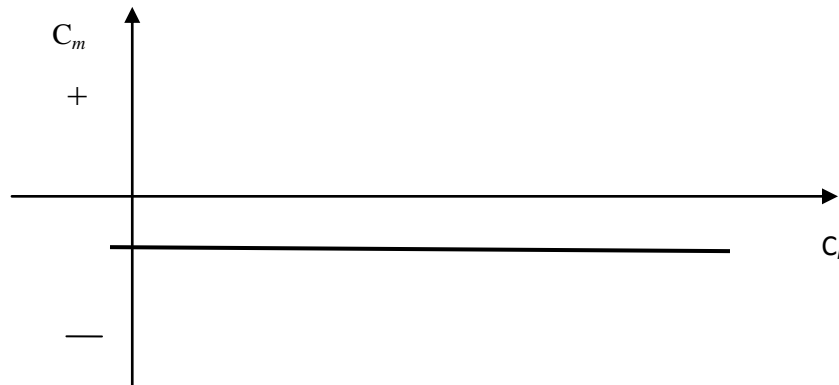


*Figure 5.14. The variations of pitching moment coefficient versus lift coefficient*

## 2. The variations of pitching moment coefficient versus angle of attack

Figure 5.13 shows the typical variations of pitching moment coefficient versus angle of attack for a positive cambered airfoil. The slope of this graph is usually negative and it is in the region of negative $C_m$ for typical range angle of attacks. The negative slope is desirable, since it stabilizes the flight, if the angle of attack is disturbed by a gust. The negative $C_m$ is sometimes referred to as nose-down pitching moment. This is due to its negative direction about y-axis which means the aircraft nose will be pitched down by such moment.

Figure 5.14 also illustrates the typical variations of pitching moment coefficient versus lift coefficient for a positive cambered airfoil. The magnitude of $C_m$ is almost constant for the typical ranges of lift coefficient. The typical magnitude is usually about -0.02 to -0.05. The design objective is to have the $C_m$ close to zero as much as possible. The reason is that the aircraft must be in equilibrium in cruising flight. This pitching moment must be nullified by another component of the aircraft, such as tail. Thus, the higher $C_m$ (more negative) results in a larger tail, which means the heavier aircraft. Therefore the airfoil which has the lower $C_m$ is more desirable. It is interesting to note that the pitching moment coefficient for a symmetrical airfoil section is zero.
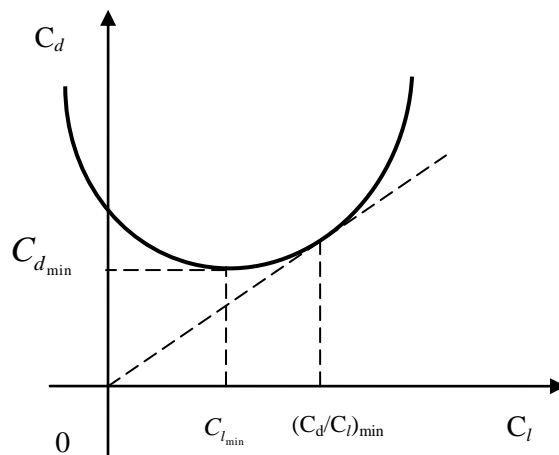


*Figure 5.15. The typical variations of drag coefficient versus lift coefficient*

## 3. The variations of drag coefficient as a function of lift coefficient

Figure 5.15 shows the typical variations of drag coefficient as a function of lift coefficient for a positive cambered airfoil. The lowest point of this graph is called minimum drag coefficient ( $C_{d_{min}}$ ). The corresponding lift coefficient to the minimum drag coefficient is called $C_{l_{min}}$. As the drag is directly related to the cost of flight, the $C_{d_{min}}$ is of great importance in airfoil design or airfoil selection. A typical value for $C_{d_{min}}$ is about 0.003 to 0.006. Therefore the airfoil which has the lower $C_{d_{min}}$ is more desirable.

A line drawn through the origin and tangent to the graph locates a point that denotes to the minimum slope. This point is also of great importance, since it indicates the flight situation that maximum $C_l$-to-$C_d$ ratio is generated, since $(C_d/C_l)_{min} = (C_l/C_d)_{max}$. This is an important output of an airfoil, and it is referred to as the maximum lift-to-drag ratio. In addition of requirement of lowest $C_{d_{min}}$, the highest $(C_l/C_d)_{max}$ is also desired. These two objectives may not happen at the same time in one airfoil, but based on aircraft mission and weight of each design requirement, one of them gets more attention.

The variation of drag coefficient as a function of lift coefficient (figure 5.15) may be mathematically modeled by the following second order equation:

$$C_d = C_{d_{min}} + K\left(C_l - C_{l_{min}}\right)^2 \tag{5.8}$$

where K is called section drag factor. The parameter K can be determined by selecting a point on the graph ($C_{l_1}$ and $C_{d_1}$) and plugging in the equation 5.8.
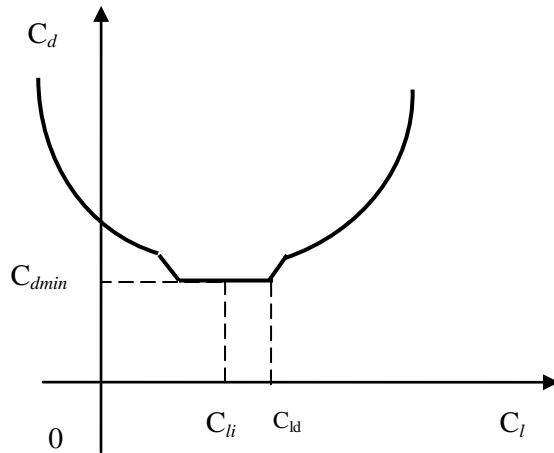


*Figure 5.16. The variations of $C_l$ versus $C_d$ for a laminar airfoil*

Figure 5.16 shows the typical variations of drag coefficient as a function of lift coefficient for a laminar airfoil; such as in 6-series NACA airfoils. This graph has a unique feature which is the bucket, due to the bucket shape of the lower portion of the graph. The unique aspect of the bucket is that the $C_{dmin}$ will not vary for a limited range of $C_l$. this is very significant, since it implies that the pilot can stay at the lowest drag point while changing the angle of attack. This situation matches with the cruising flight, since the aircraft weight is reduces as the fuel is burned. Hence, the pilot can bring aircraft nose down (decrease the angle of attack) with being worried about an increase in the aircraft drag. Therefore it is possible to keep the engine throttle low during cruising flight.

The middle point of the bucket is called ideal lift coefficient ($C_{l_i}$), while the highest $C_l$ in the bucket region is referred to as design lift coefficient ($C_{l_d}$). These two points are among the list of significant criteria to select/design an airfoil. Remember that the design lift coefficient occurs at the point whose $C_d/C_l$ is minimum or $C_l/C_d$ is maximum. For some flight operations

(such as cruising flight), flying at the point where lift coefficient is equivalent with $C_{l_i}$ is the goal, while for some other flight operations (such as loiter), the objective is to fly at the point where lift coefficient is equivalent with $C_{l_d}$. This airfoil lift coefficient is a function of aircraft cruise lift coefficient ($C_{Li}$) as will be discussed later in this chapter.

### 4. The variations of lift-to-drag ratio ($C_l/C_d$) as a function of angle of attack

The last interesting graph that is utilized in the process of airfoil selection is the variations of lift-to-drag ratio ($C_l/C_d$) as a function of angle of attack. Figure 5.17 illustrates the typical variations of lift-to-drag ratio versus angle of attack. As it is noted, this graph has one maximum point where the value of the lift-to-drag ratio is the highest at this point. The angle of attack corresponding to this point is an optimum candidate for a loitering flight ($\alpha_l$).

The application of these four graphs and twelve parameters in the airfoil selection process will be introduced in the later sections.
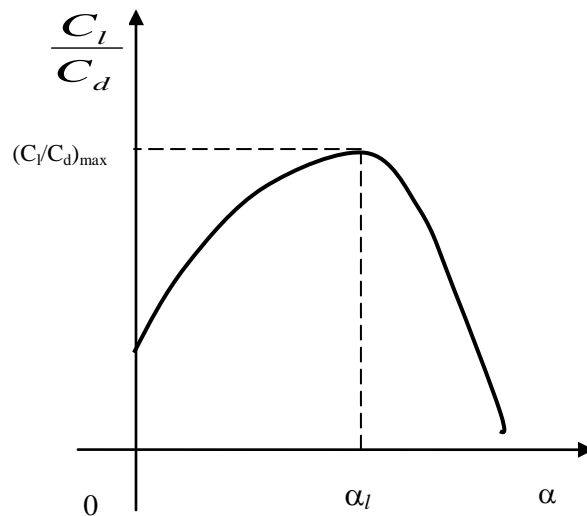


*Figure 5.17. The typical variations of lift-to-drag ratio versus angle of attack*

### 5.4.4. Airfoil Selection Criteria
Selecting an airfoil is a part of the overall wing design. Selection of an airfoil for a wing begins with the clear statement of the flight requirements. For instance, a subsonic flight design requirements are very much different from a supersonic flight design objectives. On the other hand, flight in the transonic region requires a special airfoil that meets mach divergence requirements. The designer must also consider other requirements such as airworthiness, structural, manufacturability, and cost requirements. In general, the following are the criteria to select an airfoil for a wing with a collection of design requirements:

1. The airfoil with the highest maximum lift coefficient ($C_{l_{max}}$).

---

2. The airfoil with the proper ideal or design lift coefficient ($C_{l_d}$ or $C_{l_i}$).
3. The airfoil with the lowest minimum drag coefficient ($C_{d_{min}}$).
4. The airfoil with the highest lift-to-drag ratio (($C_l/C_d)_{max}$).
5. The airfoil with the highest lift curve slope ($C_{l_{\alpha_{max}}}$).
6. The airfoil with the lowest pitching moment coefficient ($C_m$).
7. The proper stall quality in the stall region (the variation must be gentile, not sharp).
8. The airfoil must be structurally reinforceable. The airfoil should not that much thin that spars cannot be placed inside.
9. The airfoil must be such that the cross section is manufacturable.
10. The cost requirements must be considered.
11. Other design requirements must be considered. For instance, if the fuel tank has been designated to be places inside the wing inboard section, the airfoil must allow the sufficient space for this purpose.
12. If more than one airfoil is considered for a wing, the integration of two airfoils in one wing must be observed. This item will be discussed in more details in section 5.8.

Usually, there is no unique airfoil that that has the optimum values for all above-mentioned requirements. For example, you may find an airfoil that has the highest $C_{l_{max}}$, but not the highest

$$\left( \frac{C_l}{C_d} \right)_{max}$$

. In such cases, there must be compromise through a weighting process, since not all design requirements have the same importance. The weighting process will be discussed later in this chapter.

As a guidance, the typical values for the airfoil maximum thickness-to-chord ratio of majority of aircraft are about 6% to 18%.

1- For a low speed aircraft with a high lift requirement (such as cargo aircraft), the typical wing $(t/c)_{max}$ is about 15% - 18%.
2- For a high speed aircraft with a low lift requirement (such as high subsonic passenger aircraft), the typical wing $(t/c)_{max}$ is about 9% - 12%.
3- For the supersonic aircraft, the typical wing $(t/c)_{max}$ is about 6% - 9%.

The details of airfoil selection procedure will be presented in section 5.3.7. Figure 5.17 illustrates a few sample airfoils.

### 5.4.5. NACA Airfoils
The main focus of this section is how to select a wing airfoil from the available list of NACA airfoils, so this section is dedicated to the introduction of NACA airfoils. One of the most reliable resources and widely used data base is the airfoils that have been developed by NACA (predecessor of NASA) in 1930s and 1940s. Three following groups of NACA airfoils are more interesting:
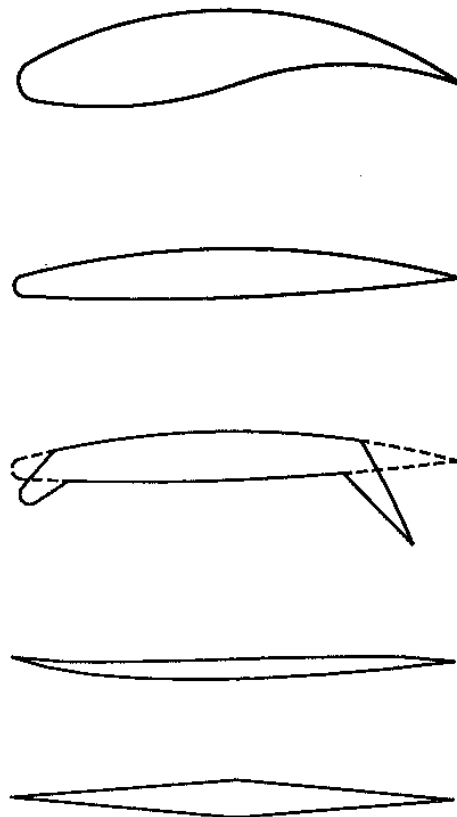
- *Four-digit NACA airfoils*
- *Five-digit NACA airfoils*

- *6-series NACA airfoils*

As the names imply, four digit airfoils are named by four digits (such as 2415), five digit airfoils are named by five digits (such as 23018), but 6-series airfoils names begin by number 6 (in fact, the have 5 main digits). Figure 5.18 illustrates a four-digit, a five-digit and a 6-series airfoils.

### a. Four-digit NACA airfoils

The four-digit NACA airfoil sections are the oldest and simplest NACA airfoils to generate. The camber of a four-digit airfoil has made up of two parabolas. One parabola generates the camber geometry from the leading edge to the maximum camber, and another parabola produces the camber shape from the maximum camber to the trailing edge. In a Four-digit NACA airfoil, the first digit indicates the maximum camber in percent chord. The second digit indicates the position of maximum camber in tenths of chord length. The last two digits represent the maximum thickness-to-chord ratio. A zero in the first digit means that this airfoil is a symmetrical airfoil section. For example, the NACA **1408** airfoil section (see figure 5.19a) has a 8 percent $(t/c)_{max}$ (the last two digits), its maximum camber is 10 percent, and its maximum camber is located at 40 percent of the chord length. Although these airfoils are easy to produce, but they generate high drag compared with new airfoils.



*Figure 5.18. Five sample airfoils*
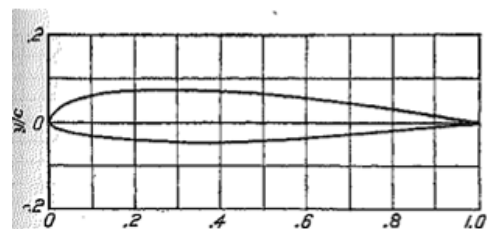
## b. Five-digit NACA airfoils

The camber of a five-digit airfoil section has made up of one parabola and one straight line. The parabola generates the camber geometry from the leading edge to the maximum camber, and then a straight line connects the end point the parabola to the trailing edge. In a five-digit NACA airfoil section, the first digit represents the 2/3 of ideal lift coefficient (see figure 5.16) in tenths. It is an approximate representation of maximum camber in percent chord. The second digit indicates the position of maximum camber in two hundredths of chord length. The last two digits represent the maximum thickness-to-chord ratio. A zero in the first digit means that this airfoil is a symmetrical airfoil section. For example, the NACA **23012** airfoil section (see figure 5.19b) has a 15% $(t/c)_{max}$,. The ideal lift coefficient of this airfoil is 0.3 (the second digit), since $2/3 \times C_{li}$ = 2/10, thus, $C_{li} = 0.2/(2/3) = 0.3$. Finally its maximum camber is located at 12% of the chord length.

## c. The 6-series NACA airfoils

The four- and five-digit airfoil sections where designed simply by using parabola and line. They were not supposed to satisfy major aerodynamic design requirements, such as laminar flow and no flow separation. When it became clear that the four- and five-digit airfoils have not been carefully designed, NACA researchers begin the investigation to develop new series of airfoils that have been driven by design requirements. On the other hands, newly designed faster aircraft require more efficient airfoil sections. Several series of airfoils were designed at that time, but the 6-series were found to be the best. The six series airfoils were designed to maintain laminar flow over a large part of the chord, thus they maintain lower $Cd_{min}$ compared with four- and five-digit airfoils. The 6-series NACA airfoils are designated by five main digits and begin with number 6. Some 6-series airfoils have a subscript number after the second digit. There is also a "-" between the second digit and the third digit.
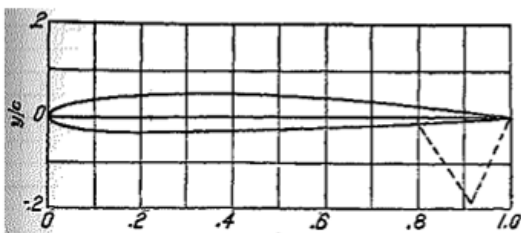


a. NACA 1408 airfoil section



b. NACA 23012 airfoil section



c. NACA $63_3$-218 airfoil section

The meaning of each digit is as follows. The first digit is always 6; that is the series designation. The second digit represents the chordwise position of minimum pressure in tenths of chord for the basic symmetrical section at zero lift. The third digit indicates the ideal lift coefficient in tenths. The last two digits represent the maximum thickness-to-chord ratio. In case that the airfoil name has a subscript after the second digit, it indicate the lift coefficient range in tenths above and below the value of ideal lift coefficient in which favorable pressure gradient and low drag exist. A zero in the third digit means that this airfoil is a symmetrical airfoil section.
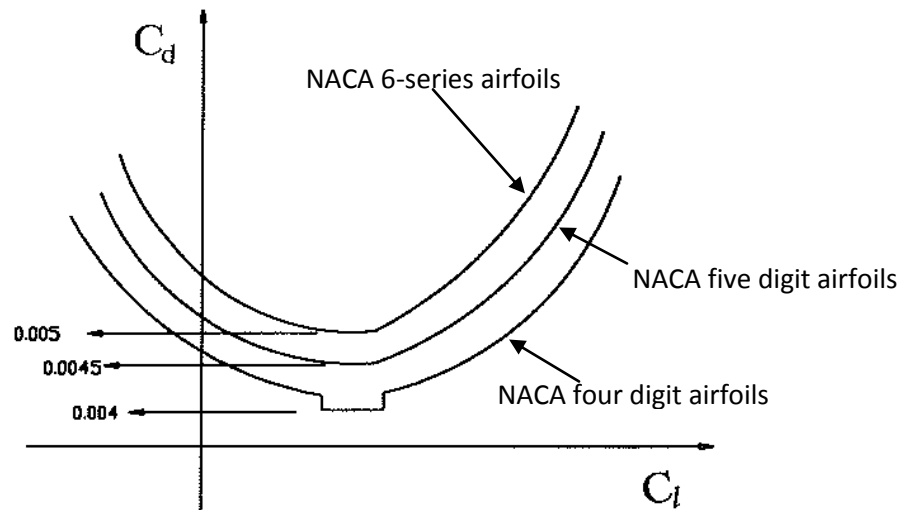


*Figure 5.20. A general comparison between four-digit, five-digit and 6-series airfoil sections*

| No | Airfoil section | $C_{lmax}$ at $Rn=3\times10^6$ | $\alpha_s$ (deg) | $C_{mo}$ | $(C_l/C_d)_{max}$ | $C_{li}$ | $C_{dmin}$ | $(t/c)_{max}$ |
|----|----------|------|----|--------|----|-----|--------|-----|
| 1 | 0009 | 1.25 | 13 | 0 | 39 | 0 | 0.0052 | 9% |
| 2 | 4412 | 1.5 | 13 | -0.09 | 71 | 0.4 | 0.006 | 12% |
| 3 | 2415 | 1.4 | 14 | -0.05 | 86 | 0.3 | 0.0065 | 15% |
| 4 | 23012 | 1.6 | 16 | -0.013 | 60 | 0.3 | 0.006 | 12% |
| 5 | 23015 | 1.5 | 15 | -0.008 | 52 | 0.1 | 0.0063 | 15% |
| 6 | $63_1$-212 | 1.55 | 14 | -0.004 | 67 | 0.2 | 0.0045 | 12% |
| 7 | $63_2$-015 | 1.4 | 14 | 0 | 61 | 0 | 0.005 | 15% |
| 8 | $63_2$-618 | 1.3 | 14 | -0.1 | 52 | 0.5 | 0.0052 | 18% |
| 9 | 64-210 | 1.4 | 12 | -0.042 | 57 | 0.2 | 0.004 | 10% |
| 10 | $65_4$-221 | 1.1 | 16 | -0.025 | 46 | 0.1 | 0.0048 | 21% |

*Table 5.2. Characteristics of several NACA airfoil sections*

For example, the NACA **$63_3$-218** airfoil section (see figure 5.19c) has 18% thickness-to-chord ratio. The position of the minimum pressure in this airfoil is located at 30 percent of the chord (the second digit). The ideal lift coefficient of the airfoil is 0.2 (the third digit). Finally, the lift

coefficient range above and below the value of ideal lift coefficient is 0.3 (the subscript). It demonstrates that the bucket in $C_d$-$C_l$ diagram (see figure 5.20) begins from lift coefficient of 0 (since 0.3 - 0.3 = 0) and ends at 0.6 (since 0.3 + 0.3 = 0.6).

| No | Aircraft name | First flight | Max speed (knot) | Root airfoil | Tip airfoil | Average $(t/c)_{max}$ |
|----|---------------|--------------|------------------|--------------|-------------|-----------------------|
| 1 | Cessna 550 | 1994 | 275 | 23014 | 23012 | 13% |
| 2 | Beech Bonanza | 1945 | 127 | 23016.5 | 23015 | 14.25% |
| 3 | Cessna 150 | 1957 | 106 | 2412 | 2412 | 12% |
| 4 | Piper Cherokee | 1960 | 132 | $65_2$-415 | $65_2$-415 | 15% |
| 5 | Dornier Do-27 | 1955 | 145 | 23018 | 23018 | 18% |
| 6 | Fokker F-27 | 1955 | 227 | $64_4$-421 | $64_4$-421 | 21% |
| 7 | Lockheed L100 | 1954 | 297 | 64A-318 | 64A-412 | 15% |
| 8 | PC-7 | 1978 | 270 | $64_2$-415 | $64_1$-415 | 15% |
| 9 | Hawker Siddely | 1960 | 225 | 23018 | 4412 | 15% |
| 10 | Beagle 206 | 1967 | 140 | 23015 | 4412 | 12.5% |
| 11 | Beech Super king | 1970 | 294 | 23018-23016.5 | 23012 | 14.5% |
| 12 | Lockheed Orion | 1958 | 411 | 0014 | 0012 | 13% |
| 13 | Moony M20J | 1976 | 175 | $63_2$-215 | 641-412 | 13.5% |
| 14 | Lockheed Hercules | 1951 | 315 | 64A318 | 64A412 | 15% |
| 15 | Thurston TA16 | 1980 | 152 | $64_2$-A215 | $64_2$-A215 | 15% |
| 16 | ATR 42 | 1981 | 269 | 43 series (18%) | 43 series (13%) | 15.5% |
| 17 | AIRTECH CN-235 | 1983 | 228 | $65_3$-218 | $65_3$-218 | 18% |
| 18 | Fokker 50 | 1987 | 282 | $64_4$-421 | $64_4$-415 | 18% |

*Table 5.3. The wing airfoil section of several prop-driven aircraft (Ref. 4)*

Figure 5.20 shows a general comparison between four-digit, five-digit and 6-series airfoil sections. Figure 5.21 demonstrates $C_l$-$\alpha$, $C_m$-$\alpha$, and $C_d$-$C_l$ graphs for NACA $63_2$-615 airfoil section. There are two groups of graphs, one for flap up and another one for flap down (60 degrees split flap). As noted, the flap deflection has doubled the airfoil drag (in fact $Cd_{min}$), increased pitching moment tremendously, but at the same time, has increased the lift coefficient by 1.2.

Besides NACA airfoil sections, there are variety of other airfoil sections that have been designed in the past several decades for different purposes. Few examples are peaky, supercritical, modern, supersonic airfoils. Table 5.2 illustrates the characteristics of several NACA airfoil sections. Table 5.3 illustrates the wing airfoil sections for several prop-driven aircraft. Table 5.4 illustrates the wing airfoil sections for several jet aircraft. As noted, all are employing NACA airfoils, from Cessna GA aircraft to F-16 fighter aircraft.
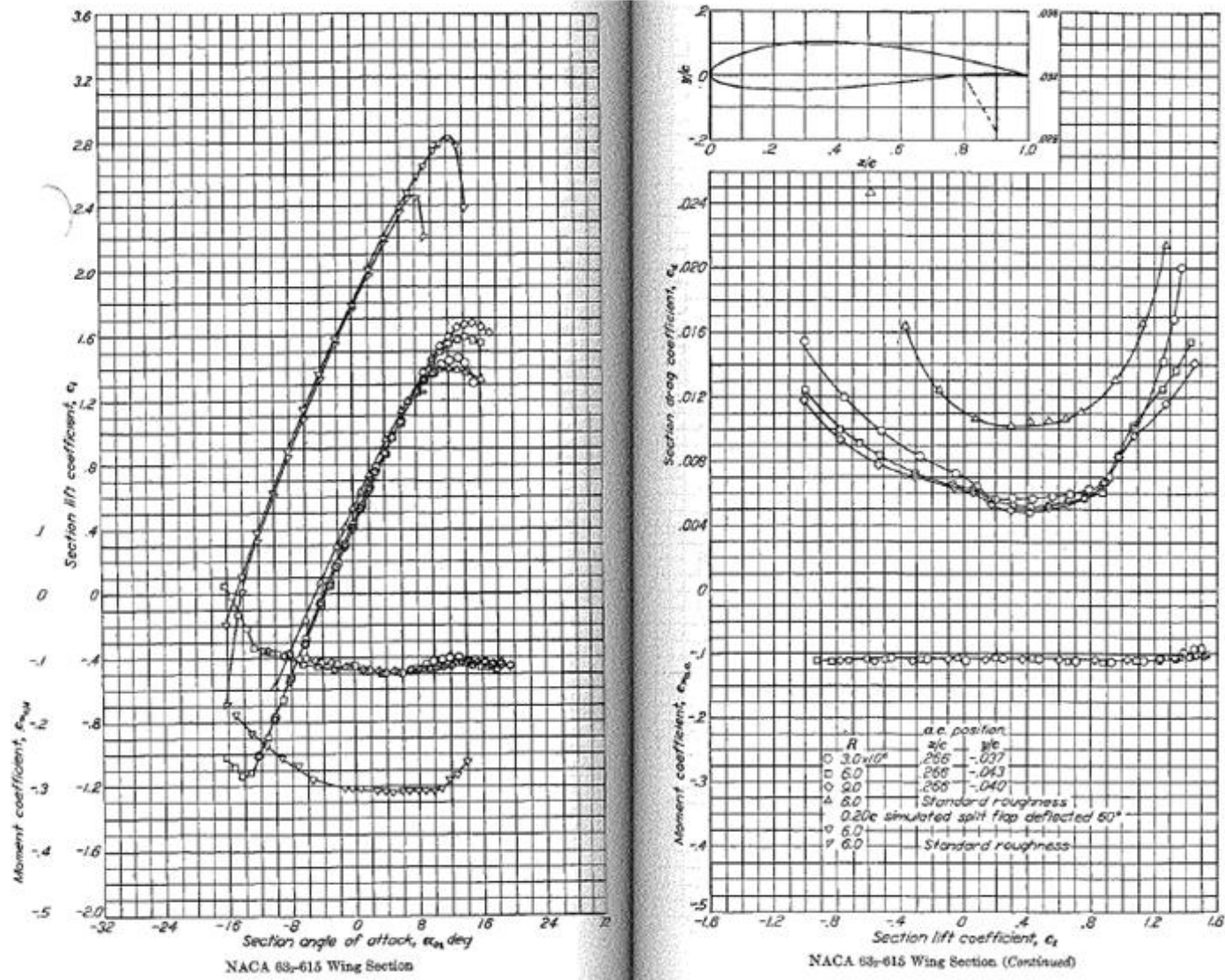
*Figure 5.21. $C_l$-$\alpha$, $C_m$-$\alpha$, and $C_d$-$C_l$ graphs of NACA 63$_2$-615 airfoil section (Ref. 2)*

| No | Aircraft name | First flight | Max speed (knot) | Root airfoil | Tip airfoil | Average $(t/c)_{max}$ |
|---|---|---|---|---|---|---|
| 1 | F-15E | 1982 | Mach 2.5 | 64A (6.6%) | 64A (3%) | 4.8% |
| 2 | Beech Starship | 1988 | 468 | 13.2% | 11.3% | 12.25% |
| 3 | Lockheed L-300 | 1963 | - | 0013 | 0010 | 11.5% |
| 4 | Cessna 500 Citation Bravo | 1994 | 275 | 23014 | 23012 | 12% |
| 5 | Cessna 318 | 1954 | 441 | 2418 | 2412 | 15% |
| 6 | Gates Learjet 25 | 1969 | 333 | 64A-109 | $64_4$-109 | 9% |
| 7 | Aero Commander | 1963 | 360 | $64_1$-212 | $64_1$-212 | 12% |
| 8 | Lockheed Jetstar | 1957 | 383 | 63A-112 | 63A-309 | 10.5% |
| 9 | Airbus 310 | 1982 | 595 | 15.2% | 10.8% | 13% |
| 10 | Rockwell/DASA X-31A | 1990 | 1485 | Transonic airfoil | Transonic airfoil | 5.5% |
| 11 | Kawasaki T-4 | 1988 | 560 | Supercritical airfoil (10.3%) | Supercritical airfoil (7.3%) | 8.8% |
| 12 | Gulfstream IV-SP | 1985 | 340 | Sonic rooftop (10%) | Sonic rooftop (8.6%) | 9.3% |
| 13 | Lockheed F-16 | 1975 | Mach 2.1 | 64A-204 | 64A-204 | 4% |
| 14 | Fokker 50 | 1985 | 282 | $64_4$-421 | $64_4$-415 | 18% |

*Table 5.4. The wing airfoil sections of several jet aircraft. (Ref. 4)*

## Example 5.1

Identify $C_{li}$, $C_{dmin}$, $C_m$, $(C_l/C_d)_{max}$, $\alpha_o$ (deg), $\alpha_s$ (deg), $C_{lmax}$, $a_o$ (1/rad), $(t/c)_{max}$ of the NACA 63-209 airfoil section (flap-up). You need to indicate the locations of all parameters on the airfoil graphs.

**Solution:**

By referring to figure 5.22, the required values for all parameters are as determined follows:

| $C_{li}$ | $C_{dmin}$ | $C_m$ | $(C_l/C_d)_{max}$ | $\alpha_o$ (deg) | $\alpha_s$ (deg) | $C_{lmax}$ | $C_{l\alpha}$ (1/rad) | $(t/c)_{max}$ |
|---|---|---|---|---|---|---|---|---|
| 0.2 | 0.0045 | -0.03 | 66.7 | -1.5 | 12 | 1.45 | 5.73 | 9% |

The locations of all points of interest are illustrated in figure 5.22.
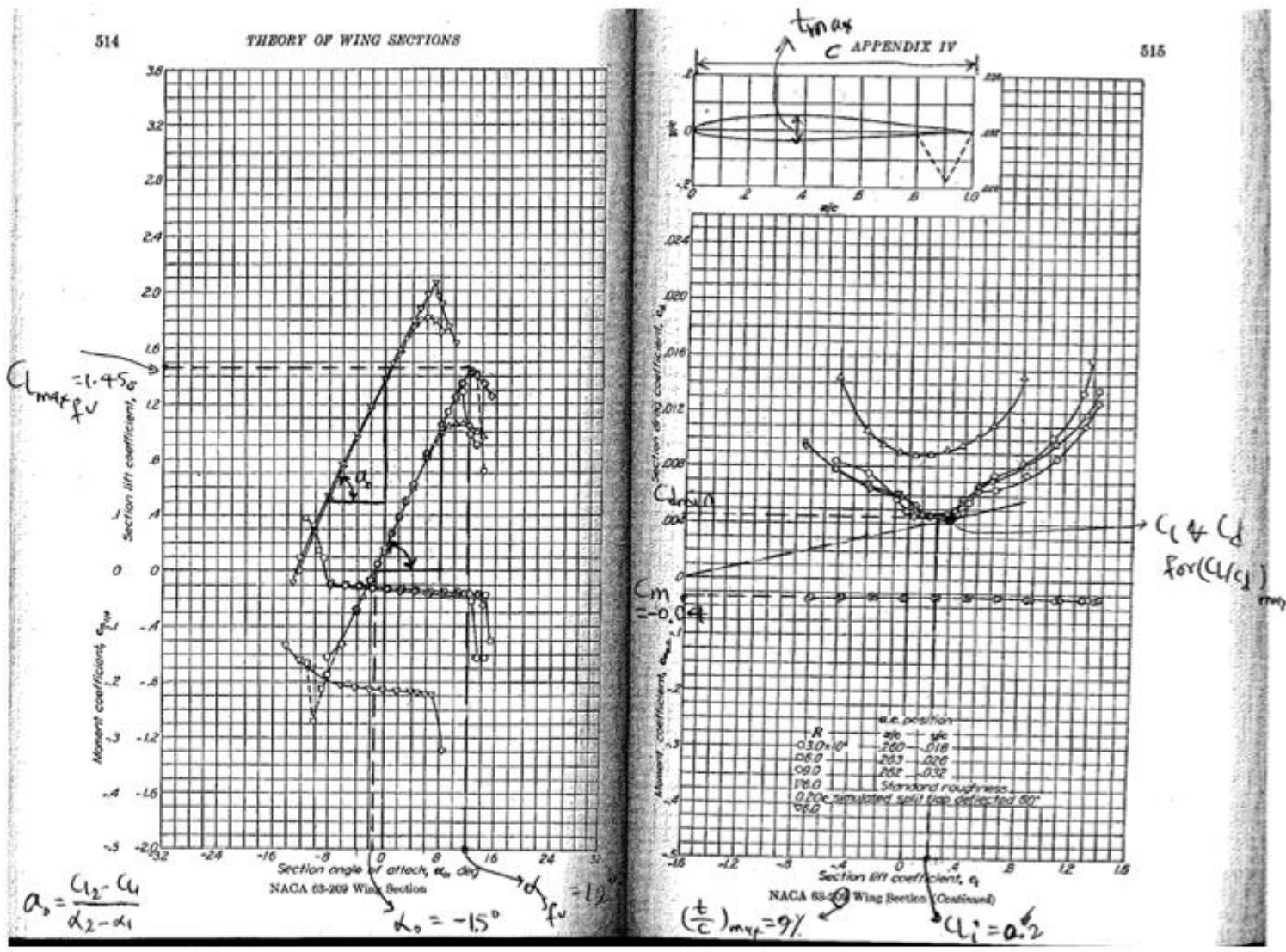
*Figure 5.22. The locations of all points of interest of NACA 63-209 airfoil section (flap-up)*

### 5.4.6. Practical Steps for Wing Airfoil Section Selection

In the previous sections, the geometry of an airfoil section, airfoil design tools, NACA airfoil sections, significant airfoil parameters, and criteria for airfoil section are covered. In this section, the practical steps for wing airfoil section selection will be presented. It is assumed that an airfoil section data base (such as *NACA* or *Eppler*) is available and the wing designer is planning to select the best airfoil from the list. The steps are as follows:

1. Determine the average aircraft weight ($W_{avg}$) in cruising flight:

$$W_{avg} = \frac{1}{2}\left(W_i + W_f\right)$$  (5.9)

   where $W_i$ is the initial aircraft weight at the beginning of cruise and $W_f$ is the final aircraft weight at the end of cruise.

2. Calculate the aircraft ideal cruise lift coefficient ($C_{L_C}$). In a cruising flight, the aircraft weight is equal to the lift force (equation 5.1), so:

$$C_{L_C} = \frac{2W_{ave}}{\rho V_c^2 S}$$  (5.10)

   where $V_c$ is the aircraft cruise speed, $\rho$ is the air density at cruising altitude, and S is the wing planform area.

3. Calculate the wing cruise lift coefficient ($C_{L_{C_w}}$). Basically, the wing is solely responsible for the generation of the lift. However, other aircraft components also contribute to the total lift; negatively, or positively; sometimes, as much as 20 percent. Thus the relation between aircraft cruise lift coefficient and wing cruise lift coefficient is a function of aircraft configuration. The contribution of fuselage, tail and other components will determine the wing contribution to aircraft lift coefficient. If you are at the preliminary design phase and the geometry of other components have not been determined yet, the following approximate relationship is recommended.

$$C_{L_{C_w}} = \frac{C_{L_C}}{0.95}$$  (5.11)

   In the later design phases; when other components are designed; this relationship must be clarified. A CFD software package is a reliable tool to determine this relationship.

4. Calculate the wing airfoil ideal lift coefficient ($C_{l_i}$). The wing is a three-dimensional body, while an airfoil is a two-dimensional section. If the wing chord is constant, with no sweep angle, no dihedral, and the wing span is assumed to be infinity; theoretically; the wing lift coefficient would be the same as wing airfoil lift coefficient. However, at this moment, the wing has not been designed yet, we have to resort to an approximate relationship. In reality, the span is limited, and in most cases, wing has sweep angle, and

non-constant chord, so the wing lift coefficient will be slightly less than airfoil lift coefficient. For this purpose, the following approximate equation[8] is recommended at this moment:

$$C_{l_i} = \frac{C_{L_{C_w}}}{0.9} \tag{5.12}$$

In the later design phases, by using aerodynamic theories and tools, this approximate relation must be modified to include the wing geometry to the required airfoil ideal coefficient.

**5.** Calculate the aircraft maximum lift coefficient ($C_{L_{max}}$):

$$C_{L_{max}} = \frac{2W_{TO}}{\rho_o V_s^2 S} \tag{5.13}$$

where $V_s$ is the aircraft stall speed, $\rho_o$ is the air density at sea level, and $W_{TO}$ is the aircraft maximum take-off weight.

**6.** Calculate the wing maximum lift coefficient ($C_{L_{max_w}}$). With the same logic that was described in step 3, the following relationship is recommended.

$$C_{L_{max_w}} = \frac{C_{L_{max}}}{0.95} \tag{5.14}$$

**7.** Calculate the wing airfoil gross maximum lift coefficient ($C_{l_{max_{gross}}}$).

$$C_{l_{max_{gross}}} = \frac{C_{L_{max_w}}}{0.9} \tag{5.15}$$

where the wing airfoil "*gross*" maximum lift coefficient is the airfoil maximum lift coefficient in which the effect of high lift device (e.g. flap) is included.

**8.** Select/Design the high lift device (type, geometry, and maximum deflection). This step will be discussed in details in section 5.12.

**9.** Determine the high lift device (HLD) contribution to the wing maximum lift coefficient ($\Delta C_{l_{HLD}}$). This step will also be discussed in details in section 5.12.

**10.** Calculate the wing airfoil "*net*" maximum lift coefficient ($C_{l_{max}}$)

$$C_{l_{max}} = C_{l_{max_{gross}}} - \Delta C_{l_{HLD}} \tag{5.16}$$

---

[8] Please note that the subscript L is used for the 3d application (wing), but subscript *l* is employed for the 2d application (airfoil).
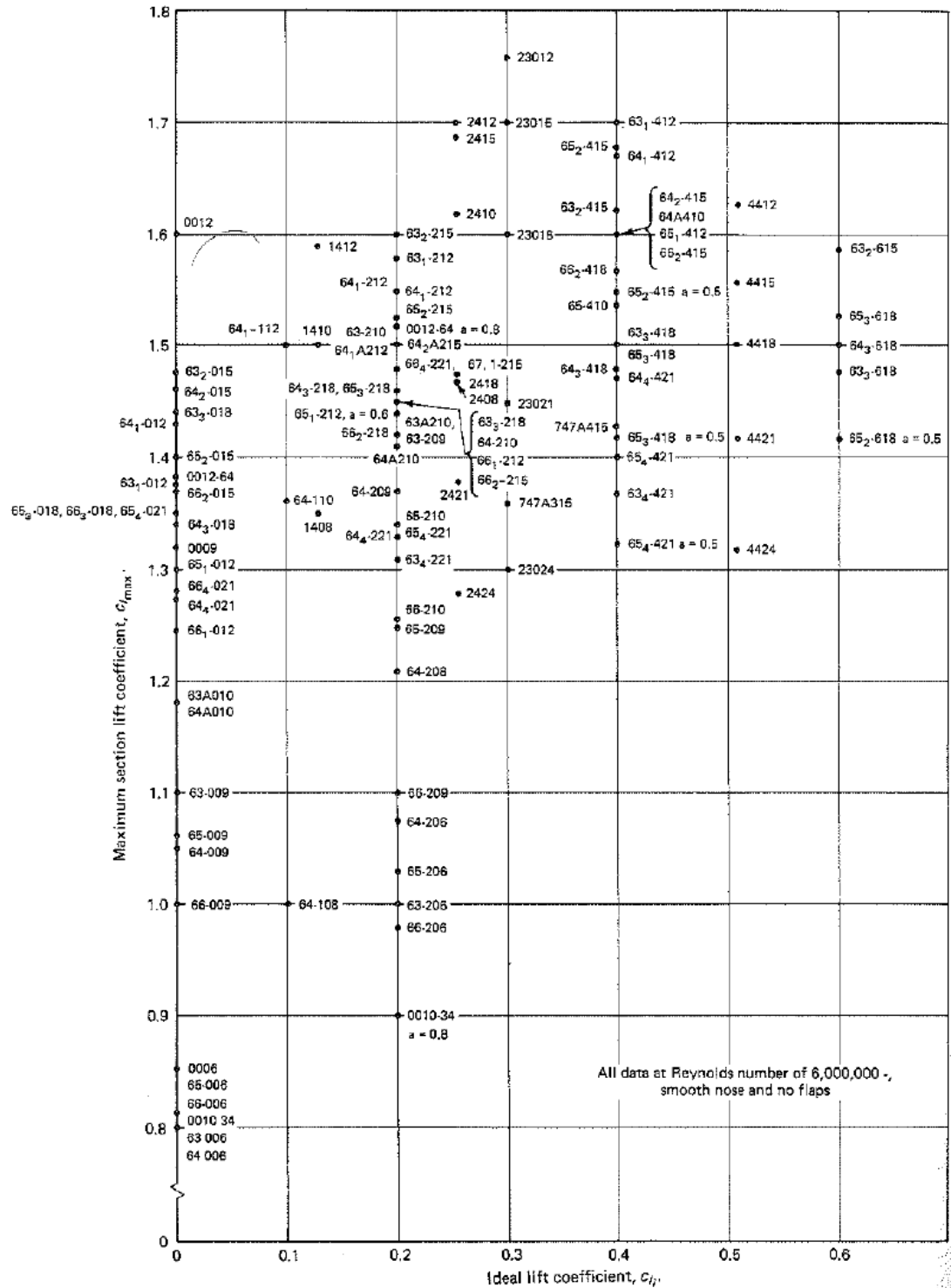
*Figure 5.23. Variation in maximum lift coefficient for various airfoil section ideal lift coefficients (Ref. 6)*

**11.** Identify airfoil section alternatives that deliver the desired $C_{li}$ (step 4) and $C_{lmax}$ (step 10). This is a very essential step. Figure 5.23 shows a collection of $C_{li}$ and $C_{lmax}$ for several

NACA airfoil sections in just one graph. The horizontal axis represents the airfoil ideal lift coefficient while the vertical axis the airfoil maximum lift coefficient. Every black circle represents one NACA airfoil section. For $C_{li}$ and $C_{lmax}$ of other airfoil sections, refer to reference 2 and reference 1. If there is no airfoil section that delivers the desired $C_{li}$ and $C_{lmax}$, select the airfoil section that is nearest to the design point (desired $C_{li}$ and $C_{lmax}$).

12. If the wing is designed for a high subsonic passenger aircraft, select the thinnest airfoil (the lowest $(t/c)_{max}$). The reason is to reduce the critical Mach number ($M_{cr}$) and drag-divergent[9] Mach number ($M_{dd}$). This allow the aircraft fly closer to Mach one before the drag rise is encountered. In general, a thinner airfoil will have a higher $M_{cr}$ than a thicker airfoil (Ref. 11). Figure 5.24 shows the variation of the drag coefficient versus Mach number for three wings with airfoil thickness ratio as a parameter. As noted, the $M_{dd}$ of the wing with 9 percent thickness-to-chord ratio occurs at the value of about 0.88. By reducing the wing $(t/c)_{max}$ to 6 and 4 percent, the magnitude of the drag rise is progressively reduced, and the value of $M_{dd}$ is increased, moving closer to mach one.
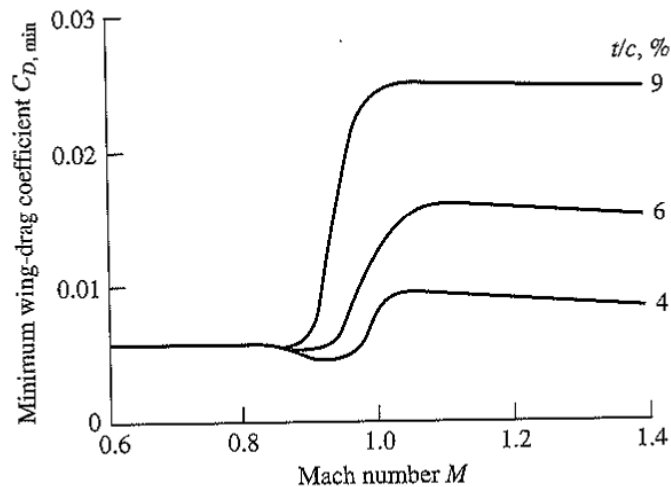


Figure 5.24. Variation of wing drag coefficient versus Mach number with airfoil thickness ratio as a parameter (Ref. 11). The wing is swept where the sweep angle is 47 degrees.

| Design objectives | Weight | Airfoil 1 | Airfoil 2 | Airfoil 3 | Airfoil 4 | Airfoil 5 |
|---|---|---|---|---|---|---|
| $C_{dmin}$ | 25% | | | | | |
| $C_{mo}$ | 15% | | | | | |
| $\alpha_s$ | 15 | | | | | |
| $\alpha_o$ | 10 | | | | | |
| $(C_l/C_d)_{max}$ | 10% | | | | | |
| $C_{l\alpha}$ | 5% | | | | | |
| Stall quality | 20% | | | | | |
| Summation | 100% | 64 | 76 | 93 | 68 | 68 |

Table 5.5. A sample table to compare the features of five airfoil sections

---

[9] $M_{dd}$ is defined as the Mach number at which the slope of the curve of $C_D$ versus M is 0.05 (Ref. 6)

**13.** Among several acceptable alternatives, select the optimum airfoil section by using a comparison table. A typical comparison table which includes a typical weight for each design requirement is shown in table 5.5. Reference 5 is a rich resource for the systematic procedure of the selection technique and table construction.

## Example 5.2

Select a NACA airfoil section for the wing for a jet non-maneuverable GA aircraft with the following characteristics:

$$m_{TO} = 4000 \text{ kg}, \ S = 30 \text{ m}^2, \ V_c = 250 \text{ knot (at 3000 m)}, \ V_s = 65 \text{ knot (sea level)}$$

The high lift device (split flap) will provide $\Delta C_L = 0.8$ when deflected.

**Solution:**

Ideal lift coefficient:

$$C_{L_C} = \frac{2W_{ave}}{\rho V_c^2 S} = \frac{2 \times 4000 \times 9.81}{0.9 \times (250 \times 0.514)^2 \times 30} = 0.176 \tag{5.10}$$

$$C_{L_{C_w}} = \frac{C_{L_C}}{0.95} = \frac{0.176}{0.95} = 0.185 \tag{5.11}$$

$$C_{l_i} = \frac{C_{L_{C_w}}}{0.9} = \frac{0.185}{0.9} = 0.205 \cong 0.2 \tag{5.12}$$

Maximum lift coefficient:

$$C_{L_{max}} = \frac{2W_{TO}}{\rho_o V_s^2 S} = \frac{2 \times 4000 \times 9.81}{1.225 \times (65 \times 0.514)^2 \times 30} = 1.909 \tag{5.13}$$

$$C_{L_{max_w}} = \frac{C_{L_{max}}}{0.95} = \frac{1.909}{0.95} = 2.01 \tag{5.14}$$

$$C_{l_{max_{gross}}} = \frac{C_{L_{max_w}}}{0.9} = \frac{2.01}{0.9} = 2.233 \tag{5.15}$$

$$C_{l_{max}} = C_{l_{max_{gross}}} - \Delta C_{l_{max_{HLD}}} = 2.233 - 0.8 = 1.433 \tag{5.16}$$

Thus, we need to look for NACA airfoil sections that yield an ideal lift coefficient of 0.2 and a net maximum lift coefficient of 1.433. Referring to figure 5.22, we find the following airfoils whose characteristics match with our design requirements (all have $C_{li} = 0.2$, $C_{lmax} = 1.43$):

$$\textbf{63}_\textbf{3}\textbf{-218, 64-210, 66}_\textbf{1}\textbf{-212, 66}_\textbf{2}\textbf{-215, 65}_\textbf{3}\textbf{-218}$$

Now we need to compare these airfoils to see which one is the best as demonstrated in table 5.6.

| No | NACA | $C_{dmin}$ | $C_{mo}$ | $\alpha_s$ (deg) Flap up | $\alpha_o$ (deg) $\delta_f = 60^o$ | $(C_l/C_d)_{max}$ | Stall quality |
|----|------|------------|----------|-------------------------|-----------------------------------|-------------------|---------------|
| 1 | $63_3$-218 | 0.005 | -0.028 | 12 | -12 | 100 | Docile |
| 2 | 64-210 | 0.004 | -0.040 | 12 | -13 | 75 | Moderate |
| 3 | $66_1$-212 | 0.0032 | -0.030 | 12 | -13 | 86 | Sharp |
| 4 | $66_2$-215 | 0.0035 | -0.028 | 14 | -13.5 | 86 | Sharp |
| 5 | $65_3$-218 | 0.0045 | -0.028 | 16 | -13 | 111 | Moderate |

*Table 5.6. A comparison among five airfoil candidates for use in the wing of Example 5.2*

The best airfoil is the airfoil whose $C_{mo}$ is the lowest, the $C_{dmin}$ is the lowest, the $\alpha_s$ is the highest, the $(C_l/C_d)_{max}$ is the highest, and the stall quality is docile.

By comparing the numbers in the above table, we can conclude the followings:

1- The NACA airfoil section $66_1$-212 yields the highest maximum speed, since it has the lowest $C_{dmin}$ (0.0032).
2- The NACA airfoil section $65_3$-218 yields the lowest stall speed, since it has the highest stall angle (16 degrees).
3- The NACA airfoil section $65_3$-218 yields the highest endurance, since it has the highest $(C_l/C_d)_{max}$ (111).
4- The NACA $63_3$-218 yields the safest flight, due to its docile stall quality.
5- The NACA airfoil sections $63_3$-218, $66_2$-215, and $65_3$-218 deliver the lowest control problem in flight, due to the lowest $C_{mo}$ (-0.028).

Since the aircraft is a non-maneuverable GA aircraft, the stall quality cannot be sharp, hence $66_1$-212 and $66_2$-215 are not acceptable. If the safety is the highest requirement, the best airfoil is NACA $63_2$-218. On the other hand, if the low cost is the most important requirement, NACA 64-210 with the lowest $C_{dmin}$ is the best. However, if the aircraft performance (stall speed, endurance or maximum speed) are of greatest important design requirement, the NACA airfoil section $65_3$-218, $65_3$-218, or $66_1$-212 are the best respectively. This may be performed by using a comparison table incorporating the weighted design requirements.

## 5.5. Wing Incidence
The wing incidence ($i_w$) is the angle between fuselage center line and the wing chord line at root (see figure 5.25). It is sometimes referred to as the wing setting angle ($\alpha_{set}$). The fuselage center line lies in the plane of symmetry and is usually defined parallel to the cabin floor. This angle could be selected to be variable during a flight operation, or be constant throughout all flight operations. If it is selected to vary during flight, there is no need to determine wing setting angle for the purpose of the aircraft manufacture. However, in this case, the mechanism to vary the wing incidence during flight phases must be designed. Thus the required wing incidence for every flight phase must be calculated. The variable wing incidence is not recommended, since

there is a huge safety and operational concerns. To allow for the wing to have a variable setting angle, there must be a single shaft around which the wing is rotated by pilot control. Such a mechanism is not 100% reliable for aviation purposes, due to fatigue, weight, and stress concentration concerns. In the history of aviation, there is only one aircraft (Vought f 8 u Crusader) whose wing had variable incidence. A flying wing; such as Northrop Grumman B-2 Spirit has no wing incidence, since there is no fuselage, however the wing angle of attack must be determined for operational purposes.
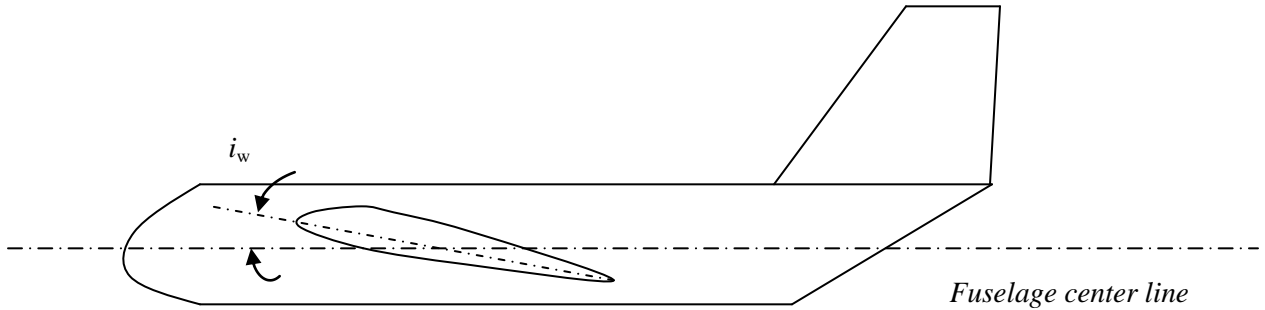


*Figure 5.25. Wing setting angle*

The second, very convenient option is to have a constant wing setting angle. The wing can be attached to the fuselage via welding, screw, or other manufacturing technique at the specified setting angle. This is much safer compared with variable setting angle. For this option, the designer must determine the angle at which the wing is attached to the fuselage. The wing incidence must satisfy the following design requirements:

1. The wing must be able to generate the desired lift coefficient during cruising flight.
2. The wing must produce minimum drag during cruising flight.
3. The wing setting angle must be such that the wing angle of attack could be safely varied (in fact increased) during take-off operation.
4. The wing setting angle must be such that the fuselage generates minimum drag during cruising flight (i.e. the fuselage angle of attack must be zero in cruise).
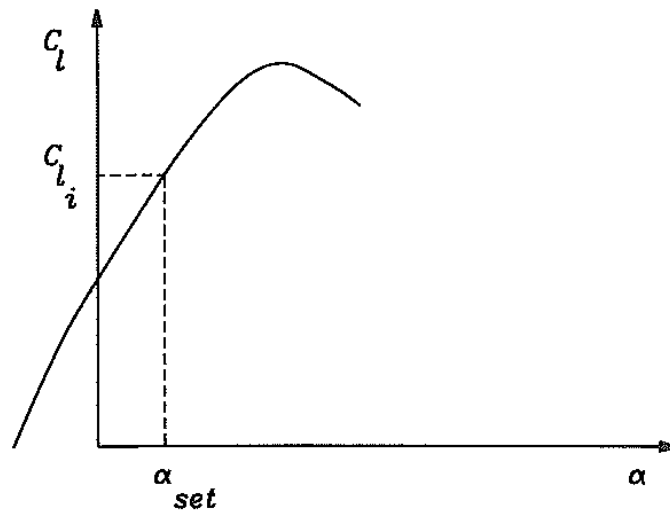


*Figure 5.26. Wing setting angle corresponds with ideal lift coefficient*

These design requirements naturally match with the wing airfoil angle of attack corresponding to the airfoil ideal lift coefficient (see figure 5.26). Therefore, as soon as the wing ideal lift coefficient is determined, a reference to $C_l$-$\alpha$ graph demonstrates the wing setting angle. Table 5.7 illustrates the wing incidence for several aircraft.

The typical number for wing incidence for majority of aircraft is between 0 to 4 degrees. As a general guidance, the wing setting angle in supersonic fighters, is between 0 to 1 degrees; in GA aircraft, between 2 to 4 degrees; and in jet transport aircraft is between 3 to 5 degrees.

| No | Aircraft | Type | Wing incidence | Cruising speed (knot) |
|----|----------|------|----------------|-----------------------|
| 1 | Airbus 310 | Jet transport | $5^o$ 30' | Mach 0.8 |
| 2 | Fokker 50 | Prop-driven transport | $3^o$ 30' | 282 |
| 3 | Sukhoi Su-27 | Jet fighter | $0^o$ | Mach 2.35 |
| 4 | Embraer FMB-120 Brasilia | Prop-driven transport | $2^o$ | 272 |
| 5 | Tucano | Turbo-Prop Trainer | $1^o$ 25' | 222 |
| 6 | Antonov An-26 | Turbo-prop Transport | $3^o$ | 235 |
| 7 | BAe Jetstream 31 | Turbo-prop Business | $3^o$ | 282 |
| 8 | BAe Harrier | V/STOL close support | $1^o$ 45' | 570 |
| 9 | Lockheed P-3C Orion | Prop-driven transport | $3^o$ | 328 |
| 10 | Rockwell/DASA X-31A | Jet combat research | $0^o$ | 1485 |
| 11 | Kawasaki | Prop-driven transport | $0^o$ | 560 |
| 12 | ATR 42 | Prop-driven transport | $2^o$ | 265 |
| 13 | Beech Super King Air B200 | Turbo-prop Transport | $3^o$ 48' | 289 |
| 14 | SAAB 340B | Turbo-prop Transport | $2^o$ | 250 |
| 15 | AVRO RJ | Jet Transport | $3^o$ 6' | 412 |
| 16 | McDonnell MD-11 | Jet Transport | $5^o$ 51' | Mach 0.87 |
| 17 | F-15J Eagle | Fighter | 0 | > Mach 2.5 |

*Table 5.7. Wing setting angle for several aircraft (Ref. 4)*

The wing setting angle may be modified as the design process progresses. For instance, a fuselage with large unsweep over the rear portion to accept aft cargo doors may have their minimum drag at a small positive angle of attack. In such cases, the wing incidence will be reduced accordingly. Another, les fundamental, consideration is that stopping performance during landing operation to get as much weight on the braked wheels as possible. Thus, there is a benefit to reduce the wing incidence slightly to the extent that the change is not felt significantly in the cabin. Reducing the nose gear length will do the same thing. This technique is limited in passenger aircraft because a level cabin floor is desirable on the ground. But, for fighter aircraft, the level floor is not a design consideration.

## 5.6. Aspect Ratio
Aspect ratio (AR)[10] is defined as the ratio between the wing span; b (see figure 5.31) to the wing Mean Aerodynamic Chord (MAC or $\overline{C}$).

---

[10] Some textbooks are using symbol A instead of AR.

$$AR = \frac{b}{\overline{C}} \tag{5.17}$$

The wing planform area with a rectangular or straight tapered shape is defined as the span times the mean aerodynamic chord:

$$S = b \cdot \overline{C} \tag{5.18}$$

Thus, the aspect ratio shall be redefined as:

$$AR = \frac{bb}{\overline{C}b} = \frac{b^2}{S} \tag{5.19}$$
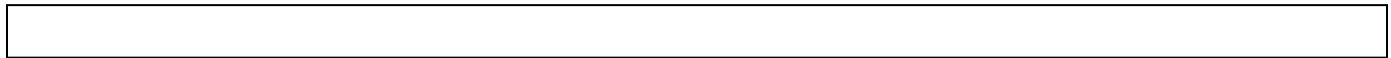
a. AR = 26.7
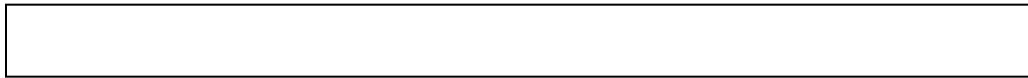
b. AR = 15

c. AR = 6.67

d. AR = 3.75

e. AR = 1

*Figure 5.27. Several rectangular wings with the same planform area but different aspect ratio*

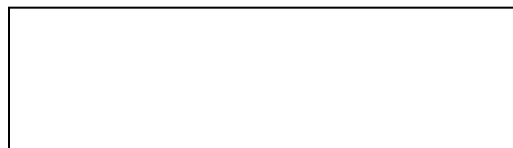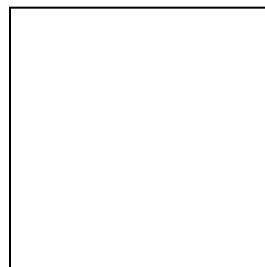This equation is not to be used for the wing with geometry other than rectangle; such as triangle, trapezoid or ellipse; except when the span is redefined. Example 5.4 clarifies this point. At this point, only wing planform area is known. The designer has infinite options to select the wing geometry. For instance, consider an aircraft whose wing reference area has been determined to be 30 m². A few design options are as follows:

1. A rectangular wing with a 30 m span and a 1 m chord (AR =30)
2. A rectangular wing with a 20 m span and a 1.5 m chord (AR =13.333)
3. A rectangular wing with a 15 m span and a 2 m chord (AR = 7.5)
4. A rectangular wing with a 10 m span and a 3 m chord (AR = 3.333)
5. A rectangular wing with a 7.5 m span and a 4 m chord (AR = 1.875)
6. A rectangular wing with a 6 m span and a 5 m chord (AR = 1.2)
7. A rectangular wing with a 3 m span and a 10 m chord (AR = 0.3)
8. A triangular (Delta) wing with a 20 m span and a 3 m root chord (AR = 13.33; please note that the wing has two sections (left and right))
9. A triangular (Delta) wing with a 10 m span and a 6 m root chord (AR = 3.33)

There are other options too; but since we have not discussed the parameter of taper ratio; we will not address them at this moment. Figure 5.27 depicts several rectangular wings with different aspect ratio. These wings have the same planform area, but their spans and chords are different. In terms of lift equation (equation 5.1), all are expected to generate the same lift, provided they have the same lift coefficient. However, the wing lift coefficient is not a function of wing area; rather, it is a function of non-dimensional aerodynamic characteristics of the wing such as airfoil and aspect ratio. It is interesting to note that the aspect ratio of the 1903 Wright Flyer was 6.

The question for a wing designer is how to select the aspect ratio, or which wing geometry is the best. To address this question, we need to discuss the effects of aspect ratio on various flight features such as aircraft performance, stability, control, cost, and manufacturability.

1. From aerodynamic points of view, as the AR is increased, the aerodynamic features of a three-dimensional wing (such as $C_{L\alpha}$, $\alpha_o$, $\alpha_s$, $C_{Lmax}$, $C_{Dmin}$) are getting closer to its two-dimensional airfoil section (such as $C_{l\alpha}$, $\alpha_o$, $\alpha_s$, $C_{lmax}$, $C_{dmin}$). This is due to reduction of the influence of wing tip vortex. The flow near the wing tips tends to curl around the tip, being forced from the high-pressure region just underneath the tips to the low-pressure region on top (Ref. 3). As a result, on the top surface of the wing, there is generally a spanwise component of flow from the tip toward the wing root, causing the streamlines over the top surface to bend toward the root. Similarly, on the bottom surface of the wing, there is generally a spanwise component of flow from the root toward the wing tip, causing the streamlines over the bottom surface to bend toward the tip.
2. Due to the first item, as the AR is increased, the wing lift curve slope ($C_{L\alpha}$) is increased toward the maximum theoretical limit of $2\pi$ 1/rad (see figure 5.28). The relationship (Ref. 3) between 3d wing lift curve slope ($C_{L\alpha}$) and 2d airfoil lift curve slope ($C_{l\alpha}$) is as follows:

$$C_{L_\alpha} = \frac{dC_L}{d\alpha} = \frac{C_{l_a}}{1 + \frac{C_{l_\alpha}}{\pi \cdot AR}} \qquad (5.20)$$
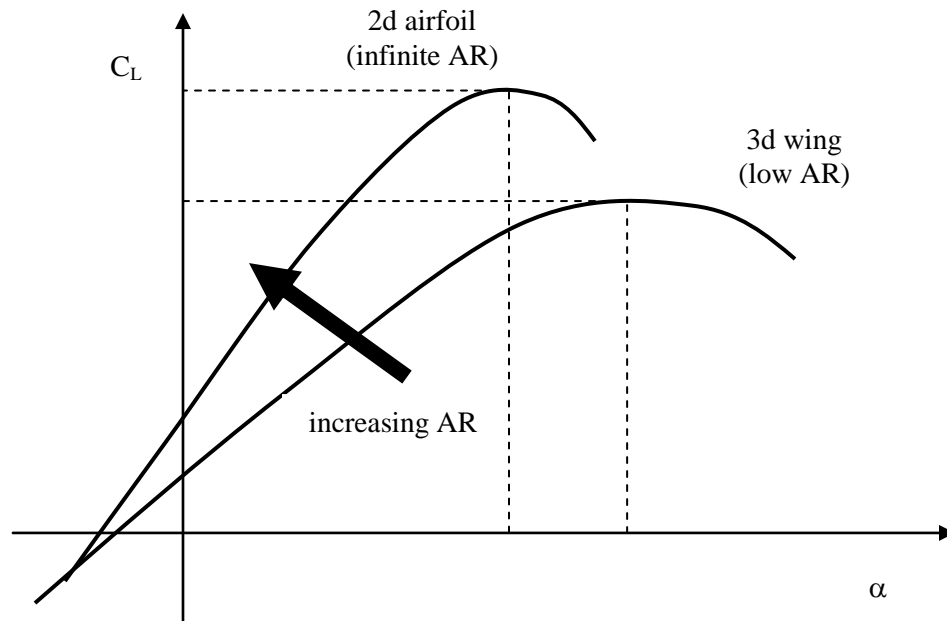
For this reason, a high AR (longer) wing is desired.



*Figure 5.28. The effect of AR on $C_L$ versus angle of attack graph*

3. As the AR is increased, the wing stall angle ($\alpha_s$) is decreased toward the airfoil stall angle. Since the wing effective angle of attack is increased (see figure 5.28). For this reason, the horizontal tail is required to have an aspect ratio lower than wing aspect ratio to allow for a higher tail stall angle. This will result in the tail to stall after wing has stalled, and allow for a safe recovery. For the same reason, a canard is desired to have an aspect ratio to be more than the wing aspect ratio. For this reason, a high AR (longer) wing is desired.

4. Due to the third item, as the AR is increased, the wing maximum lift coefficient ($C_{Lmax}$) is increased toward the airfoil maximum lift coefficient ($C_{lmax}$). This is due to the fact that the wing effective angle of attack is increased (see figure 5.28). For this reason, a high AR (longer) wing is desired.

5. As the AR is increased, the wing will be heavier. The reason is the requirement for structural stiffness. As the wing gets longer, the wing weight ($W_w$) moment arm (T) gets larger (since $T = \frac{W_w}{2}\frac{b}{2}$), and wing root will have a higher stress. Thus, the wing root must be stronger to hold the long wing. This requires a heavier wing. The more weight of the wing translates to more cost. For this reason, a low AR (shorter) wing is desired.

6. As the $\sqrt{AR}$ is increased, the aircraft maximum lift-to-drag ratio is increased. Since

$$\left(\frac{L}{D}\right)_{\text{max}} = \frac{1}{2\sqrt{KC_{D_o}}} \tag{5.21}$$

where

$$K = \frac{1}{\pi \cdot e \cdot AR} \tag{5.22}$$

where K is the wing induced drag factor, e is the Oswald span efficiency factor, and $C_{\text{Do}}$ is the aircraft zero-lift drag coefficient (Ref. 7 and 8). For the derivation of these two equations, you are referred to Reference 7. For this reason, a high AR (longer) wing is desired. This is one of the reasons that the gliders have large aspect ratio and long wing. For this reason, a high AR (longer) wing is desired.

7.  As the AR is increased, the wing induced drag is decreased, since the induced drag ($C_{Di}$) is inversely proportional to aspect ratio. For this reason, a low AR (shorter) wing is desired.

$$C_{D_i} = \frac{C_L^2}{\pi \cdot e \cdot AR} \tag{5.23}$$

8.  As the AR is increased, the effect of wing tip vortex on the horizontal tail is decreased. As explained in item 1, the tendency for the flow to leak around the wing tips establishes a circulation which trails downstream of the wing; i.e. a trailing vortex is created at each wing tip. This downward component is called downwash. If the tail is in the region of downwash, the tail effective angle of attack is reduced by downwash. This will influence the longitudinal stability and longitudinal control (Ref. 10) of the aircraft.

9.  As the AR increases, the aileron arm will be increased, since the aileron are installed outboard of the wing. This means that the aircraft has more lateral control.

10. As the AR increases, the aircraft mass moment of inertia around x-axis (Ref. 9) will be increased. This means that it takes longer to roll. In another word, this will reduces the maneuverability of aircraft in roll (Ref. 10). For instance, the Bomber aircraft B-52; that has a very long span; takes several seconds to roll at low speed, whilst the fighter aircraft F-16 takes a fraction of a second to roll. For this reason, a low AR (shorter) wing is desired for a maneuverable aircraft. The tactical supersonic missiles have a low AR of around 1 to enable them to roll and maneuver as fast as possible.

11. If the fuel tank is supposed to be inside wing, it is desirable to have a low aspect ratio wing. This helps to have a more concentrated fuel system. For this reason, a low AR (shorter) wing is desired.

12. As the aspect ratio is increased, the wing stiffness around y-axis is decreased. This means that the tendency of the wing tips to drop during a take-off is increased, while the tendency to rise during high speed flight is increased. In practice, the manufacture of a very high aspect ratio wing with sufficient structural strength is difficult.

    This wing behavior was observed during the flight of Voyager aircraft (AR = 38, b = 33.8 m) in 1986 during its record breaking flight to circle around the globe without refueling. The Voyager wing tip drop was more than 5 feet during the take-off (low sped flight), while the wing tips raised more than 4 feet during the cruising (high speed) flight.

During the Voyager's takeoff, as the plane accelerated, the tips of the wings, which were heavily loaded with fuel, were damaged as they scraped against the runway, ultimately causing pieces of winglets to break off at both ends. The aircraft accelerated very slowly and needed approximately 14,200 feet of the runway to gain enough speed to lift from the ground, the wings arching up dramatically just before take-off. The plane also continuously reminded the pilots of its pitch instability and fragility. They had to maneuver around bad weather numerous times.

Another example is the transport aircraft Boeing 747 (AR =7.7, b = 59.6 m) whose wing tips drop about 1 foot while the aircraft in on the ground prior to take-off. The wingtip drop is not desirable, especially for a take-off maneuver, since the wing tip clearance is of great importance for safety. For this reason, a low AR (shorter) wing is desired. A shorter wing is easier to build compared with a long wing. For the manufacturability reason, a low AR (shorter) wing is desired.

13. A shorter wing needs lower cost to build compared with a long wing. For the cost reason, a low AR (a shorter wing) is desired.
14. As the AR is increased, the occurrence of the aileron reversal (Ref. 10) is more expected, since the wing will be more flexible. The aileron reversal is not a desirable phenomenon for a maneuverable aircraft. For this reason, a low AR (shorter) wing is desired.

| No | Aircraft type | Aspect ratio |
|---|---|---|
| 1 | Hang glider | 4-8 |
| 2 | Glider (sailplane) | 20-35 |
| 3 | Homebuilt | 4-7 |
| 4 | General Aviation | 5-9 |
| 5 | Jet trainer | 4-8 |
| 6 | Low subsonic transport | 6-10 |
| 7 | High subsonic transport | 10-16 |
| 8 | Supersonic fighter | 3-5 |
| 9 | Tactical missile | 0.3-1 |
| 10 | Hypersonic aircraft | 1-3 |

*Table 5.8. Typical values of wing aspect ratio*

As noted, aspect ratio has several influences over the aircraft features. For some design requirements, a low aspect ratio wing is favorable, while for other design requirements, a high aspect ratio wing is desirable. The exact value of the AR will be determined through a thorough investigation and lots of calculation over aircraft performance, stability, control, manufacturability, and cost.

A systems engineering technique (Ref. 5) by using a weighted parametric table must be employed to determine the exact value of the aspect ratio. Table 5.8 illustrates the typical values of aspect ratio for different aircraft type. Table 5.9 illustrates the aspect ratio for several aircraft. As noted, the aspect ratio ranges from 2.2 for fighter aircraft Eurofighter 2000 to 32.9 for high altitude long endurance (HALE) aircraft Socata.

| No | Aircraft | Type | Engine | $V_{max}$ (knot) | S (m²) | AR | λ |
|----|----------|------|--------|------------------|--------|-----|-----|
| 1 | Cessna 172 | GA | Piston | 121 | 16.2 | 7.52 | 0.67 |
| 2 | Air Tractor AT-402B | Agricultural | Turboprop | 174 | 27.3 | 8.9 | 1 |
| 3 | Piper Comanche | GA | Piston | 170 | 16.5 | 7.3 | 0.46 |
| 4 | McDonnell DC-9 | Transport | Turbofan | Mach 0.84 | 86.8 | 8.56 | 0.25 |
| 5 | Lockheed L-1011 | Transport | Turbofan | Mach 0.86 | 321 | 7.16 | 0.29 |
| 6 | Boeing 747-400 | Transport | Turbofan | Mach 0.92 | 525 | 6.96 | 0.3 |
| 7 | Tucano | Trainer | Turboprop | Mach 0.4 | 19.2 | 6.4 | 0.465 |
| 8 | Airbus 310 | Transport | Turbofan | Mach 0.9 | 219 | 8.8 | 0.26 |
| 9 | Jetstream 41 | Regional Airliner | Turboprop | 295 | 32.59 | 10.3 | 0.365 |
| 10 | Lockheed F-16 Falcon | Fighter | Turbofan | > Mach 2 | 27.87 | 3.2 | 0.3 |
| 11 | SAAB 39 Gripen | Fighter | Turbofan | > Mach 2 | 27 | 2.6 | 0.25 |
| 12 | Grumman B-2 Spirit | Bomber | Turbofan | - | 465.5 | 5.92 | 0.24 |
| 13 | Schweizer SA 2-38A | Surveillance | Piston | 157 | 21 | 18.2 | 0.4 |
| 14 | Grob G 850 Strato 2C | Surveillance | Piston | 280 | 145 | 22 | 0.25 |
| 15 | Stemme S10 | Motor glider | Piston | 97 | 18.7 | 28.2 | 0.26 |
| 16 | Socata HALE | Surveillance | Turboprop | - | 70 | 32.9 | 0.6 |
| 17 | Voyager | Circle the globe | Piston | 106 | 30.1 | 38 | 0.25 |
| 18 | Eurofighter 2000 | Fighter | Turbofan | Mach 2 | 50 | 2.2 | 0.19 |
| 19 | Dassault Mirage 2000 | Fighter | Turbofan | Mach 2.2 | 41 | 2 | 0.08 |

*Table 5.9. Aspect ratio and taper ratio for several aircraft*

## 5.7. Taper Ratio

Taper ratio (λ) is defined as the ratio between the tip chord ($C_t$) to the root chord ($C_r$)[11]. This definition is applied to the wing, as well as the horizontal tail, and the vertical tail. Root chord and tip chord are illustrated in figure 5.31.

$$\lambda = \frac{C_t}{C_r} \tag{5.24}$$

The geometric result of taper is a smaller tip chord. In general, the taper ratio varies between zero and one.

$$0 \le \lambda \le 1$$

where three major planform geometries relating to taper ratio are rectangular, trapezoidal and delta shape (see Figure 5.29).

In general, a rectangular wing planform is aerodynamically inefficient, while it has a few advantages, such as performance, cost and ease of manufacture. A wing with a rectangular planform has a larger downwash angle at the tip than at the root. Therefore, the effective angle of attack at the tip is reduced compared with that at the root. Thus, the wing tip will tend to stall

---

[11] In some older textbooks, taper ratio was defined as the ratio between root chord and the tip chord.

later than the root. The spanwise lift distribution is far from elliptical; where it is highly desirable to minimize the induced drag. Hence, one of the reasons to taper the planform is to reduce the induced drag.



a.   Rectangle (λ =1)



b.   Trapezoid  0 < λ < 1 (straight tapered)



c.   Triangle (delta)  λ = 0
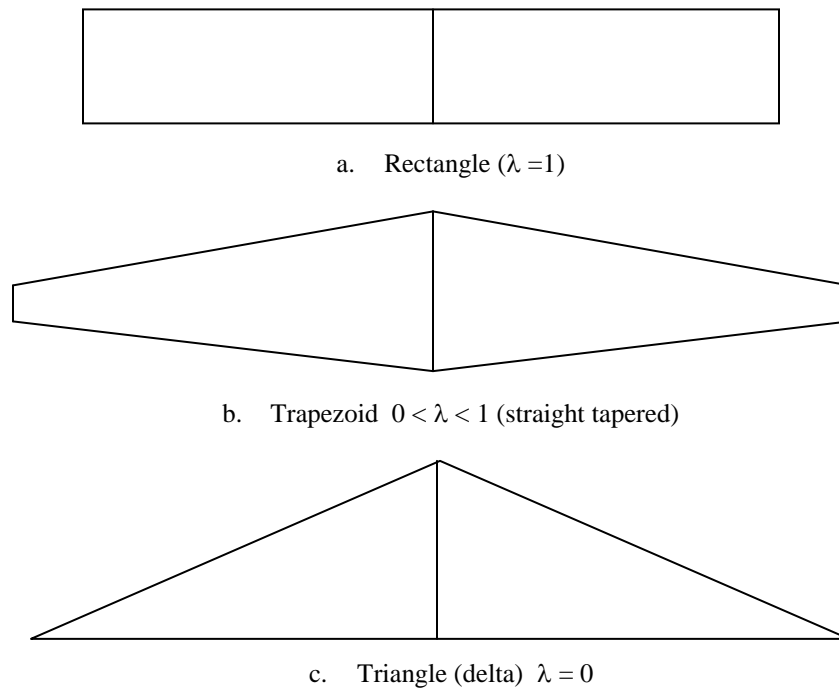
*Figure 5.29. Wings with various taper ratio*

In addition, since the tip chord is smaller than root chord, the tip Reynolds number will be lower, as well as a lower tip induced downwash angle. Both effects will lower the angle of attack at which stall occurs. This will result in the tip may stall before the root. This is undesirable from the viewpoint of lateral stability and lateral control. On the other hand, a rectangular wing planform is structurally inefficient, since there is a lot of area outboard, which supports very little lift. Wing taper will help resolve this problem as well. The effect of wing taper can be summarized as follows:

1.   The wing taper will change the wing **lift distribution**. This is assumed as an advantage of the taper, since it is a technical tool to improve the lift distribution. One of the wing design objective is to generate the lift such that the spanwise lift distribution be elliptical. The significance of elliptical lift distribution will be examined in the next section. Based on this item, the exact value for taper ratio will be determined by lift distribution requirement.

2.   The wing taper will increase the **cost** of the wing manufacture, since the wing ribs will have different shapes. Unlike a rectangular planform that all ribs are similar; each rib will have different size. If the cost is of major issue (such as for homebuilt aircraft), do not taper the wing.

3.   The taper will reduce the wing **weight**, since the center of gravity of each wing section (left and right) will move toward fuselage center line. This results in a lower bending

moment at the wing root. This is an advantage of the taper. Thus, to reduce the weight of the wing, more taper (toward 0) is desired.

4. Due to item 3, the wing mass moment of inertia about x-axis (longitudinal axis) will be decreased. Consequently, this will improve the aircraft **lateral control**. In this regard, the best taper is to have a delta wing ($\lambda = 0$).

5. The taper will influence the aircraft static **lateral stability** ($C_{l\beta}$), since the taper usually generates a sweep angle (either on the leading edge or on quarter chord line). The effect of the weep angle on the aircraft stability will be discussed in section 5.8.

As noted, taper ratio has mixed influences over the aircraft features. The aspect ratio of a conventional aircraft is a compromise between conflicting aerodynamic, structural, performance, stability, cost, and manufacturability requirements. For some design requirements (e.g. cost, manufacturability), no taper ratio wing is favorable; while for other design requirements (such as stability, performance, and safety), a tapered wing is desirable. The first estimate of the taper ratio will be determined by lift distribution calculations, as introduced in the next section. The exact value of the taper ratio will be finalized through a thorough investigation and lots of calculations over aircraft performance, stability, control, manufacturability, and cost. A systems engineering technique (Ref. 5) by using a weighted parametric table must be employed to determine the exact value of the taper ratio. Table 5.9 illustrates the taper ratio for several aircraft. The typical effect of taper ratio on the lift distribution is sketched in figure 5.30.
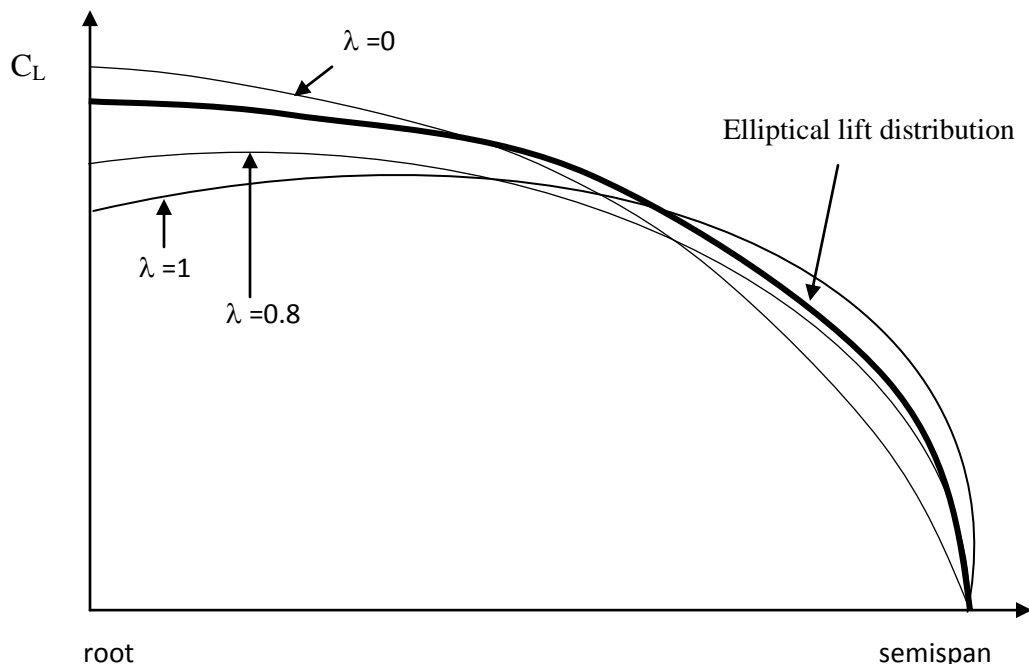


*Figure 5.30. The typical effect of taper ratio on the lift distribution*

In the normal flight range, the resultant aerodynamic forces acting on any lifting surface (e.g. lift, tail) can be represented as a lift and drag acting at the Aerodynamic Center (ac), together with a pitching moment which is independent of angle of attack. Methods for determining planform aerodynamic center locations may be found in most aerodynamic textbooks. Until

compressibility effects begin to play a role, it is experienced that the planform aerodynamic center ranges from 25 percent to about 30 percent of Mean Aerodynamic Chord (MAC or $\overline{C}$). In the transonic and supersonic speed range, the ac tends to move aft, such that at transonic speeds, the ac moves close to the 50 percent chord point on the MAC. The aerodynamic center lies in the plane of symmetry of the wing. However, in determining MAC, it is convenient to work with the half wing. For a general planform, the location of length of the MAC can be determined using the following integral:

$$\overline{C} = \frac{2}{S} \int_0^{b/2} c^2(y)dy \tag{5.25}$$

where c is the local chord and y is the aircraft lateral axis. For a constant taper and sweep angle (trapezoidal) planform, (see the geometry of figure 5.31), Mean Aerodynamic Chord is determined (Ref. 15) as follows:

$$\overline{C} = \frac{2}{3} C_r \left( \frac{1 + \lambda + \lambda^2}{1 + \lambda} \right) \tag{5.26}$$
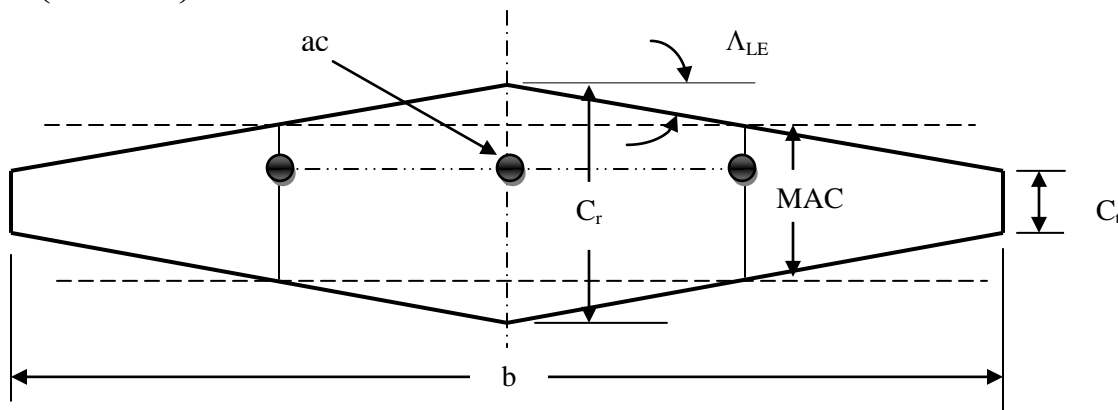


*Figure 5.31. Mean Aerodynamic Chord and Aerodynamic Center in a straight wing*

Table 5.9 illustrates the aspect ratio for several jet and prop-driven aircraft.

## 5.8. The Significance of Lift and Load Distributions

The distribution of wing non-dimensional lift (i.e. lift coefficient; $C_L$) per unit span along the wing is referred to as *lift distribution*. Each unit area of the wing along the span is producing a specific amount of lift. The total lift is equal to the summation of these individual lifts. The lift distribution goes to zero at the tips, because there is a pressure equalization from the bottom to the top of the wing precisely at y = -b/2 and +b/2. Hence no lift is generated at these two points. In addition, the variation of "lift coefficient times sectional chord ($C \cdot C_L$)" along span is referred to as the "*load distribution*". Both lift distribution and load distribution are of great importance in the wing design process. The major application of lift distribution is in aerodynamic calculation, while the primary application of the load distribution is in wing structural design as well as controllability analysis.

In the past (1930s), it was thought that for an elliptic lift distribution, the chord must vary elliptically along the span. The direct result of such logic was that the wing planform must be elliptical. For this reason, several aircraft wing planforms such as *Supermarine Spitfire*, a famous British World War II fighter were made elliptic. But, today, we know that there are various parameters that make the lift distribution elliptic, thus, there is no need for the wing planform to be planform.

The type of both lift distribution and load distribution are very important in wing design; and will influence the aircraft performance, airworthiness, stability, control, and cost. Ideally both lift distribution and load distribution are preferred to be elliptical. For the above mentioned reasons, the elliptical lift distribution and the elliptical load distribution are ideal and are the design objectives in the wing design process. An elliptical lift distribution is sketched in figure 5.32, where a front view of the wing is illustrated. The horizontal axis in figure 5.32 is y/s where y is the location is y-axis, and s denotes the semispan (s = b/2). In this figure, no high lift device (e.g. flap) is deflected and the effect of the fuselage is ignored. The elliptical lift distribution and elliptical load distribution have the following desirable properties:

1. If the wing tends to stall ($C_{Lmax}$), the wing root is stalled before the wing tip ($C_{Lroot} = C_{Lmax}$ while $C_{Ltip} < C_{Lmax}$). In a conventional aircraft, the flaps are located inboard, while the ailerons are installed outboard of the wing. In such a situation, ailerons are active, since the flow over the wing outboard section is healthy. This is of greater importance for spin recovery (which often happens after stall); since the aileron (in addition to rudder) application are very critical to stop the autorotation. Thus, the elliptical lift distribution provision guarantees the flight safety in the event of stall (see figure 5.33).
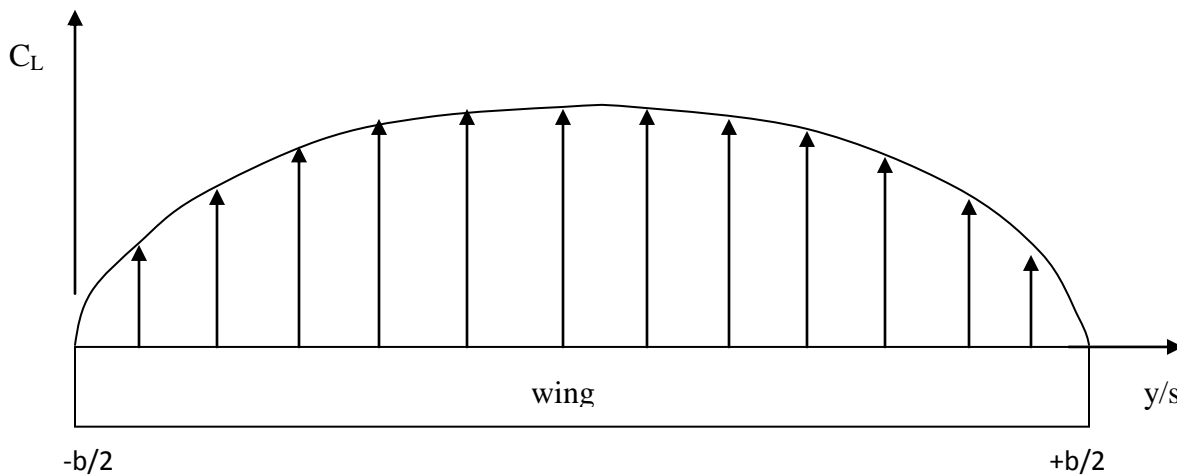


*Figure 5.32. Elliptical lift distribution over the wing*

2. The bending moment at the wing root is a function of load distribution. If the load distribution is concentrated near to the root, the bending moment is considerably less that when it is concentrated near the tip. The center of an elliptical load distribution is closer to the wing root, thus it leads to a lower bending moment, which results in a less bending stress and a less stress concentration at wing root (see figure 5.34). This

means a lighter wing spar and lighter wing structure that is always one of the design requirements. The load distribution is a function of the lift distribution.

3. The center of gravity of each wing section (left or right) for an elliptical load distribution is closer to the fuselage center line. This means a lower wing mass moment of inertia about x-axis which is an advantage in the lateral control. Basically, an aircraft rolls faster when the aircraft mass moment of inertia is smaller.

4. The downwash is constant over the span for an elliptical lift distribution (Ref. 3). This will influence the horizontal tail effective angle of attack.

5. For an elliptical lift distribution, the induced angle of attack is also constant along the span.

6. The variation of lift over the span for an elliptical lift distribution is steady (gradually increasing from tip (zero) to the root (maximum)). This will simplify the wing spar(s) design.



a. Non-elliptical (tip stalls before the root)    b. Elliptical (root stalls before the tip)
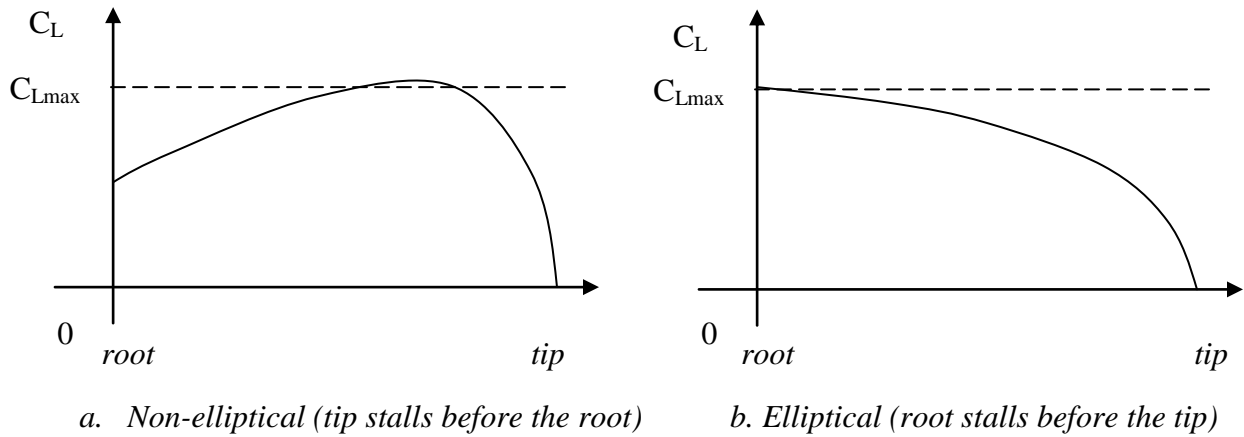
*Figure 5.33. Lift distribution over the half wing*



a. Non-elliptical (load is farther from root)    b. Elliptical (load is closer to root)
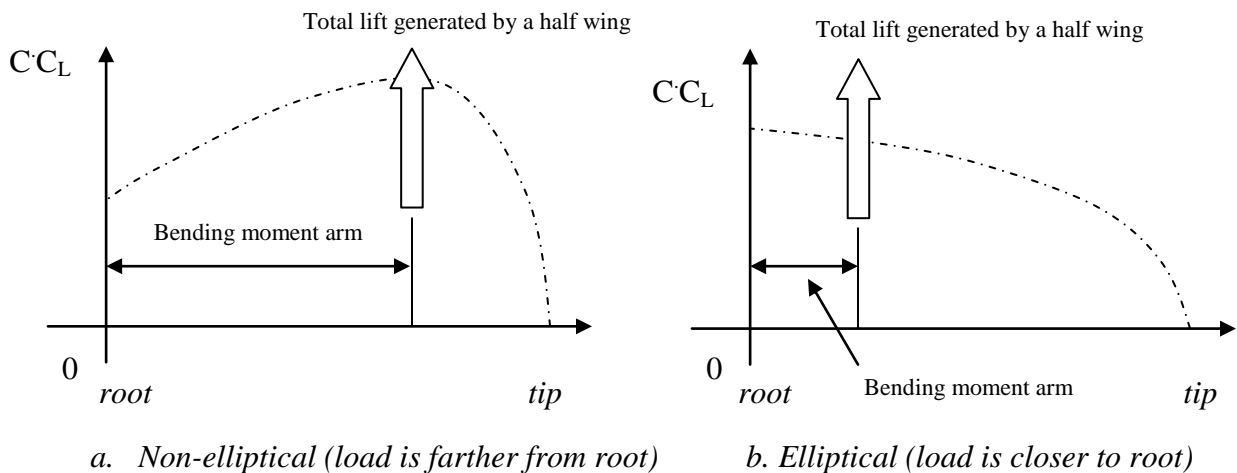
*Figure 5.34. Load distribution over a half wing*

The reader may have noticed that if the contribution of the fuselage is added to the wing lift distribution, the distribution may not be elliptical; due to negligible fuselage lift contribution.

This is true, and more realistic, since in a conventional aircraft, the wing is attached to the fuselage. What we examined here in this section is an ideal case, and the reader may modify the lift distribution by considering the fuselage contribution. Figure 5.35 depicts the fuselage contribution to a low wing configuration. Similar case may be made for the effect of flap of lift distribution when deflected. Figure 5.36 illustrates the flap contribution to the wing lift distribution. In principle, the goal in the wing design is to obtain an elliptical wing distribution without considering the contributions of fuselage, flap, or other components.
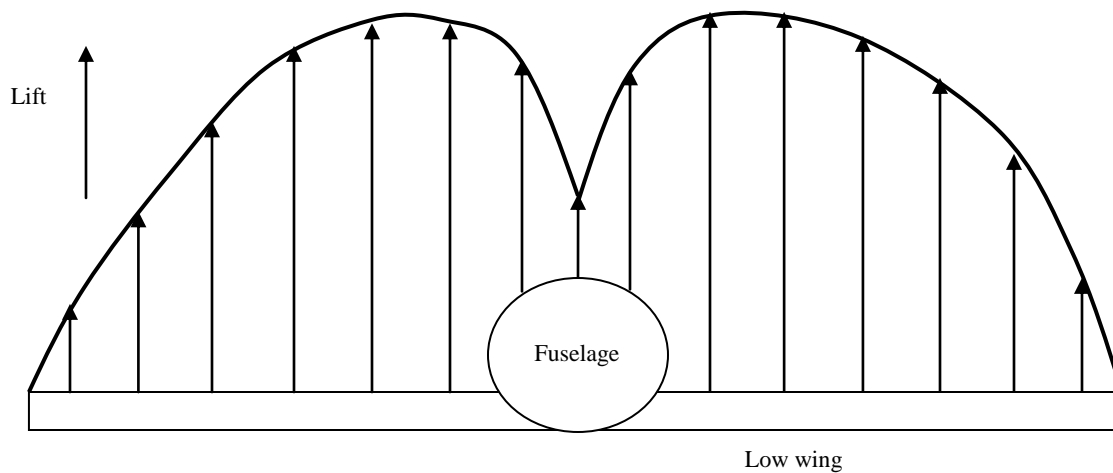


*Figure 5.35. The fuselage contribution to the lift distribution of a low wing configuration*
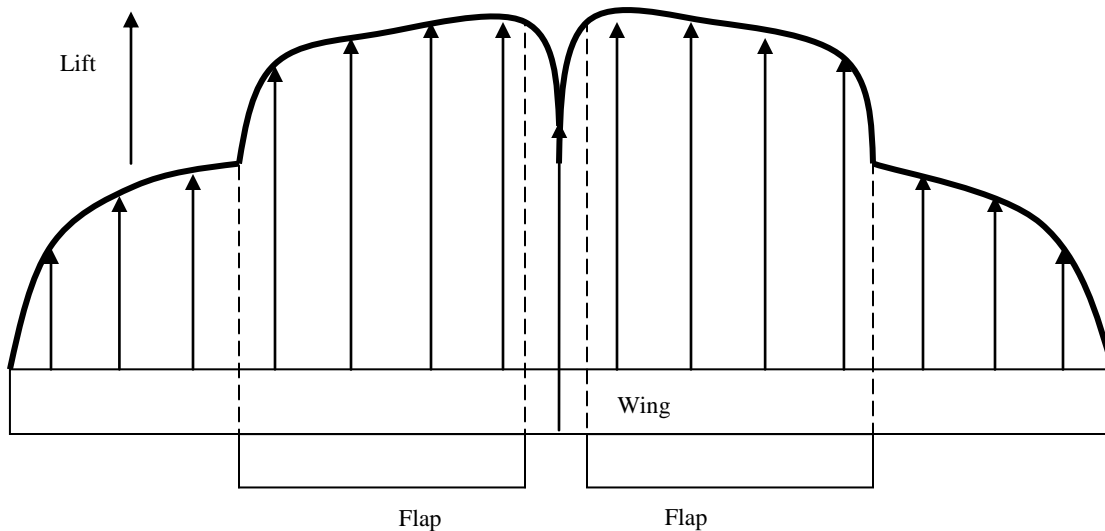


*Figure 5.36. The flap contribution to the lift distribution*

In Section 5.15, a mathematical technique will be introduced to determine the lift and load distribution along the wing.

## 5.9. Sweep Angle

Consider the top view of an aircraft. The angle between a constant percentage chord line along the semispan of the wing and the lateral axis perpendicular to the aircraft centerline (y-axis) is called leading edge sweep ($\Lambda_{LE}$). The angle between the wing leading edge and the y-axis of the aircraft is called leading edge sweep ($\Lambda_{LE}$). Similarly, the angle between the wing trailing edge and the longitudinal axis (y-axis) of the aircraft is called trailing edge sweep ($\Lambda_{TE}$). In the same fashion, the angle between the wing quarter chord line and the y-axis of the aircraft is called quarter chord sweep ($\Lambda_{C/4}$). And finally, the angle between the wing 50 percent chord line and the y-axis of the aircraft is 50 percent chord sweep ($\Lambda_{C/2}$).
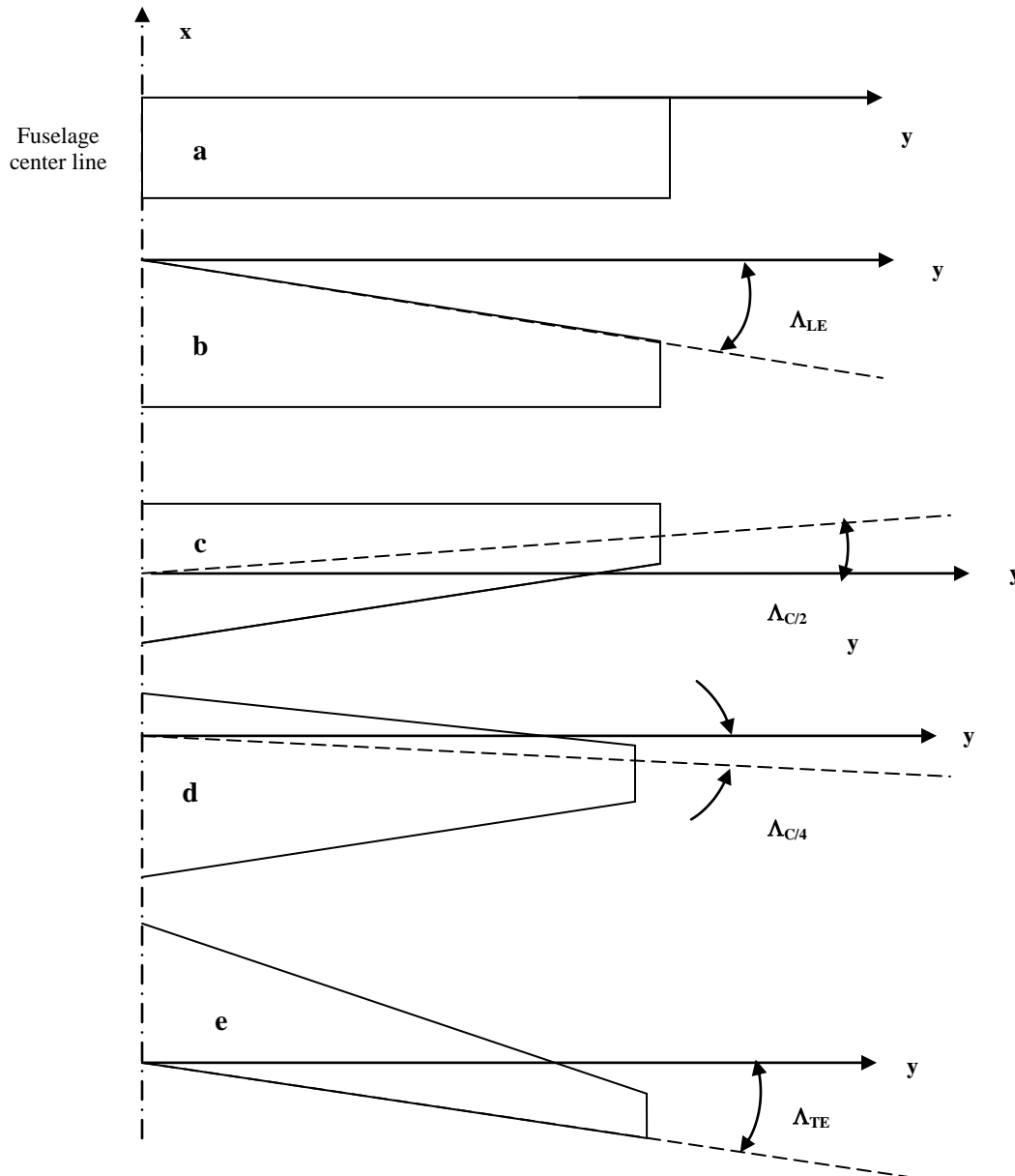


*Figure 5.37. Five wings with different sweep angles*

If the angle is greater than zero (i.e. wing to inclined toward tail), it is called aft sweep or simply sweep; otherwise it is referred to as forward sweep. Figure 5.37 shows five wings with various sweep angles. Figure 5.37a illustrates a wing without sweep, while figures 5.37b through 5.37d show four swept wing. The leading edge sweep is depicted in the wing of figure 5.37b, while trailing edge sweep is shown in the wing of figure 5.37e. In addition, the quarter chord sweep is illustrated in the wing of figure 5.37d, and the 50 percent chord sweep is illustrated in the wing of figure 5.37c. Most high-speed airplanes designed since the middle 1940s – such as North American F-86 Saber - have swept wings. On sweptback tapered wing, typical of almost all high speed aircraft, the leading edge has more sweep than the trailing edge.

With reference to the definition of sweep angle, a particular wing may have aft leading edge sweep, while it has forward trailing edge sweep. Among four types of sweep angles, the quarter chord sweep and leading edge sweep are the most important ones. The subsonic lift due angle of attack normally acts at the quarter chord. In addition, the crest is usually close to the quarter chord. The discussion in this section regarding the characteristics (advantages and disadvantages) of sweep angle is mostly about leading edge sweep angle, unless otherwise stated.
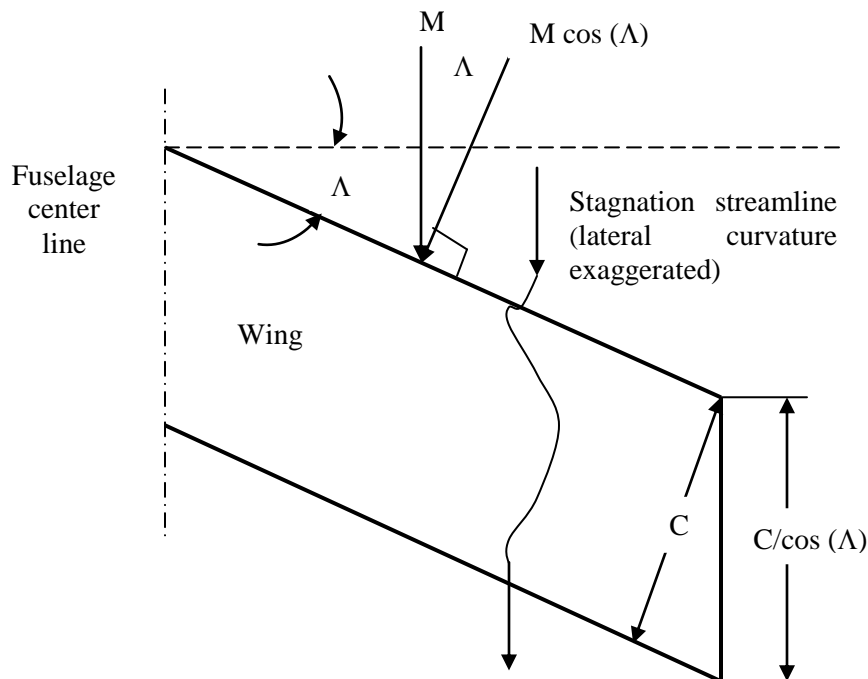


*Figure 5.38. The effective of the sweep angle of the normal Mach number*

Basically, a wing is being swept for the following four design goals:

1. Improving the wing aerodynamic features (lift, drag, pitching moment) at transonic, supersonic and hypersonic speeds by delaying the compressibility effects.
2. Adjusting the aircraft center of gravity.
3. Improving longitudinal and directional stability
4. Increasing pilot view (especially for fighter pilots)

These items will be described in more details in this section. For more information, the reader needs to refer to technical textbooks that are listed at the end of this chapter. The practical influence of the sweep angle on various flight features are as follows:

1. The sweep angle, in practice, tends to increase the distance between leading edge and trailing edge. Accordingly, the pressure distribution will vary.
2. The effective chord length of a swept wing is longer (see Figure 5.38) by a factor of 1/cos ($\Lambda$). This makes the effective thickness-to-chord ratio thinner, since the thickness remains constant.
3. Item 2 can be also translated into the reduction of Mach number ($M_n$) normal to the wing leading edge to M cos ($\Lambda$). Hence, by sweeping the wing, the flow behaves as if the airfoil section is thinner, with a consequent increase in the critical Mach number of the wing. For this reason, a classic design feature used to increase $M_{cr}$ is to sweep the wing (Ref. 11).
4. The effect of the swept wing is to curve the streamline flow over the wing as shown in figure 5.38. The curvature is due to the deceleration and acceleration of flow in the plane perpendicular to the quarter chord line. Near the wing tip the flow around the tip from the lower surface to the upper surface obviously alters the effect of sweep. The effect is to unsweep the spanwise constant-pressure lines; isobar. To compensate, the wing tip may be given additional structural sweep.
5. The wing aerodynamic center (ac) is moved aft by the wing aft sweep at about few percent. The aft movement of the ac with increase in sweptback angle occurs because the effect of the downwash pattern associated with a swept wing is to raise the lift coefficient on the outer wing panel relative to the inboard lift coefficient. Since sweep movers the outer panel aft relative to the inner portion of the wing, the effect on the center of lift is an aft ward movement. The effect of wing sweep on ac position is shown in figure 5.39 for aspect ratios of 7 and 10 and for taper ratios of 0.25 and 0.5.
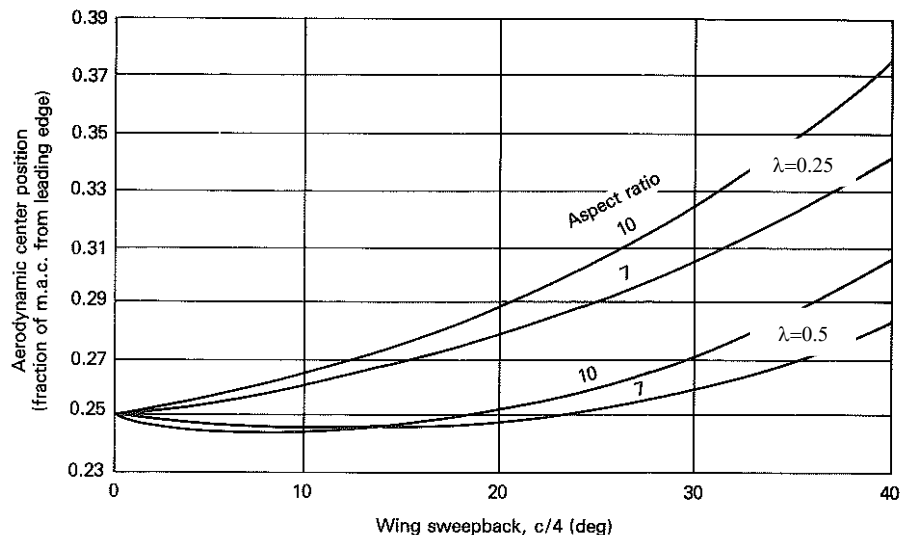


*Figure 5.39. Effect of wing sweepback on ac position for several combinations of AR and $\lambda$ (Ref.6)*

6. The effective dynamic pressure is reduced, although not by as much as in cruise.
7. The sweep angle tends to change the lift distribution as sketched in figure 5.40. The reason becomes clear by looking at the explanations in item 5. As the sweep angle is increased, the Oswald efficiency factor (e) will decrease (Equation 5.25).
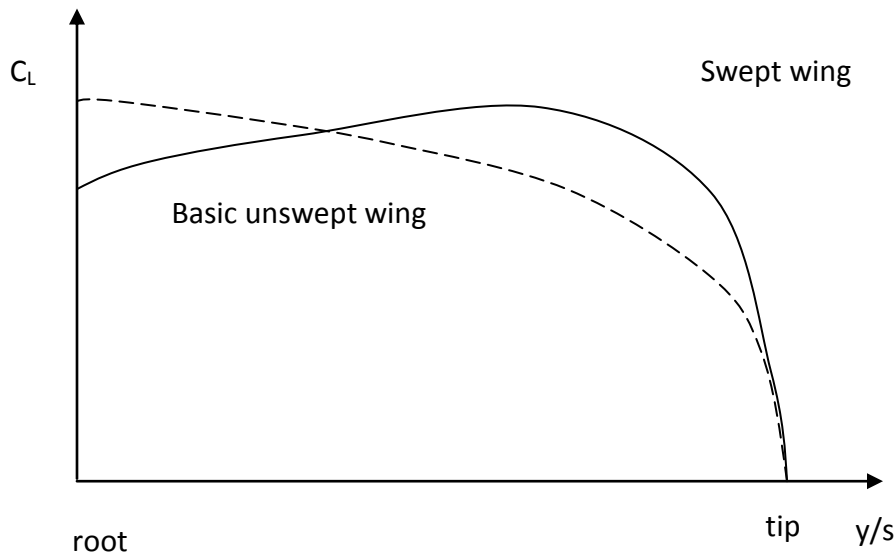


*Figure 5.40. Typical effect of sweep angle on lift distribution*

The Oswald span efficiency for a straight wing and swept wing are given respectively by equation 5.27a and 5.27b (Ref. 14).

$$e = 1.78(1 - 0.045AR^{0.68}) - 0.64 \qquad (5.27a)$$

$$e = 4.61(1 - 0.045AR^{0.68})[\cos(\Lambda_{LE})]^{0.15} - 3.1 \qquad (5.27b)$$

Equation 5.27a is for a straight wing and Equation 5.27b is for a swept wing where sweep angle is more than 30 degrees. When the Oswald span efficiency is equal to 1, it indicates that the lift distribution is elliptical, otherwise it is non-elliptic.

8. The wing maximum lift coefficient can actually increase with increasing sweep angle. However, the maximum useful lift coefficient actually decreases with increasing sweep angle, due to loss of control in pitch up situation. Whether or not pitch up occurs depends not only on the combination of sweep angle and aspect ratio, but also an airfoil type, twist angle, and taper ratio. Thus, the sweep angle tends to increase stall speed ($V_s$).
The maximum lift coefficient of the basic wing without high lift device is governed by the following semi-empirical relationship (Ref. 6):

$$C_{L\max_{(\Lambda \neq 0)}} = C_{l\max}[0.86 - 0.002(\Lambda)] \qquad (5.28)$$

where sweep angle ($\Lambda$) is in degrees and $C_{lmax}$ denotes the maximum lift coefficient for the outer panel airfoil section.

9. Wing sweep tends to reduce the wing lift curve slope ($C_{L\alpha}$). A modified equation based on Prandtl-Glauert approximation is introduced by Ref. 6 as follows:

$$C_{L_\alpha} = \frac{2\pi AR}{2 + \sqrt{AR^2\left(1 + \tan^2\Lambda - M^2\right) + 4}}$$ (5.29)

10. The aircraft pitching moment will be increased, provided the aircraft cg is forward of aircraft ac. The reason is that wing aerodynamic center is moving aft with increase in sweep angle.

11. An aft swept wing tends to have tip stall because of the tendency toward outboard, spanwise flow. This causes the boundary layer to thicken as it approaches the tips. For the similar reason, a swept forward wing would tend toward root stall. This tends to have an influence opposite to that of wing twist.

12. On most aft swept wing aircraft, the wing tips are located behind the aircraft center of gravity. Therefore, any loss of lift at the wing tips causes the wing center of pressure to move forward. This in turn will cause the aircraft nose to pitch up. This pitch up tendency can cause the aircraft angle of attack to increase even further. This may result in a loss of aircraft longitudinal control. For the similar reason, a forward swept wing aircraft would exhibit a pitch down tendency in a similar situation.

13. Tip stall on a swept wing is very serious. If the outboard section of a swept wing stalls, the lift loss is behind the wing aerodynamic center. The inboard portion of the wing ahead of the aerodynamic center maintains its lift and produces a strong pitch-up moment, tending to throw the aircraft deeper into the stall. Combined with the effect of tip stall on the pitching moment produced by the tail, this effect is very dangerous and must be avoided by options such as wing twist.

14. A swept wing produce a negative rolling moment because of a difference in velocity components normal to the leading edge between the left and right wing sections (Ref. 13). The rolling moment due to aft sweep is proportional to the sine of twice the leading edge sweep angle.

$$C_{l_\beta} \propto \sin(2\Lambda_{LE})$$ (5.30)

This makes the dihedral effect ($C_{l_\beta}$) more negative and it means that a swept wing has an inherent dihedral effect. Hence, a swept wing may not need a dihedral or anhedral to satisfy lateral-directional stability requirements. Thus, the sweep angle tends to reinforce the dihedral effect. It is interesting to note that making the dihedral effect ($C_{l_\beta}$) more negative will make an aircraft more spirally stable. At the same time, the dutch-roll damping ratio tends to decrease. This presents a design conflict (Ref. 13) which must be resolved through some compromise.

15. In supersonic flight, the sweep angle tends to reduce the shock wave drag. The drag generated by the oblique shock wave is referred to as wave drag, which is inherently related to the loss of total pressure and increase of entropy across the oblique shock waves created by the wing. For this purpose, the sweep angle must be greater (see figure 5.41) than Mach angle, $\mu$ (Ref. 11):

$$\mu = \sin^{-1}\left(\frac{1}{M}\right) \tag{5.31}$$

$$\Lambda = 1.2 \times (90 - \mu) \tag{5.32}$$

where M is the aircraft cruising Mach number. A 20 percent higher sweep angle will guarantee the low wave drag at supersonic speeds.

16. In a hypersonic speed (e.g. Space Shuttle), if the oblique shock wave is very close to the wing leading edge; due to a low sweep angle; it generates very high temperature due to aerodynamic heating (about 3000 $^o$F) such that the wing leading edge surface may be melted. Thus, the sweep angle must be such that wing leading edge surface survive very high temperature. This ensures that the wing is located inside Mach cone.
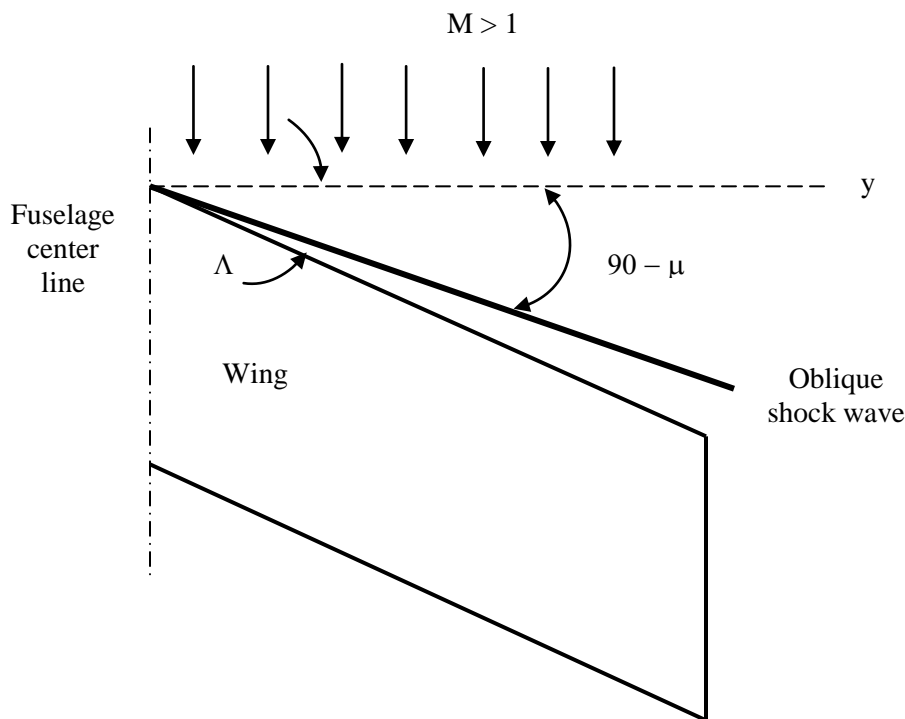


*Figure 5.41. The sweep angle and Mach angle in supersonic flight*

17. With the application of the sweep angle, the wing effective span ($b_{eff}$) with be shorter than original theoretical span. This results in a lower wing mass moment of inertia about x-axis, which increases the lateral controllability of the aircraft. Hence, the higher the sweep angle, allows for better maneuverability.

**Sweep angle selection guideline:** As noted, sweep angle has several advantages and disadvantages such that can only be decided through a compromise. The following guidelines help the reader to select the initial value and to update the value throughout the design iterative process.

a. **Low subsonic aircraft:** If the aircraft maximum speed is less than Mach 0.3 (the borderline to include the compressibility effect), no sweep angle is recommended for the wing, since its advantages negates all the improvement it produced. For instance, by using 5 degrees of sweep angle, you may have reduced the aircraft drag by say 2 percent. But you have increased the cost by say 15 percent as well as adding complexity to the wing manufacturing. Thus a straight wing is recommended.

b. **High subsonic and supersonic aircraft:** The initial value can be determined through equation 5.32 as a function of aircraft cruising speed. However, the final value will be finalized after a series of calculations and analysis on aerodynamics, performance, stability, control, structure, as well as cost, and manufacturability. Remember, if the wing is tapered, it must have a sweep angle anyway.

Table 5.10 shows sweep angles of several aircraft along with their maximum speeds. As noted, as the maximum speed is increased, so do the sweep angel.

| No | Aircraft | Type | First flight | Max speed (Mach, knot) | $\Lambda_{LE}$ (deg) |
|----|----------|------|-------------|------------------------|----------------------|
| 1 | Cessna 172 | Single piston engine GA | 1955 | 121 knot | 0 |
| 2 | Tucano | Turboprop trainer | 1983 | 247 knot | 4 |
| 3 | AIRTECH | Turboprop Transport | 1981 | 228 knot | 3º 51' 36'' |
| 4 | ATR 42 | Turboprop Transport | 1984 | 265 knot | 3º 6' |
| 5 | Jetstream 31 | Turboprop business | 1967 | Mach 0.4 | 5º 34' |
| 6 | Beech Starship | Turboprop business | 1991 | Mach 0.78 | 20 |
| 7 | DC-9 series 10 | Jet Passenger | 1965 | Mach 0.84 | 24 |
| 8 | Falcon 900B | Business Jet | 1986 | Mach 0.87 | 24º 30' |
| 9 | Gulfstream V | Business Jet | 1996 | Mach 0.9 | 27 |
| 10 | Boeing 777 | Jet Transport | 1994 | Mach 0.87 | 31.6 |
| 11 | B-2A Spirit | Strategic Bomber | 1989 | Mach 0.95 | 33 |
| 12 | MD-11 | Jet Transport | 2001 | Mach 0.945 | 35 |
| 13 | Boeing 747 | Jet Transport | 1969 | Mach 0.92 | 37º 30' |
| 14 | Airbus 340 | Jet Transport | 1991 | Mach 0.9 | 30 |
| 15 | F-16 | Fighter | 1974 | > Mach 2 | 40 |
| 16 | F/A-18 | Fighter | 1992 | > Mach 1.8 | 28 |
| 17 | Mig-31 | Fighter | 1991 | Mach 2.83 | 40 |
| 18 | Su-34 | Fighter | 1996 | Mach 2.35 | 42 |
| 19 | Eurofighter Typhoon | Fighter | 1986 | Mach 2 | 53 |
| 20 | Mirage 2000 | Fighter | 1975 | Mach 2.2 | 58 |
| 21 | Concorde | Supersonic Jet Transport | 1969 | Mach 2.2 | 75 inboard 32 outboard |
| 22 | Space Shuttle | Spacecraft (flies in air during return mission) | 1981 | Mach 21 | 81 inboard 44 outboard |

*Table 5.10. Sweep angles for several low and high speed aircraft*

The following practical comments; including a few drawbacks; will help the designer to make the right decision on the wing sweep angle:

1. **Variable sweep:**

If the aircraft needs to have different sweep angles at various flight conditions, an ideal option is to select the variable sweep wing. This is an ideal objective from few design aspects, but on the other hand, it generates design problems. The example is a fighter aircraft that spends the vast majority of its flight time at subsonic speeds, using its supersonic capability for short 'supersonic dashes", depending on its mission.

A variable-sweep wing is a wing that may be swept back and then returned to its original position during flight. It allows the wing's geometry be modified in flight. Typically, a swept wing is more suitable for high speeds (e.g. cruise), while an unswept wing is suitable for lower speeds (e.g. take off and landing), allowing the aircraft to carry more fuel and payload, as well as improving field performance. A variable-sweep wing allows a pilot to select the exact wing configuration for the intended speed. The variable-sweep wing is most useful for those aircraft that are expected to function at both low and high speed, thus it has been used primarily in fighters.

A number of successful designs; such as Bell X-5, Grumman F-14 Tomcat, General Dynamics F-111, Rockwell supersonic Bomber B-1B, Mig-23, and Sukhoi Su-27; were introduced from the 1940s through the 1970s. However, the recent advances in flight control technology and structural materials have allowed designers to closely tailor the aerodynamics and structure of aircraft, removing the need for variable geometry to achieve the required performance. Aerodynamically, the exact sweep angle will generate the lowest possible drag while produce the highest possible lift and control. The drawback is the loose structural integrity as well as the sweep angle control mechanism problem (manual or automatic). The last variable-sweep wing military aircraft to date was the Soviet Tupolev Tu-160 "Blackjack", which first flew in 1980.

2. **Wing-fuselage interference:**

It is at the wing root that the straight fuselage sides more seriously degrade the sweep effect by interfering with the curved flow of figure 3.36. Wing airfoils are often modified near the root to change the basic pressure distribution to compensate for the distortion to the swept wing flow. Since the fuselage effect is to increase the effective airfoil camber, the modification is to reduce the root airfoil camber and in some cases to use negative camber. The influence of the fuselage then changes the altered root airfoil pressure back to the desired positive camber pressure distribution existing farther out along the wing span (Ref. 6). This same swept wing root compensation can be achieved by adjusting the fuselage shape to match the natural swept wing streamlines. This imposes serious manufacturing burdens and passenger cabin arrangement problems. Thus the airfoil approach is more preferred for transport aircraft. Instead, the employment of large fillet or even fuselage shape variation is appropriate for fighter aircraft.

3. **Non-constant sweep:**

In some cases, one sweep angle cannot satisfy all design requirements. For instance, a very high sweep angle wing satisfies the high speed cruise requirements, however, at low subsonic speed, the aircraft is not satisfactorily controllable or laterally stable. One solution is to divide the wing

sections into inboard plane, and outboard plane; each having different sweep angles (see figure 5.42). The supersonic transport aircraft Concorde and Space Shuttle have such feature.
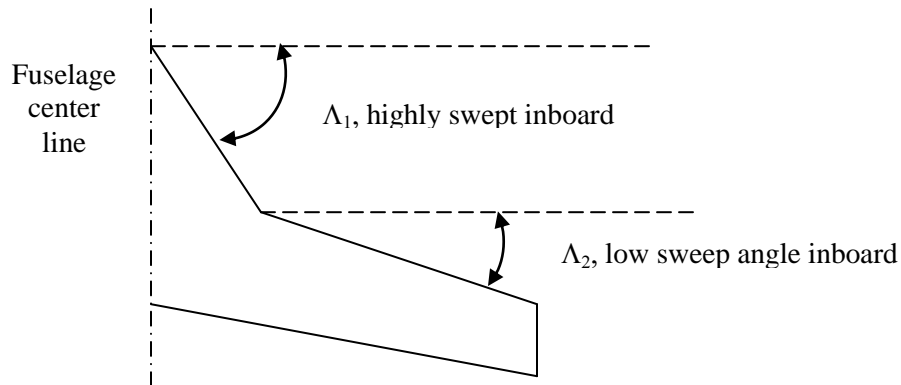


*Figure 5.42. Top view of a wing with two sweep angels*

### 4. Control surfaces:

The sweep angel will influence the performance of high lift device (such as flap) as well as control surfaces (such as ailerons). In practice, since both high lift device and control surface have to have sweep angles (with slightly different values); their lifting forces will be spoiled. Consequently, the high lift device's contribution to generate lift at low speed will be reduced. With the same logic, it can be shown that the aileron will also produce less lateral control. To compensate for these shortcomings, both control surface and high lift device must have slightly larger areas.

### 5. Spar

When the wing has a sweep angle, the wing spar can no longer be one piece, since two wing sections (left and right) have opposite sweep angles. This is assumed to be a disadvantage of sweep angle, since the wing structural integrity will be negatively influenced. This adds to the complexity of the wing manufacturing as well.

### 6. Effective span ($b_{eff}$) and Effective Aspect Ratio ($AR_{eff}$):

With the presence of the sweep angle, the wing span (b) will have slightly different meaning, so the new parameter of effective span ($b_{eff}$) is introduced. When the 50 percent chord line sweep angle is not zero, the wing span will be greater than wing effective span. Wing span in a straight wing is basically defined as the distance between two wing tips parallel to aircraft the lateral axis (y-axis). However, in a swept wing, wing span is defined as twice the distance between one wing tip to fuselage center line parallel to 50 percent sweep chord line. Thus, the effective wing span in a swept wing is defined as the distance between wing tips parallel to aircraft lateral axis (y-axis). Figure 5.43 depicts the difference between span and effective span. This indicates that wing sweep angle alters the wing span to effective span which is smaller.

$$AR_{eff} = \frac{b_{eff}^2}{S} \tag{5.33}$$

The technique to determine effective span is based on the laws of triangle. The application of the technique is illustrated in the examples 5.3 and 5.4. Figure 5.46 illustrates sweep angles of fighter F-16, Space Shuttle, and Cessna T-303 Crusader.
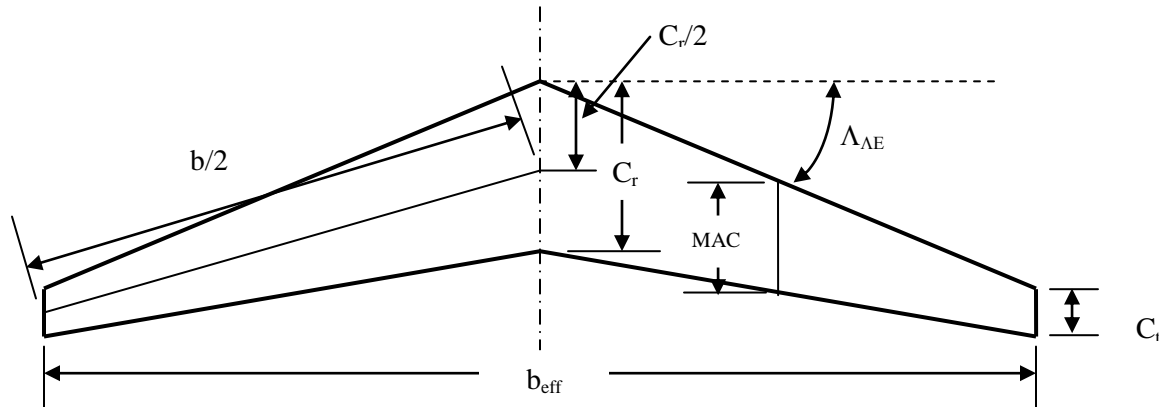


*Figure 5.43. Effective wing span in a swept wing*

## Example 5.3

An aircraft has a wing area of S = 20 m$^2$, aspect ratio AR = 8, and taper ratio of $\lambda$ = 0.6. It is required that the 50 percent chord line sweep angle be zero. Determine tip chord, root chord, mean aerodynamic chord, and span, as well as leading edge sweep, trailing edge sweep and quarter chord sweep angles.

**Solution:**

To determine the unknown variables, we first employ the following equations:

$$AR = \frac{b^2}{S} \Rightarrow b = \sqrt{S \cdot AR} = \sqrt{20 \times 8} \Rightarrow b = 12.65 \quad m \tag{5.19}$$

$$AR = \frac{b}{\overline{C}} \Rightarrow \overline{C} = \frac{b}{AR} = \frac{12.65}{8} \Rightarrow \overline{C} = 1.58 \quad m \tag{5.18}$$

$$\overline{C} = \frac{2}{3}C_r\left(\frac{1+\lambda+\lambda^2}{1+\lambda}\right) \Rightarrow 1.58 = \frac{2}{3}C_r\left(\frac{1+0.6+0.6^2}{1+0.6}\right) \Rightarrow C_r = 1.936 \quad m \tag{5.26}$$

$$\lambda = \frac{C_t}{C_r} \Rightarrow 0.6 = \frac{C_t}{1.935} \Rightarrow C_t = 1.161 \quad m \tag{5.24}$$

---

Since the 50 percent chord line sweep angle is zero ($\Lambda_{C/2} = 0$), the leading edge, trailing edge, and quarter chord sweep angel are determined using the triangle law in triangle ABC (see figure 5.44) as follows:
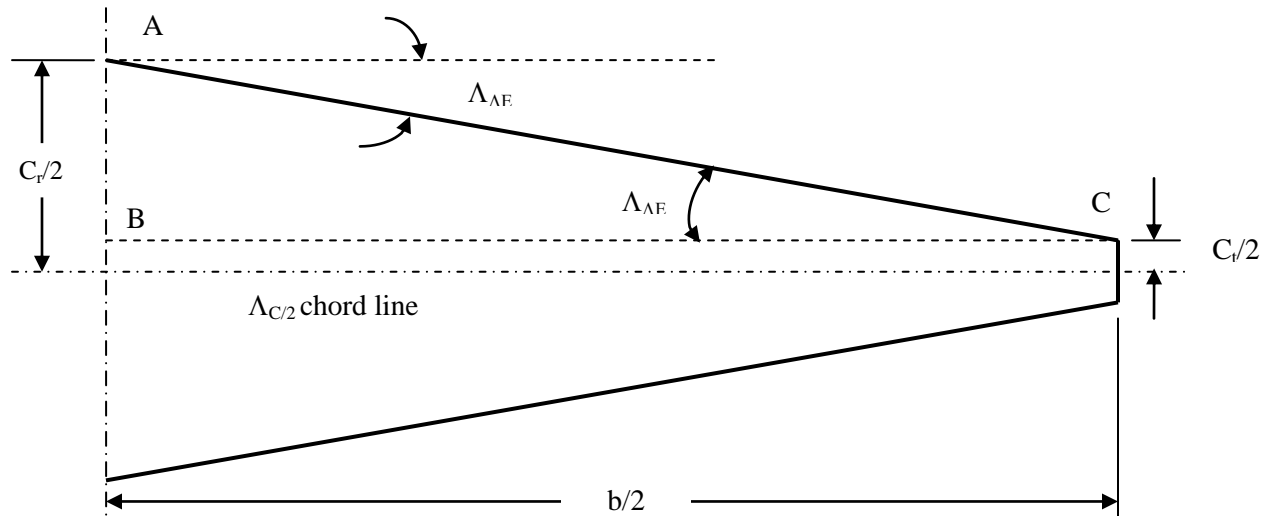


*Figure 5.44. The wing of Example 5.3($\lambda$ and angles are exaggerated)*

$$\tan(\Lambda_{LE}) = \frac{AB}{BC} \Rightarrow \Lambda_{LE} = \tan^{-1}\left(\frac{\dfrac{C_r}{2} - \dfrac{C_t}{2}}{b/2}\right) = \tan^{-1}\left(\frac{\dfrac{1.936 - 1.161}{2}}{12.65/2}\right) \Rightarrow \Lambda_{LE} = 3.5 \text{ deg (sweep back)}$$

The wing is straight, thus the trailing edge sweep angle would be:

$\Lambda_{TE} = -3.5$ deg (swept forward)

The quarter chord sweep angle is determined using tangent law in a similar triangle as follows:

$$\Lambda_{C/4} = \tan^{-1}\left(\frac{\dfrac{C_r - C_t}{4}}{b/2}\right) = \tan^{-1}\left(\frac{\dfrac{1.936 - 1.161}{4}}{12.65/2}\right) \Rightarrow \Lambda_{C/4} = 1.753 \text{ deg} \qquad \text{(sweep back)}$$

In it interesting to note that, although the wing is straight ($\Lambda_{C/2} = 0$), but the leading edge, trailing edge and quarter chord line all are swept.

## Example 5.4

An aircraft has a wing area of S = 20 m², aspect ratio AR = 8, and taper ratio of $\lambda$ = 0.6. It is required that the 50 percent chord line sweep angle be 30 degrees. Determine tip chord, root

chord, mean aerodynamic chord, span, and effective span, as well as leading edge sweep, trailing edge sweep and quarter chord sweep angles.

**Solution:**

To determine the unknown variables, we first employ the following equations:

$$AR = \frac{b^2}{S} \Rightarrow b = \sqrt{S \cdot AR} = \sqrt{20 \times 8} \Rightarrow b = 12.65 \quad m \tag{5.19}$$

$$AR = \frac{b}{\overline{C}} \Rightarrow \overline{C} = \frac{b}{AR} = \frac{12.65}{8} \Rightarrow \overline{C} = 1.58 \quad m \tag{5.18}$$

$$\overline{C} = \frac{2}{3} C_r \left( \frac{1 + \lambda + \lambda^2}{1 + \lambda} \right) \Rightarrow 1.58 = \frac{2}{3} C_r \left( \frac{1 + 0.6 + 0.6^2}{1 + 0.6} \right) \Rightarrow C_r = 1.936 \quad m \tag{5.26}$$

$$\lambda = \frac{C_t}{C_r} \Rightarrow 0.6 = \frac{C_t}{1.935} \Rightarrow C_t = 1.161 \quad m \tag{5.24}$$

Since the 50 percent chord line sweep angle is 30 degrees ($\Lambda_{C/2}$ = 30 deg), the leading edge, trailing edge, and quarter chord sweep angel are determined using the triangle law (see figure 5.45). But we first need to calculate a few parameters.

In the right triangle CIF that includes 50 percent chord sweep angle ($\Lambda_{C/2}$), we can write:

$$\sin(\Lambda_{C/2}) = \frac{FI}{b/2} \Rightarrow FI = \frac{12.65}{2} \sin(30) = 3.1625 \quad m$$

$$(CI)^2 + (FI)^2 = (CF)^2 \Rightarrow CI = \sqrt{(CF)^2 - (FI)^2} \Rightarrow \frac{b_{eff}}{2} = \sqrt{\left( \frac{12.65}{2} \right)^2 - 3.1625^2} \Rightarrow b_{eff} = 10.955 \quad m$$

Hence, the effective span is less than regular span. Consequently, the effective aspect ratio is reduced to:

$$AR_{eff} = \frac{b_{eff}^2}{S} = \frac{10.955^2}{20} \Rightarrow AR_{eff} = 6 \tag{5.33}$$

In is noted that the AR has been reduced from 8 to 6. The distance IH is:

$$IH = FI - \frac{C_t}{2} = 3.1625 - \frac{1.161}{2} = 2.582 \quad m$$

In the right triangle AKH that includes leading edge sweep angle ($\Lambda_{LE}$), we have:

$$\tan(\Lambda_{LE}) = \frac{KH}{AK} = \frac{KI + IH}{\dfrac{b_{eff}}{2}} = \frac{\dfrac{C_r}{2} + 2.582}{\dfrac{10.955}{2}} = \frac{\dfrac{1.936}{2} + 2.582}{\dfrac{10.955}{2}} = 0.648 \Rightarrow \Lambda_{LE} = 33 \ \text{deg (aft sweep)}$$
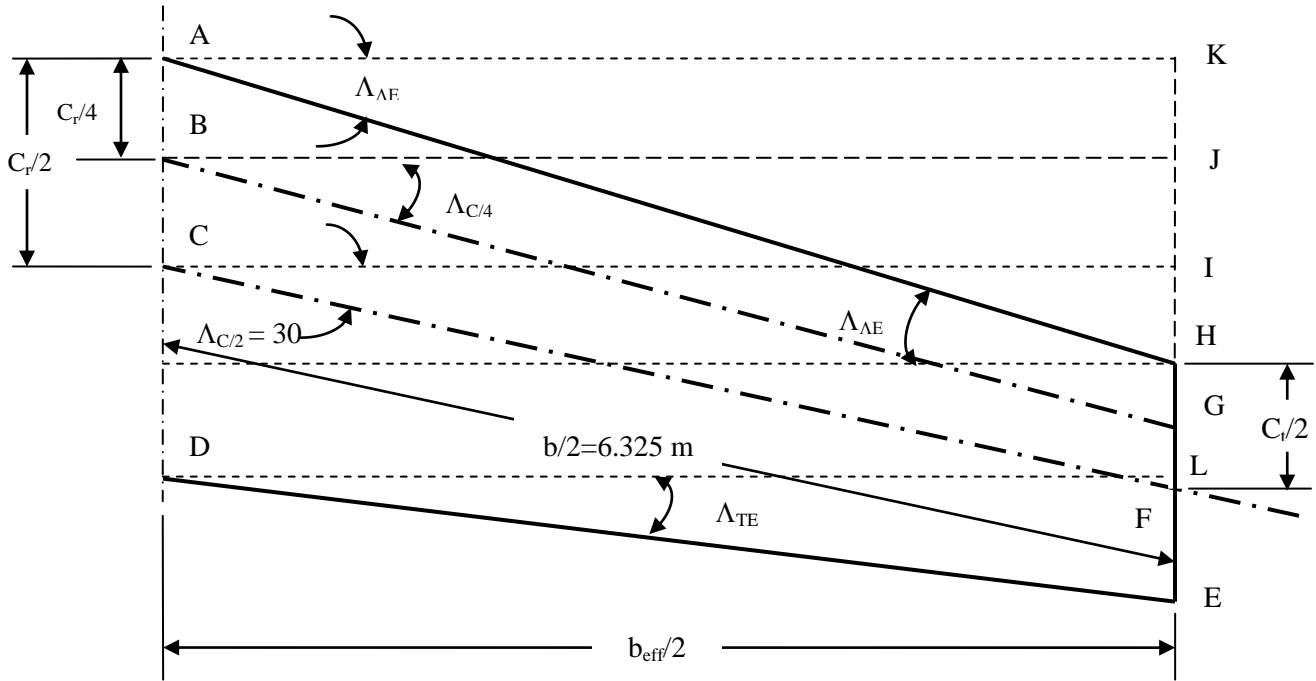


*Figure 5.45. The top view of the right wing of Example 5.4*

In the right triangle GJB that includes quarter chord sweep angle ($\Lambda_{C/4}$), we have:

$$\tan(\Lambda_{C/4}) = \frac{GJ}{BJ} = \frac{GH + JH}{\dfrac{b_{eff}}{2}} = \frac{\dfrac{C_t}{4} + KH - KJ}{\dfrac{b_{eff}}{2}} = \frac{\dfrac{C_t}{4} + (KI + IH) - KJ}{\dfrac{b_{eff}}{2}} = \frac{\dfrac{C_t}{4} + \left(\dfrac{C_r}{2} + 2.582\right) - \dfrac{C_r}{4}}{\dfrac{b_{eff}}{2}}$$

$$= \frac{\dfrac{1.161}{4} + \left(\dfrac{1.936}{2} + 2.582\right) - \dfrac{1.936}{4}}{\dfrac{10.955}{2}} = 0.613 \Rightarrow \Lambda_{C/4} = 31.5 \ \text{deg} \quad (\text{aft sweep})$$

This reveals that both leading edge sweep and quarter chord sweep angles are greater than 50 percent chord line sweep angle.

Finally, in the right triangle DLE that includes trailing edge sweep angle ($\Lambda_{TE}$), we have:

$$\tan(\Lambda_{TE}) = \frac{EL}{LD} = \frac{EK - KL}{\frac{b_{eff}}{2}} = \frac{EK - C_r}{\frac{b_{eff}}{2}} = \frac{\frac{C_t}{2} + KH - C_r}{\frac{b_{eff}}{2}} = \frac{\frac{C_t}{2} + (KI + IH) - C_r}{\frac{b_{eff}}{2}}$$

$$= \frac{\frac{C_t}{2} + \left(\frac{C_r}{2} + 2.582\right) - C_r}{\frac{b_{eff}}{2}} = \frac{\frac{1.161}{2} + (2.582) - \frac{1.936}{2}}{\frac{10.955}{2}} = 0.401 \Rightarrow \Lambda_{TE} = 21.85 \text{ deg } (aft \ sweep)$$

The trailing edge sweep angel is considerably less than 50 percent chord line sweep angle.



F-16        Space Shuttle        Cessna T303 Crusader
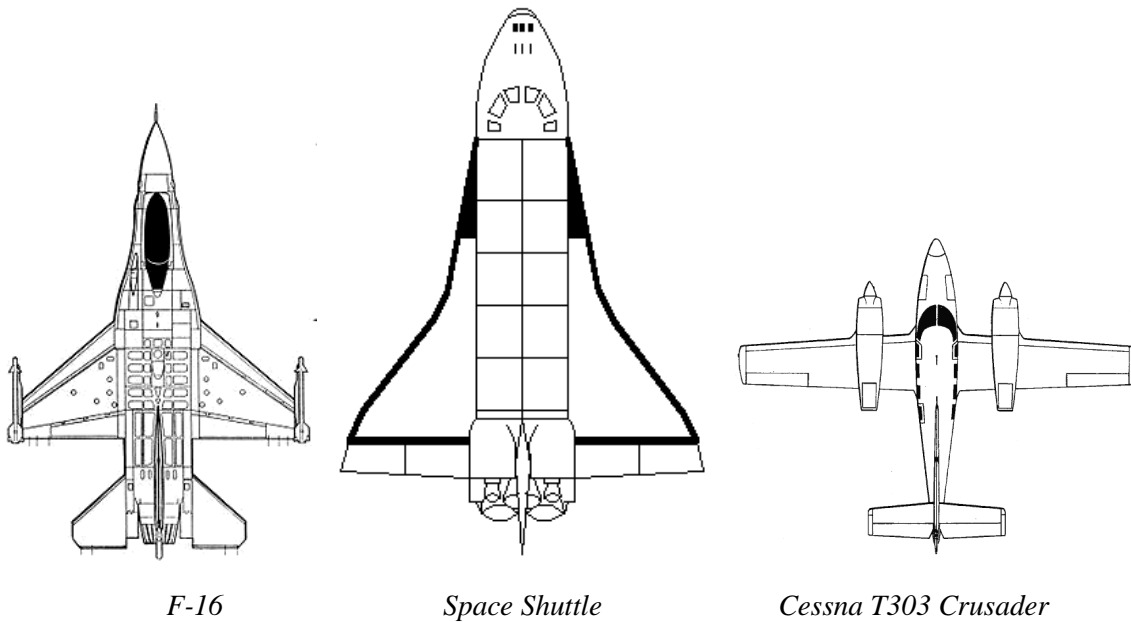
*Figure 5.46. Sweep angles for three aircraft*

## 5.10. Twist Angle

If the wing tip is at a lower incidence than the wing root, the wing is said to have negative twist or simply twist ($\alpha_t$) or washout. On the other hand, if the wing tip is at a higher incidence than the wing root, the wing is said to have positive twist or wash-in. The twist is usually negative; which means the wing tip angle of attack is lower than root angle of attack as sketched in figure 5.47a. This indicates that wing angle of attack is reduced along the span. The wings on a number of modern aircraft have different airfoil sections along the span, with different values of zero lift angle of attack; this is called aerodynamic twist. The wing tip airfoil section is often thinner than root airfoil section as sketched in figure 5.47b. Sometimes, the tip and root airfoil sections have the same thickness-to-chord ratio, but the root airfoil section has higher zero-lift angle of attack (i.e. more negative) than tip airfoil section.
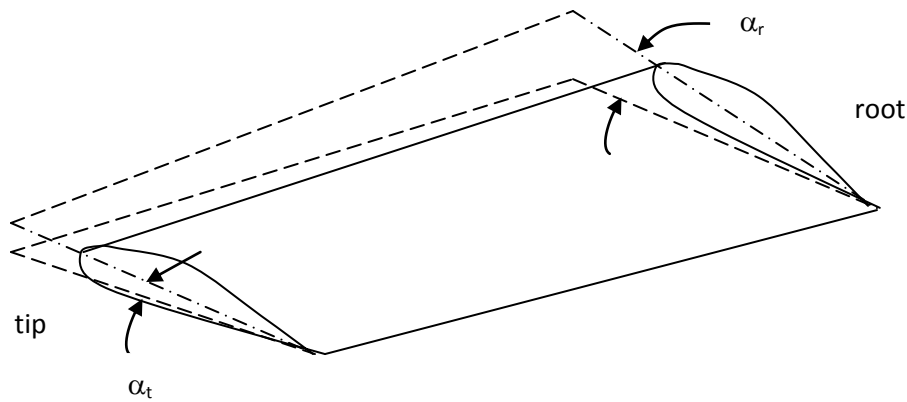
*a. geometric twist*
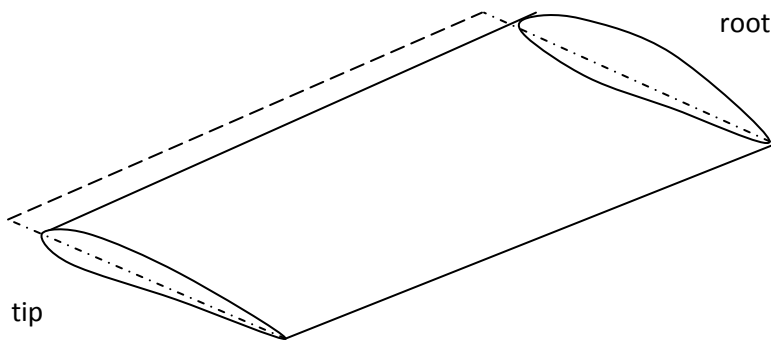


*b. Aerodynamic twist*

*Figure 5.47. Wing twist*

When the tip incidence and root incidence are not the same, the twist is referred to as *geometric twist*. However, if the tip airfoil section and root airfoil section are not the same, the twist is referred to as *aerodynamic twist*. Both types of twist have advantages and disadvantages by which the designer must establish a selection that satisfies the design requirement. The application of twist is a selection as a decision making, but the amount of twist is determined via calculations. In this section, both items will be discussed.

In practice, the application of aerodynamic twist is more convenient than the geometric twist. The reason is that in aerodynamic twist, a part of the wing has different ribs than another part, while all parts of the wing have the same incidence. The difficulty in the application of geometric twist arises from manufacturing point of view. Every portion of the wing has a unique incidence, since the angle of attack must be decreased (usually linearly) from wing setting angle; $i_w$ (at root) to a new value at the tip. This technique is applied by twisting the main wing spar, through which wing (rib) twist is automatically applied. The alternative solution is to divide each section of the wing (left and right) into two portions; inboard portion and outboard portion. Then, the inboard portion has the incidence equal to wing setting angle, while the outboard portion has the value such that the twist is produced. If situation allows, both geometric and aerodynamic twist may be employed.

There are two major goals for the employing the twist in wing design process:

1. Avoiding tip stall before root stall
2. Modification of lift distribution to elliptical one

In addition to two above-mentioned desired goals, there is another one unwanted output in twist:

3. Reduction in lift

When the wing root enters the stall before the wing tip, the pilot is able to utilize the aileron to control the aircraft, since the fair low at outboard section has not yet been stalled. This provision improves the safety of the aircraft in the advent of wing stall. The significance of the elliptical lift distribution has been described in section 5.7. The major drawback in twist is the loss of lift, since the twist is usually negative. As the angle of attack of a wing section is decreased, lift coefficient will be decreased too. The criterion and the limit for the wing twist is that the twist angle must not be such high that it results in a negative lift in the outer wing portions. Since any section has a zero-lift angle of attack ($\alpha_o$), the criterion is formulated as follows:

$$|\alpha_t| + i_w \geq |\alpha_o| \tag{5.34}$$

When a portion of the outboard of the wing generates a negative lift, the overall lift is decreased. This is not desirable and must be avoided in the twist angle determination process. The typical value for the geometric twist is between -1 to - 4 degrees (i.e. negative twist). The exact value of the twist angle must be determined such that the tip stalls after root as well as the lift distribution be elliptic. Figure 5.48 illustrates the typical effect of a (negative) twist angle on the lift distribution. Table 5.11 shows twist angles for several aircraft. As noted, several aircraft such as Cessna 208, Beech 1900D, Beechjet 400A, AVRO RJ100, and Lockheed C-130 Hercules have both geometric and aerodynamic twists.
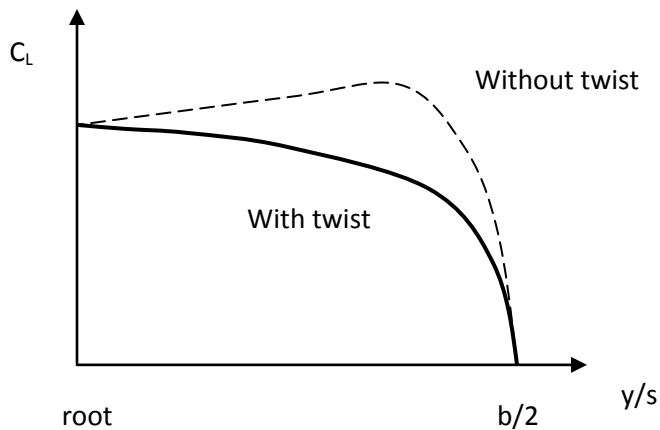


*Figure 5.48. The typical effect of a (negative) twist angle on the lift distribution*

| No | Aircraft | MTOW (lb) | Wing incidence at root ($i_w$) (deg) | Wing angle at tip (deg) | Twist (deg) |
|----|----------|-----------|-------------------------------------|-------------------------|-------------|
| 1 | Fokker 50 | 20,800 | +3.5 | +1.5 | -2 |
| 2 | Cessna 310 | 4,600 | +2.5 | -0.5 | -3 |
| 3 | Cessna Citation I | 11,850 | +2.5 | -0.5 | -3 |
| 4 | Beech King Air | 11,800 | +4.8 | 0 | -4.8 |
| 5 | Beech T-1A JawHawk | 16,100 | +3 | -3.3 | -6.3 |
| 6 | Beech T-34C | 4,300 | +4 | +1 | -3 |
| 7 | Cessna StationAir 6 | 3,600 | +1.5 | -1.5 | -3 |
| 8 | Gulfstream IV | 73,000 | +3.5 | -2 | -5.5 |
| 9 | Northrop-Grumman E-2C Hawkeye | 55,000 | +4 | +1 | -3 |
| 10 | Piper Cheyenne | 11,200 | +1.5 | -1 | -2.5 |
| 11 | Beech Super King | 12,500 | + 3° 48' | -1° 7' | |
| 12 | Beech starship | 14,900 | +3 | -5 | -3.5 |
| 13 | Cessna 208 | 8000 | 2° 37' | -36' | |
| 14 | Beech 1900D | 16,950 | 3° 29' | -1° 4' | 4° 25' |
| 15 | Beechjet 400A | 16,100 | 3 | -3° 30' | -6° 30' |
| 16 | AVRO RJ100 | 101,500 | 3° 6' | 0 | -3° 6' |
| 17 | Lockheed C-130 Hercules | 155,000 | 3 | 0 | -3 |
| 18 | Pilatus PC-9 | 4,960 | 1 | -1 | -2 |
| 19 | Piper PA-28-161 Warrior | 2,440 | 2 | -1 | -3 |

*a. Geometric twist (Ref. 4 and 12)*

| No | Aircraft | MTOW (lb) | Root airfoil section | Tip airfoil section | $\Delta t/C$ (%) |
|----|----------|-----------|---------------------|--------------------|------------------|
| 1 | Cessna 208 | 8000 | NACA 23017.424 | NACA 23012 | 5 |
| 2 | Beech 1900D | 16,950 | NACA 23018 | NACA 23012 | 6 |
| 3 | Beechjet 400A | 16,100 | t/C = 13.2% | t/C = 11.3 | 1.9 |
| 4 | AVRO RJ100 | 101,500 | t/C = 15.3% | t/C = 12.2% | 3.1 |
| 5 | Lockheed C-130 Hercules | 155,000 | NACA 64A318 | NACA 64A412 | 6 |
| 6 | Gulfstream IV-SP | 74,600 | t/C = 10% | t/C = 8.6% | 1.4% |
| 7 | Boeing 767 | 412,000 | t/C = 15.1% | t/C = 10.3% | 4.8 |
| 8 | Harrier II | 31,000 | t/C = 11.5% | t/C = 7.5% | 4 |
| 9 | BARE Sea Harrier | 26,200 | t/C = 10% | t/C = 5% | 5 |
| 10 | Kawasaki T-4 | 12,544 | t/C = 10.3% | t/C = 7.3% | 3 |

*b. Aerodynamic twist (Ref. 4)*

*Table 5.11. Twist angles for several aircraft*

## 5.11. Dihedral Angle

When you look at the front view of an aircraft, the angle between the chord-line plane of a wing with the "xy" plane is referred to as the wing dihedral ($\Gamma$). The chord line plane of the wing is an imaginary plane that is generated by connecting all chord lines across span. If the wing tip is higher than the xy plane, the angle is called positive dihedral or simply dihedral, but when the wing tip is lower than the xy plane, the angle is called negative dihedral or anhedral (see figure 5.49). For the purpose of aircraft symmetricity, both right and left sections of a wing must have the same dihedral angle. There are several advantages and disadvantages for dihedral angle. In this section, these characteristics are introduced, followed by the design recommendations to determine the dihedral angle.
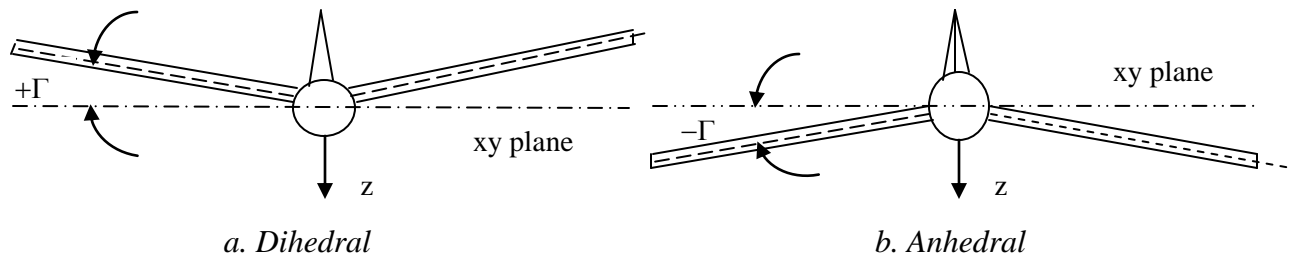


a. Dihedral                    b. Anhedral

*Figure 5.49. Dihedral, anhedral (aircraft from view)*

The primary reason of applying the wing dihedral is to improve the lateral stability of the aircraft. The lateral stability is mainly a tendency of an aircraft to return to original trim level-wing flight condition if disturbed by a gust and rolls around the x axis. In some references, it is called *dihedral stability*, since a wing dihedral angle provides the necessary restoring rolling moment. The lateral static stability in primarily represented by a stability derivative called aircraft dihedral effect ($C_{l_\beta} = \dfrac{dC_l}{d\beta}$) that is the change in aircraft rolling moment coefficient due to a change in aircraft sideslip angle ($\beta$).

Observe a level-wing aircraft that has experienced a disturbance (see figure 5.50) which has produced an undesired rolling moment (e.g. a gust under one side of the wing). When the aircraft rolls, one side of the wing (say left) goes up, while other side (say right) goes down. This is called a positive roll. The right wing section that has dropped has temporally lost a few percentage of its lift. Consequently, the aircraft will accelerates and slip down toward the right wing which produces a sideslip angle ($\beta$). This is equivalent to a wing approaching from the right of the aircraft, the sideslip angle is positive. In response, a laterally statically stable aircraft must produce a negative rolling moment to return to the original wing-level situation. This is technically translated into a negative dihedral effect ($C_{l_\beta} < 0$). The role of the wing dihedral angle is to induce a positive increase in angle of attack ($\Delta\alpha$). This function of the wing dihedral angle is done by producing a normal velocity ($V_n = V\Gamma$).

$$\Delta\alpha \approx \frac{V\Gamma}{U} \approx \frac{U\beta\Gamma}{U} \approx \beta\Gamma \tag{5.35}$$

where U is the airspeed component along x-axis, and where V is the airspeed component along y-axis. It is this increment in angle of attack which produces a corresponding increment in lift. This in turn results is a negative rolling moment contribution. It is interesting that the left wing section experiences exactly the opposite effect which also results in a negative rolling moment. Therefore, the rolling moment due to sideslip due to geometric wing dihedral is proportional to the dihedral angle. Basically, a positive wing geometric dihedral causes the rolling moment due to sideslip derivative $C_{l_\beta}$; to be negative. Aircraft must have a certain minimum amount of negative rolling moment due to sideslip; dihedral effect. This is needed to prevent excessive spiral instability. Too much dihedral effect tends to lower dutch roll damping. More negative $C_{l_\beta}$ means more spiral stability, but at the same time, less dutch roll stability.
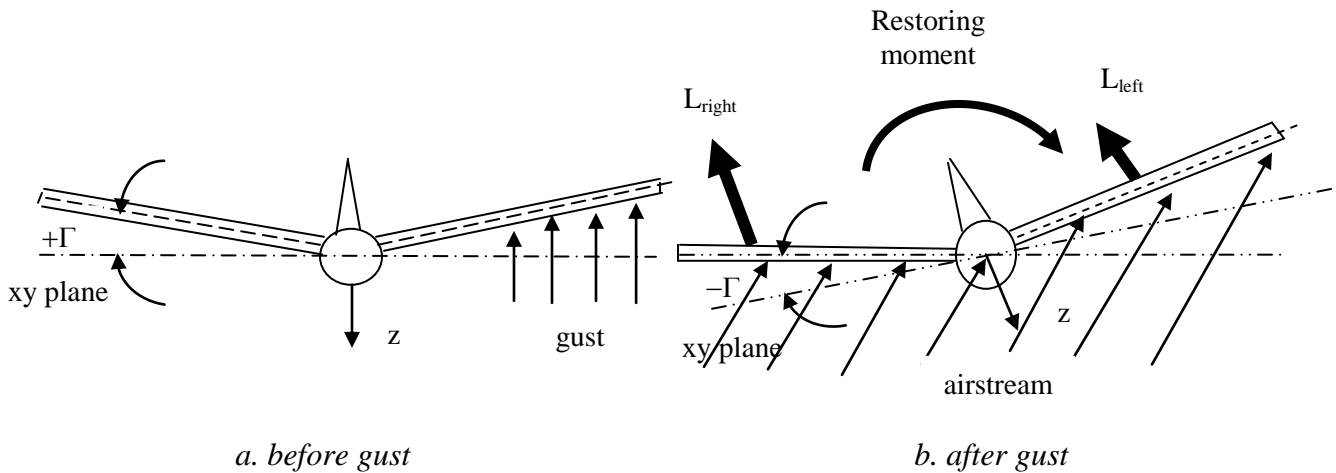


*Figure 5.50. The effect of dihedral angle on a disturbance in roll (aircraft from view)*

The anhedral has exactly the opposite function. In another word, the anhedral is laterally destabilizing. The reason for using anhedral in some configuration is to balance between the roles of wing parameters (such as sweep angle and wing vertical position) in lateral stability. The reason is that, the more laterally stable aircraft means the less rolling controllable aircraft. In the wing design, one must be careful to determine the wing parameters such that satisfy both stability and controllability requirements. Since the primary reason for the wing dihedral angle is the lateral stability, but wing sweep angles and wing vertical position are driven by not only lateral stability, but also performance requirements, and operational requirements.

For instance a cargo aircraft has usually a high wing to satisfy the loading and unloading operational requirements. The high wing contribution to lateral stability is highly positive, that means the aircraft is laterally stable more than necessary. In order to make the aircraft less laterally stable, one of the designer's option is to add an anhedral to the wing. This decision does not alter the operational characteristics of the aircraft, but improve the rolling controllablity of the aircraft. In general, high wing aircraft have inherent dihedral effect while low wing aircraft tend to be deficient in inherent dihedral effect; $C_{l_\beta}$. For this reason, low wing aircraft tend to have considerably greater dihedral angle than high wing aircraft. On the other hand, swept wing

aircraft tend to have too much dihedral effect; $C_{l_\beta}$ due to sweep angle. This can be offset in high wing aircraft by giving the wing negative dihedral (i.e. anhedral). The balance between lateral stability and roll control is a major criterion for the determination of dihedral angle.
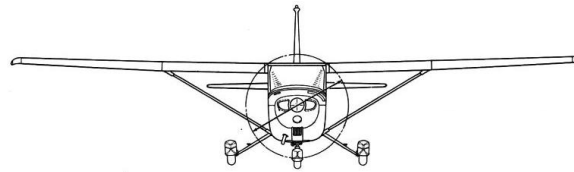


*Cessna 172 Skyhawk (GA)*
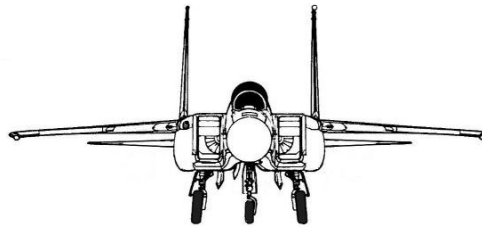


*F-15C (Fighter)*



*C-17 Globemaster III (Cargo)*
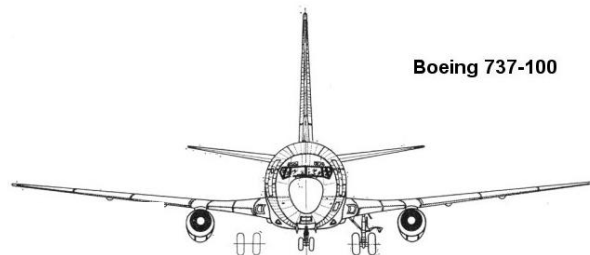


*Boeing 737-100 (Transport)*

*Figure 5.51. Four aircraft with different dihedral angles*

Another effect of wing dihedral effect is to alter the ground and water clearance, since aircraft wings, nacelles and propellers must have a minimum amount of ground and water clearance. It is clear that dihedral would increase ground and water clearance, while anhedral would decrease ground and water clearance. In aircraft with high aspect ratio and highly elastic wings (such as record breaker Voyager) the elastic deformation of the wing in flight generates extra dihedral angle. This must be considered in the wing design of such aircraft.

When the dihedral angle is applied on a wing, the wing effective planform area ($S_{eff}$) is reduced. This in turn will reduce the lift generated by the wing without dihedral, which is undesirable. If you need to apply the dihedral angle to a wing, consider the lowest value for the dihedral to minimize the lift reduction. The effective wing planform area as a function of dihedral angle is determined as follows:

$$S_{eff} = S_{ref} \cos(\Gamma) \tag{5.36}$$

| No | Aircraft | Type | Wing position | Dihedral (deg) |
|----|----------|------|---------------|----------------|
| 1 | Pilatus PC-9 | Turboprop Trainer | Low-wing | 7 (outboard) |
| 2 | MD-11 | Jet Transport | Low-wing | 6 |
| 3 | Cessna 750 Citation X | Business Jet | Low-wing | 3 |
| 4 | Kawasaki T-4 | Jet Trainer | High-wing | -7 |
| 5 | Boeing 767 | Jet Transport | Low-wing | 4° 15' |
| 6 | Falcon 900 B | Business Jet Transport | Low-wing | 0° 30' |
| 7 | C-130 Hercules | Turboprop Cargo | High-wing | 2° 30' |
| 8 | Antonov An-74 | Jet STOL Transport | Parasol-wing | -10 |
| 9 | Cessna 208 | Piston Engine GA | High-wing | 3 |
| 10 | Boeing 747 | Jet Transport | Low-wing | 7 |
| 11 | Airbus 310 | Jet Transport | Low-wing | 11° 8' |
| 12 | F-16 Fighting Falcon | Fighter | Mid-wing | 0 |
| 13 | BAE Sea Harrier | V/STOL Fighter | High-wing | -12 |
| 14 | MD/BAe Harrier II | V/STOL Close Support | High-wing | -14.6 |
| 15 | F-15J Eagle | Fighter | High-wing | -2.4 |
| 16 | Fairchild SA227 | Turboprop Commuter | Low-wing | 4.7 |
| 17 | Fokker 50 | Turboprop Transport | High-wing | 3.5 |
| 18 | AVRO RJ | Jet Transport | High-wing | -3 |
| 19 | MIG-29 | Fighter | Mid-wing | -2 |

*Table 5.12. Dihedral (or Anhedral) angles for several aircraft*

Table 5.12 illustrates dihedral (and anhedral) angles for several aircraft along with their wing vertical position. As noted, the typical dihedral angle is a value between -15 to +10 degrees. Figure 5.51 illustrates four aircraft with different dihedral angles. Table 5.13 shows typical values of dihedral angle for swept or unswept wings of various wing vertical positions. This table is a recommended reference for the starting point. You can select an initial value for the dihedral angle from this table. However, the exact value of the dihedral angle is determined during the stability and control analysis of whole aircraft. When other aircraft components (e.g. fuselage, tail) are designed, evaluate the lateral stability of the whole aircraft.

The suggested value for aircraft dihedral effect ($C_{l_\beta}$) to have an acceptable lateral controllability and lateral stability is a value between -0.1 to +0.4 1/rad. Then you can adjust the dihedral angle to satisfy all design requirements. If one dihedral angle for whole wing does not satisfy all design requirements, you may divide the wing into inboard and outboard sections;

each with different dihedral angle. For instance, you may apply dihedral angle to the outboard plane, in order to keep the wing level in the inboard plane.

| No | Wing | Low wing | Mid-wing | High wing | Parasol wing |
|----|------|----------|----------|-----------|--------------|
| 1 | Unswept | 5 to 10 | 3 to 6 | -4 to -10 | -5 to -12 |
| 2 | Low subsonic swept | 2 to 5 | -3 to +3 | -3 to -6 | -4 to -8 |
| 3 | High subsonic swept | 3 to 8 | -4 to +2 | -5 to -10 | -6 to -12 |
| 4 | Supersonic swept | 0 to -3 | 1 to -4 | 0 to -5 | NA |
| 5 | Hypersonic swept | 1 to 0 | 0 to -1 | -1 to -2 | NA |

*Table 5.13. Typical values of dihedral angle for various wing configurations*

## 5.12. High Lift Device

### 5.12.1. The Functions of High Lift Device

One of the design goals in wing design is to maximize the capability of the wing in the generation of the lift. This design objective is technically shown as maximum lift coefficient ($C_{L_{max}}$). In a trimmed cruising flight, the lift is equal to weight. When the aircraft generates its maximum lift coefficient, the airspeed is referred to as stall speed.

$$L = W \Rightarrow \frac{1}{2} \rho V_s^{\,2} S C_{L_{max}} = mg \tag{5.37}$$

Two design objectives among the list of objectives are: 1. maximizing the payload weight, 2. minimizing the stall speed ($V_s$). As the equation 5.36 indicates, increasing the $C_{L_{max}}$ tends to increase the payload weight (W) and decrease the stall speed. The lower stall speed is desirable since a safe take-off and landing requires a lower stall speed. On the other hand, the higher payload weight will increase the efficiency of the aircraft and reduce the cost of flight. A higher $C_{L_{max}}$ allows the aircraft to have a smaller wing area that results in a lighter wing. Hence, in a wing design, the designer must find way to maximize the $C_{L_{max}}$. In order to increase the lift coefficient, the only in-flight method is to temporarily vary (increase) the wing camber. This will happen only when the high lift device is deflected downward.

The primary applications of high lift devices are during take-off and landing operations. Since the airspeed is very low compared with cruising speed, the wing must produce more lift coefficient. The aircraft speed during take-off and landing is slightly greater than stall speed. Airworthiness standards specify the relationship between take-off speed and landing speed with stall speed. As a general rule, we have:

$$V_{TO} = k \cdot V_S \tag{5.38}$$

where *k* is about 1.1 for fighter aircraft, and about 1.2 for jet transports and GA aircraft.

The application of the high lift device tends to change the airfoil section's and wing's camber (in fact the camber will be positively increased). This in turn will change the pressure distribution along the wing chord as sketched in figure 5.52. In this figure, $C_P$ denotes the pressure coefficient.

On the other hand, the leading edge high lift device tends to improve the boundary layer energy of the wing. Some type of high lift device has been used on almost every aircraft designed since the early 1930s. High lift devices are the means to obtain the sufficient increase in $C_{Lmax}$.

At the airfoil level, a high lift device deflection tends to cause the following six changes in the airfoil features:

1. Lift coefficient ($C_l$) is increased,
2. Maximum lift coefficient ($C_{lmax}$) is increased,
3. Zero-lift angle of attack ($\alpha_o$) in changed,
4. Stall angle ($\alpha_s$) is changed,
5. Pitching moment coefficient is changed, and
6. Drag coefficient is increased.
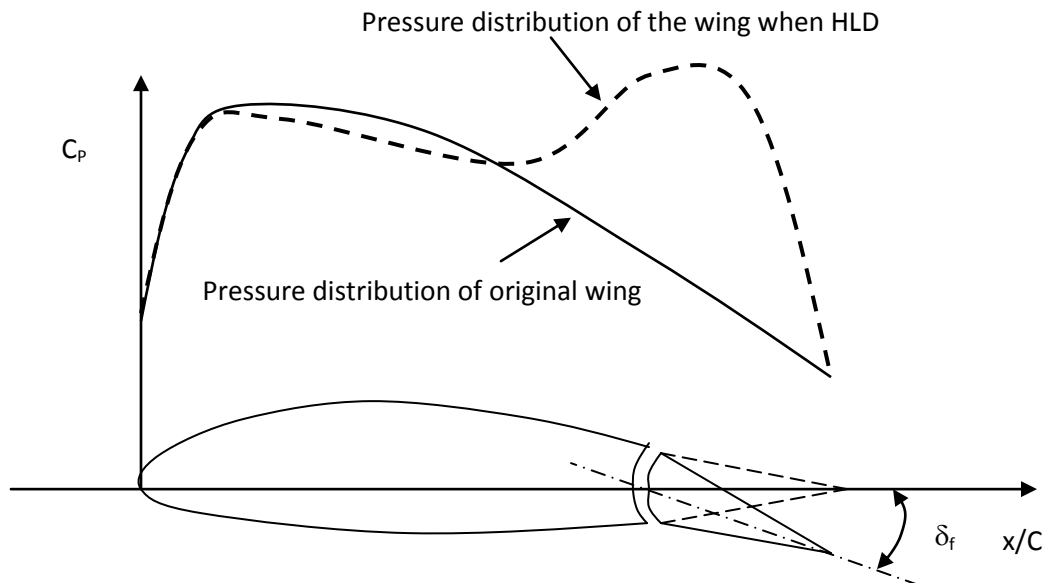7. Lift curve slope is increased.



*Figure 5.52. Example of pressure distribution with the application of a high lift device*

These effects are illustrated in figure 5.53. Along with three desirable advantages (first two items) to the application of high lift devices; there are a few negative side-effects (the last five items) as well. A plain flap tends to decrease stall angle, while a slotted flap and leading edge slat tend to increase the stall angle. In addition, among all types of flaps, the Fowler flap and leading edge slat tend to increase the lift curve slope ($C_{L\alpha}$). On the other hand, leading edge flap tend to increase (shift to the right) the zero-lift angle of attack ($\alpha_o$).

A reduction in stall angle is undesirable, since the wing may stall at a lower angle of attack. During the take-off and landing operation, a high angle of attack is required to successfully take-off and land. The high angle of attack will also tend to reduce the take-off run and landing run that is desirable in the airport at which have a limited runway length. An increase in pitching moment coefficient requires higher horizontal tail area to balance the aircraft. An increase in

drag coefficient decreases the acceleration during take-off and landing. Although the application of high lift device generates three undesirable side effects, but the advantages outweigh the disadvantages.

If the natural Value of $C_{Lmax}$ for an aircraft is not high enough for safe take-off and landing, it can be temporarily increased by mechanical high lift devices. Thus, employing the same airfoil section; one is able to increase $C_{Lmax}$ temporarily as needed without actually pitching the aircraft. Two flight operations at which the $C_{Lmax}$ needs to be increased are take-off and landing. Table 5.14 shows the maximum lift coefficient for several aircraft.
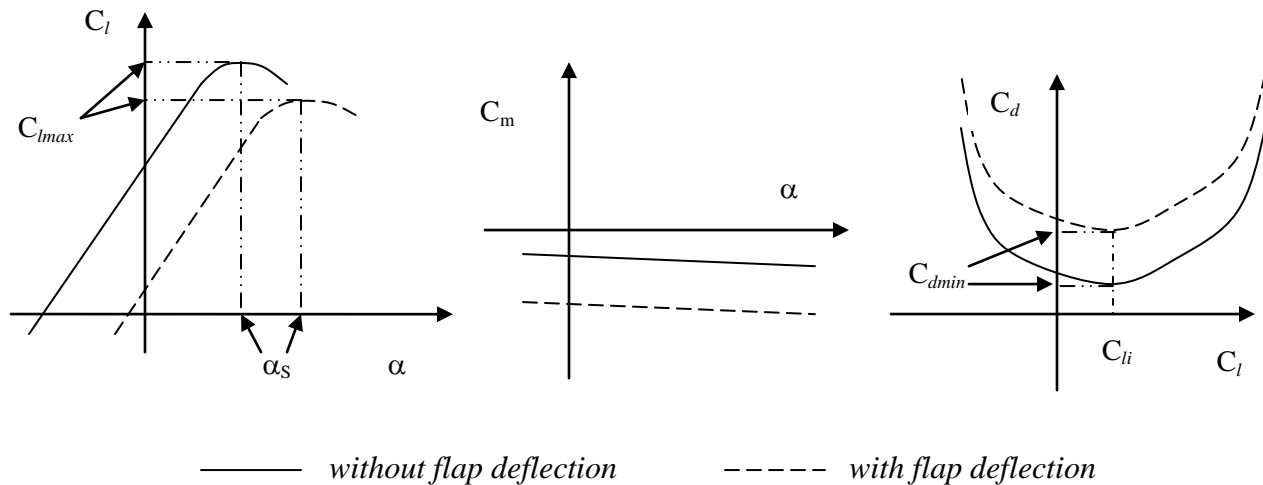


—— *without flap deflection*          - - - - - *with flap deflection*

*Figure 5.53. Typical effects of high lift device on wing airfoil section features*

In a cruising flight, there is no need to utilize the maximum lift coefficient since the speed is high. These mechanical devices are referred to as High Lift Devices (HLD). High Lift Devices are parts of wings to increase the lift when deflected down. They are located at inboard section of the wing and usually employed during take-off and landing.

| $C_{Lmax}$ | Cessna 172 | Piper Cherokee | Short Skyvan 3 | Gulfstream II | DC-9 | Boeing 727 | Airbus 300 | Learjet 25 |
|---|---|---|---|---|---|---|---|---|
| **Take-Off** | 1.5 | 1.3 | 2.07 | 1.4 | 1.9 | 2.35 | 2.7 | 1.37 |
| **Landing** | 2.1 | 1.74 | 2.71 | 1.8 | 2.4 | 2.75 | 3 | 1.37 |

*Table 5.14. Maximum lift coefficient for several aircraft*

### 5.12.2. High Lift Device Classification
Two main groups of high lift devices are:

1. leading edge high lift device (LEHLD or flap), and
2. trailing edge high lift devices (TEHLD).

There are many types of wing trailing edge flaps that the most common of them are split flap, plain flap, single-slotted flap, double-slotted flap, triple-slotted flap, and fowler flap as

illustrated in figure 5.54a. They are all deflected downward to increase the camber of the wing, so $C_{Lmax}$ will be increased. The most common of leading edge devices are leading edge flap, leading edge slat, and Kruger flap as shown by in figure 5.54b.

A common problem with the application of high lift devices is how to deal with the gap between high lift device and the main wing. This gap can be either sealed or left untouched. In both cases, there are undesirable side effects. If the gap left open, the airflow from downside escapes to the upper surface which in turn degrades the pressure distribution. On the other hand, if the gap is sealed by a means such diaphragm, it may be blocked by ice during flight into colder humid air. In both cases, it needs special attention as an operational problem. In the following, the technical features of various high lift devices are discussed.
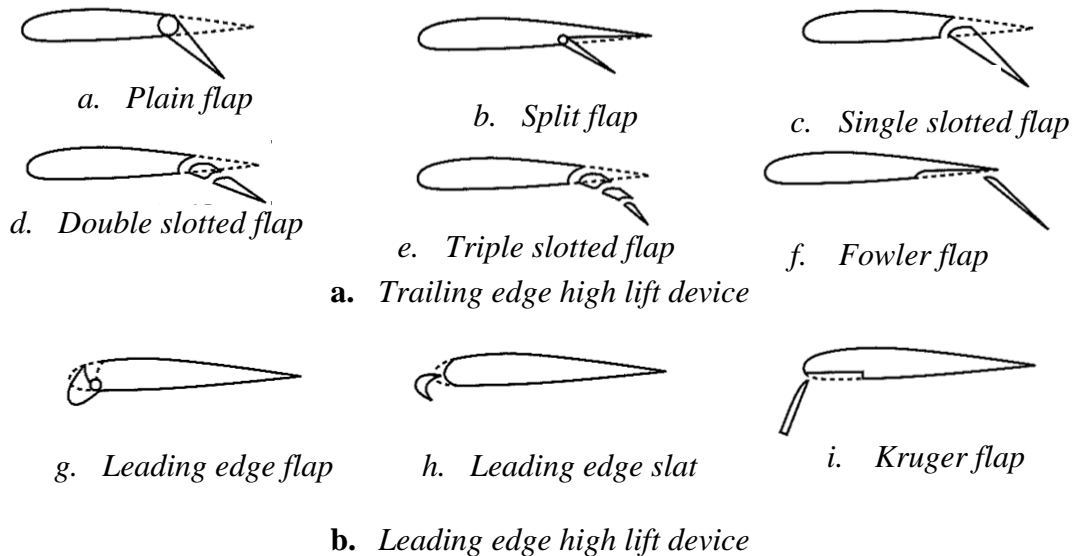


a.  *Plain flap*

b.  *Split flap*

c.  *Single slotted flap*

d.  *Double slotted flap*

e.  *Triple slotted flap*

f.  *Fowler flap*

**a.**  *Trailing edge high lift device*

g.  *Leading edge flap*

h.  *Leading edge slat*

i.  *Kruger flap*

**b.**  *Leading edge high lift device*

*Figure 5.54. Various types of high lift devices*

1.  The *plain flap* (figure 5.54-a) is the simplest and earliest type of high lift device. It is an airfoil shape that is hinged at the wing trailing edge such that it can be rotated downward and upward. However, the downward deflection is considered only. A plain flap increases the lift simply by mechanically increasing the effective camber of the wing section. In terms of cost, a plain flap is the cheapest high lift device. In terms of manufacturing, the plain flap is the easiest one to build. Most home build aircraft and many General Aviation aircraft are employing the plain flap. The increment in lift coefficient for a plain flap at 60 degrees of deflection (full extension) is about 0.9. If it is deflected at a lower rate, the $C_L$ increment will be lower. Some old GA aircraft such as Piper 23 Aztec D has a plain flap. It is interesting to know that the modern fighters such aircraft F-15E Eagle and MIG-29 also employ plain flaps.

2.  In the *split flap* (figure 5.54-b), only the bottom surface of the flap is hinged so that it can be rotated downward. The split flap performs almost the same function as a plain flap. However, the split flap produces more drag and less change in the pitching moment compared to a plain flap. The split flap was invented by Orville Wright in 1920, and it was employed, because of

its simplicity, on many of the 1930s and 1950s aircraft. However, because of the higher drag associated with split flap, they are rarely used on modern aircraft.

3. The *single slotted flap* (figure 5.54-c) is very similar to a plain flap, except it has two modifications. First, the leading edges of these two trailing edge flaps are different as shown in figure 5.51. The leading edge of a single slotted flap is carefully designed such that it modifies and stabilizes the boundary layer over the top surface of the wing. A low pressure is created on the leading edge that allows a new boundary layer to form over the flap which in turn causes the flow to remain attached to very high flap deflection. The second modification is to allow the flap move aftward during the deflection (i.e. the slot). The aft movement of single slotted flap actually increases the effective chord of the wing which in turn increases the effective wing planform area. The larger wing planform area naturally generated more lift.
Thus a single slotted flap generates considerably higher lift than a plain and split flap. The main disadvantage is the higher cost and the higher degree of complexity in the manufacturing process associated with the single slotted flap. Single slotted flap are in common use on modern light, general aviation aircraft. In general, the stall angle is increased by the application of the slotted flap. Several modern GA light aircraft such as Beech Bonanza F33A and several turboprop transport aircraft such as Beech 1900D and Saab 2000 has deployed single slotted flap.

4. The *double slotted flap* is similar to a single slotted flap, except it has two slots; I.e. the flap is divided into two segments, each with a slot as sketched in figure 5.54-d. A flap with two slots almost doubles the advantages of a single slotted flap. This benefit is achieved at the cost of increased mechanical complexity and higher cost. Most modern turboprop transport aircraft such as ATR-42; and several jet aircraft such as and jet trainer Kawasaki T-4 employ the double slotted flap. The jet transport aircraft Boeing 767 has single slotted outboard flap and double slotted inboard flap. It is a common practice to deflect the first segment (slot) of the flap during a take-off operation, but employs full deflection (both segments) during landing. The reason is that more lift coefficient is needed during a landing that a take-off.

5. A *triple slotted flap* (figure 5.54-e) is an extension to a double slotted flap; i.e. has three slots. This flap is mechanically the most complex; and costly most expensive flap in design and operation. However, a triple slotted flap produces the highest increment in lift coefficient. It is mainly used in heavy weight transport aircraft which have high wing loading. The jet transport aircraft Boeing 747 has employed the triple slotted flap.

6. A *Fowler flap* (figure 5.54-f) has a special mechanism such that when deployed, not only deflects downward, but also translates or tracks to the trailing edge of the wing. The second feature increases the exposed wing area; which means a further increase in lift. Because of this benefit, the concept of the Fowler flap may be combined with the double slotted and triple slotted flaps. For instance jet transport aircraft Boeing B-747 has utilized triple slotted Fowler flap. In general, the wing lift curve slope is slightly increased by the application of the Fowler flap. Maritime patrol aircraft Lockheed Orion P-3 with 4 turboprop engines has a Fowler engine.

**7.** A *leading edge flap (or droop)* in illustrated in figure 5.54-g. This flap is similar to trailing edge plain flap, except it is installed at the leading edge of the wing. Hence, the leading edge pivots downward, increasing the effective camber. A feature of the leading edge flap is that the gap between the flap and main wing body is sealed with no slot. In general, the wing zero-lift angle of attack is shifted to the right by the application of leading edge flap. Since the leading edge flap has a lower chord compared with the trailing edge flaps, it generates a lower increment in lift coefficient ($\Delta C_L$ is about 0.3).

**8.** The *leading edge slat* (see figure 5.54-h) is a small, highly cambered section, located slightly forward of the leading edge the wing body. When deflected, a slat is basically a flap at the leading edge, but with an unsealed gap between the flap and the leading edge. In addition to the primary airflow over the wing, there is a secondary flow that takes place through the gap between the slat and the wing leading edge. The function of a leading edge slat is primarily to modify the pressure distribution over the top surface of the wing. The slat itself, being highly cambered, experiences a much lower pressure over its top surface; but the flow interaction results in a higher pressure over the top surface of the main wing body. Thus it delays flow separation over the wing and mitigates to some extent the otherwise strong adverse pressure gradient that would exist over the main wing section.

  By such process, the lift coefficient is increased with no significant increase in drag. Since the leading edge slat has a lower chord compared with the trailing edge flaps, it generates a lower increment in lift coefficient ($\Delta C_L$ is about 0.2). Several modern jet aircraft such as two seat fighter aircraft Dassault Rafale, Eurofighter 2000, Bombardier BD 701 Global Express, MD-80, and Airbus A-300 have leading edge slat. In general, the wing lift curve slope is slightly increased by the application of leading edge slat.

**9.** A *Kruger flap* is demonstrated in figure 5.54-i. This leading edge high lift device is essentially a leading edge slat which is thinner, and which lies flush with the bottom surface of the wing when not deflected. Therefore, it is suitable for use with thinner wing sections. The most effective method used on all large transport aircraft is the leading edge slat. A variant on the leading edge slat is a variable camber slotted Kruger flap used on the Boeing 747. Aerodynamically, this is a slat, but mechanically it is a Kruger flap.

| No | High lift device | $\Delta C_L$ |
|----|------------------|--------------|
| 1 | Plain flap | 0.7-0.9 |
| 2 | Split flap | 0.7-0.9 |
| 3 | Fowler flap | 1-1.3 |
| 4 | Slotted flap | 1.3 $C_f/C$ |
| 5 | Double slotted flap | 1.6 $C_f/C$ |
| 6 | Triple slotted flap | 1.9 $C_f/C$ |
| 7 | Leading edge flap | 0.2-0.3 |
| 8 | Leading edge slat | 0.3-0.4 |
| 9 | Kruger flap | 0.3-0.4 |

*Table 5.15. Lift coefficient increment by various types of high lift devices (when deflected 60 degrees)*

As a general comparison, table 5.15 shows the typical values of maximum wing lift coefficient for various types of high lift devices. In this table, the symbol $C_f/C$ denotes the ratio between the chord of high lift device to the chord of the main wing body as shown in figure 5.55. Table 5.16 demonstrates various features for high lift devices of several aircraft.

### 5.12.3. Design Technique

In designing the high lift device for a wing, the following items must be determined:

1. High lift device location along the span
2. The type of high lift device (among the list in figure 5.51)
3. High lift device chord ($C_f$)
4. High lift device span ($b_f$)
5. High lift device maximum deflection (down) ($\delta_{fmax}$)

The last three parameters are sketched in figure 5.55. The first and second item must be selected through an evaluation and analysis technique considering all advantages and disadvantages of each option regarding design requirements. However, the last three parameters must be determined through a series of calculations. In the following, the design technique for high lift device to determine the above five items will be presented.
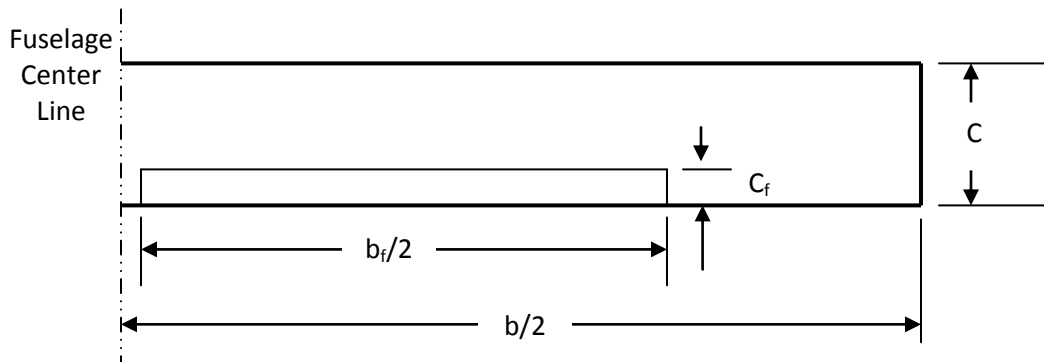


*a.   Top-view of the right wing*
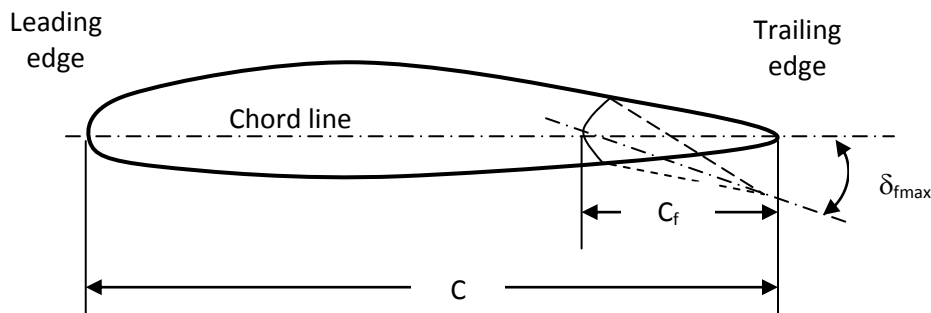


*b.   The side-view of the inboard wing (flap deflected)*

*Figure 5.55. High lift device parameters*

### a. HLD Location

The best location for high lift device is the inboard portion of both left and right of the wing sections. When high lift device is applied symmetrically on the left and right wing sections, it will prevent any rolling moment; hence the aircraft will remain laterally trimmed. The deflection of high lift device will increase the lift on both inboard sections, but since they are generated symmetrically, both lift increments will cancel each other's rolling moments.

There are two reasons for the selection of inboard section. First of all, it produces a lower bending moment on the wing root. This makes the wing structure lighter and causes less fatigue on the wing in the long run. The second reason is that it allows the aileron to have a large arm, which is employed on the outboard wing trailing edge. The larger arm for the aileron, when installed on the outboard panels, means the higher lateral control and a faster roll. The design of the aileron will be discussed in chapter 12.

### b. Type of High Lift Device

The options for the high lift device are introduced in Section 5.11.2. Several design requirements will affect the decision on the type of high lift device. They include, but not limited to: 1. Performance requirements (i.e. the required lift coefficient ($\Delta C_L$) increment during take-off and landing); 2. Cost considerations; 3. Manufacturing limitations; 4. Operational requirements; 5. Safety considerations; and 6. Control requirements. The following guideline will help the designer to make the right decision.

The final decision is the outcome of a compromise among all options using a table including the weighted design requirements. For a homebuilt aircraft designer, the low cost is the number one priority, while for a fighter aircraft designer the performance is the first priority. A large transport passenger aircraft designer, believe that the airworthiness must be on the top of the list of priorities.

The following are several guidelines that relate the high lift device options to the design requirements:

1. A more powerful high lift device (higher $\Delta C_L$) is usually more expensive. For instance, a double slotted flap is more expensive than a split flap.
2. A more powerful high lift device (higher $\Delta C_L$) is usually more complex to build. For example, a triple slotted flap is more complex in manufacturing than a single slotted flap.
3. A more powerful high lift device (higher $\Delta C_L$) is usually heavier. For instance, a double slotted flap is heavier than a single slotted flap.
4. The more powerful high lift device (higher $\Delta C_L$), results in a smaller wing area.
5. The more powerful high lift device (higher $\Delta C_L$), results in a slower stall speed, which consequently means a safer flight.
6. A heavier aircraft requires a more powerful high lift device (higher $\Delta C_L$).
7. A more powerful high lift device results in a shorter runway length during take-off and landing.
8. A more powerful high lift device (higher $\Delta C_L$) allows a more powerful aileron.

**9.** A simple high lift device requires a simpler mechanism to operate (deflect or retract) compared with a more complex high lift device such as a triple slotted flap.

When the low cost is the number one priority, select the least expensive high lift device that is the plain flap. If the performance is the number one priority, select the high lift device that satisfies the performance requirements. If only one high lift device such as a single slotted flap does not satisfy the performance requirements, add another high lift device such as leading edge flap to meet the design requirements. The other option is to combine two high lift devices into one new high lift device. For instance, the business jet Gulfstream IV and Dassault Falcon 900B employ single slotted Fowler flap that is a combination of the single slotted flap and the Fowler flap.

All large aircraft use some forms of slotted flap. The drag and lift of slotted flaps depend on the shape and dimensions of the vanes and flaps, their relative position, and the slot geometry. Mounting hinges and structure may seriously degrade flap performance if not carefully designed to minimize flow separation. Typical examples are DC-8 original flap hinges and the DC-9 original slat design, both of which were redesigned during the flight test stage to obtain the required $C_{Lmx}$ and low drag.

The triple slotted flap is almost the ultimate in mechanical complexity. For this reason, in the interest of lower design and production cost, some recent aircraft designs have returned to simpler mechanism. For example, the Boeing 767 has single slotted outboard flap and double slotted inboard flap.

Leading edge high lift devices such as slats functions very differently compared with trailing edge high lift devices. The lift coefficient at a given angle of attack is increased very little, but the stall angle is greatly increased. One disadvantage of slats is that the aircraft must be designed to fly at a high angle of attack for take-off and landing to utilize the high available lift increment. This clearly affects the design of the windshield, because of the pilot visibility requirements. Despite disadvantages of slats, they are so powerful in high lift that high speed transport aircraft designed since about 1964 use some form of slats in addition to trailing edge flaps. If leading edge devices serve simply to shorten take-off and/or landing runway lengths below the required values and wing area cannot be reduced (say because of fuel tank requirement), the weight and complexity due to the application of leading edge device ate not justified.

Leading edge devices intended to substantially raise the $C_{Lmax}$ must extend along the entire leading edge except for a small cutout near the fuselage to trigger the inboard stall. Some designs utilize a less powerful device, such as Kruger flap, on the inboard part of the wing to ensure inboard initial stall. Table 5.16 illustrates the type of the high lift device for several aircraft.

### c. HLD Span

The spanwise extent of high lift devices depends on the amount of span required for ailerons. In general, the outer limit of the flap is at the spanwise station where the aileron begins. The exact span needed for aileron depend on aircraft lateral controllability requirements. Low speed GA aircraft utilize about 30 percent of the total semispan for aileron. This means that flaps can start

at the side of the fuselage and extent to the 70 percent semispan station. In large transport aircraft, a small inboard aileron is often provided for gentle maneuver at high speeds, and this serves to reduce the effective span of the flaps. However, in fighter aircraft which are highly maneuverable, aileron requires all wing span stations, so there is theoretically no space for flap. This leads to the idea of flaperon that serves as an aileron as well as a flap. The high lift device span is usually introduced as the ratio to the wing span (i.e. $b_f/b$). In some references, $b_f/b$ refers to the ratio between flap span to net wing span (i.e. from root to tip, not from center line to tip).

Table 5.16 illustrates the ratio of the high lift device span to the wing span for several aircraft. As an initial value, it is recommended to allocate 70 percent of the wing span to the high lift device. The exact value must be determined through the calculation of lift increment due to this span ($b_f$) for high lift device. There are several aerodynamic tools to accomplish this analysis. An aerodynamic technique called *lift line theory* will be introduced in Section 5.13. Such technique can be employed to calculate the lift increment for each high lift device span. You can then adjust the HLD span ($b_f$) to achieve the required lift increment. An example at the end of this chapter will illustrate the application.

### d. HLD Chord

Since the high lift device is employed temporarily in a regular flight mission that is during the take-off and landing, the lease amount of wing chord must be intended for a high lift device. The wing structural integrity must be considered when allocating part of the wing chord to a high lift device. The chord of the high lift device is often introduced as the ratio to the wing chord (i.e. $C_f/C$). It is important to note that the deflection of a high lift device will increase the wing drag. Hence, the high lift device chord must not be that much high that the drag increment; due to its deflection; nullifies its advantages. On the other hand, as the high lift device chord is increased, the power required to deflect the device is increased. If the pilot is using the manual power to move the high lift device, the longer high lift device chord requires more pilot power. Therefore, the shorter high lift device is better in many aspects.

Another consideration about the high lift device chord is that the designer can extend the chord up to the rear spar of the wing. Since in most aircraft, rear spar is an important in the wing structural integrity, do not try to cut the rear spar in order to extend the high lift device chord. The high lift device chord and span can be interchanged in some extent. If you have to reduce the span of the high lift device, due to aileron requirements, you can increase the high lift device chord instead. The opposite is also true. If you have to reduce the chord of the high lift device, due to structural considerations, you can increase the high lift device span instead. If the wing is tapered, you may taper the flap as well. So the high lift device chord does not have a constant chord.

Table 5.16 illustrates the ratio of the high lift device chord to the wing chord ($C_f/C$) for several aircraft. As an initial value, it is recommended to allocate 20% of the wing chord to the high lift device. The exact value must be determined through the calculation of lift increment due to this chord for high lift device. There are several aerodynamic tools to accomplish this analysis. Such aerodynamic technique as *lift line theory* can be employed to calculate the lift increment for each high lift device chord. You can then adjust the HLD chord ($C_f$) to achieve the required lift increment. An example at the end of this chapter will illustrate the application.

### e. HLD Maximum Deflection

Another parameter that must be determined in the design of high lift device is the amount of its deflection ($\delta_{fmax}$). The exact value of the deflection must be determined through the calculation of lift increment due to the high lift device deflection. Table 5.16 illustrates the high lift device deflection ($\delta_{fmax}$) for several aircraft. As an initial value, it is recommended to consider the deflection of 20 degrees during a take-off and 50 degrees for the landing. There are several aerodynamic tools to accomplish this analysis. Such aerodynamic technique as *lift line theory* can be employed to calculate the lift increment for each high lift device deflection. You can then adjust the HLD chord ($C_f$) to achieve the required lift increment. An example at the end of this chapter will illustrate the application.

| No | Aircraft | Engine | HLD | $C_f/C$ | $b_f/b$ | $\delta_{fmax}$ TO | $\delta_{fmax}$ Landing |
|----|----------|--------|-----|---------|---------|------|---------|
| 1 | Cessna 172 | Piston | Single slotted | 0.33 | 0.46 | 20 | 40 |
| 2 | Piper Cherokee | Piston | Single slotted | 0.17 | 0.57 | 25 | 50 |
| 3 | Lake LA-250 | Piston | Single slotted | 0.22 | 0.57 | 20 | 40 |
| 4 | Short Skyvan 3 | Turboprop | Double slotted | 0.3 | 0.69 | 18 | 45 |
| 5 | Fokker 27 | Turboprop | Single slotted | 0.313 | 0.69 | 16 | 40 |
| 6 | Lockheed L-100 | Turboprop | Fowler | 0.3 | 0.7 | 18 | 36 |
| 7 | Jetstream 41 | Turboprop | Double slotted | 0.35 | 0.55 | 24 | 45 |
| 8 | Boeing 727 | Turbofan | Triple slotted + LE flap | 0.3 | 0.74 | 25 | 40 |
| 9 | Airbus A-300 | Turbofan | Double slotted + LE flap | 0.32 | 0.82 | 15 | 35 |
| 10 | Learjet 25 | Turbofan | Single slotted | 0.28 | 0.61 | 20 | 40 |
| 11 | Gulfstream II | Turbofan | Fowler | 0.3 | 0.73 | 20 | 40 |
| 12 | McDonnell DC-9 | Turbofan | Double slotted | 0.36 | 0.67 | 15 | 50 |
| 13 | Antonov 74 | Turbofan | Double slotted + triple slotted + LE flap | 0.24 | 0.7 | 25 | 40 |
| 14 | McDonnell F-15E Eagle | Turbofan | Plain flap | 0.25 | 0.3 | - | - |
| 15 | Mikoyan MIG-29 | Turbofan | Plain flap + LE flap | 0.35 | 0.3 + 1 | - | - |

*Table 5.16. Characteristics of high lift devices for several aircraft*

In using aerodynamic techniques to calculate lift increment due the extension of trailing edge flap, it is sometime necessary to determine the increment in wing zero-lift angle of attack ($\Delta\alpha_o$). The following is an empirical equation that allow for such calculation.

$$\Delta\alpha_o \approx -10 \cdot \Delta C_L \tag{5.39}$$

This equation provides the increment in section's zero-lift angle of attack ($\Delta\alpha_o$) in degrees as a function of the increment in the lift coefficient.

## 5.13. Aileron

Aileron is very similar to a trailing edge plain flap except is deflected both up and down. Aileron is located at the outboard portion of the left and right sections of wing. Unlike flap, ailerons are deflected differentially, left up and right down; or left down and right up. The lateral control is applied on an aircraft through the differential motions of ailerons. Aileron design is part of wing design, but because of the importance and great amount of materials that needs to be covered on aileron design, it will be discussed in a separate chapter (Chapter 12).
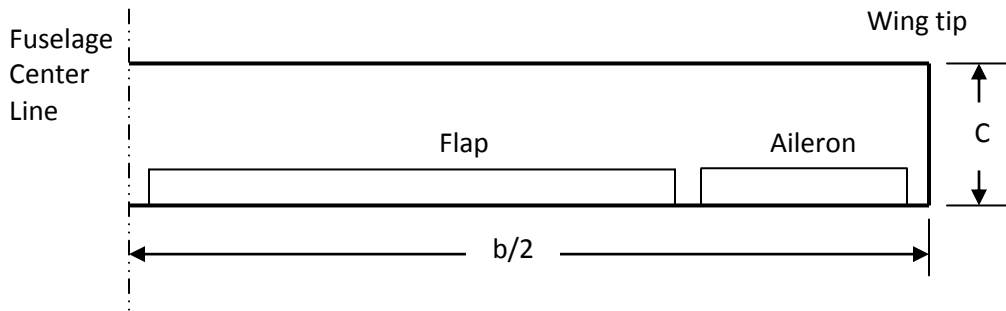


*Figure 5.56. Typical location of the aileron on the wing*

At this section, it is mainly emphasized that do not consume all wing trailing edge for flap and leave about 30 percent of the wing outboard for ailerons. Figure 5.56 illustrates the typical location of the aileron on the wing. Three major parameters that need to be determined in aileron design process are: aileron chord, aileron span, and aileron deflection (up and down). The primary design requirements in aileron design originate from roll controllability of the aircraft. The full discussion on aileron design and aileron design technique will be covered in chapter 12.

## 5.14. Lifting Line Theory

In section 5.7, it is explained that in the wing design process, the designer must calculate the lift force that a wing is generating. Then, by changing wing parameters one can finalize wing parameters to achieve the design goals while satisfying all design requirements. The technique is essentially comes from the area of Aerodynamics, however, in order to complete the discussion on the wing design, a rather straight forward, but at the same time relatively accurate technique is introduced. A wing designer must have a solid background on the topic of Aerodynamics; so this section plays the role of a review for you. For this reason, materials in this section are covered without proof. For more and detailed information, you are referred to the Reference 16.

The technique introduced in this section, allows the reader to determine the amount the lift that is generated by a wing without using sophisticated CFD software. You need to have all wing data in hand such as wing area, airfoil section and its features, aspect ratio, taper ratio, wing incidence, and high lift device type and data. By solving several aerodynamic equations simultaneously, one can determine the amount of lift that a wing is producing. Furthermore, the technique will generate the lift distribution along the span, hence one can make sure that if the lift distribution is elliptical or not.

The technique is initially introduced by Ludwig Prandtl and is called "*lifting-line theory*" in 1918. Almost every *Aerodynamics* textbook has the details of this simple and remarkably

accurate technique. The major weakness of this classical technique is that it is a linear theory; thus, it does not predict stall. Therefore, if you know the airfoil section's stall angle, do not employ this approach beyond the airfoil's stall angle. The technique can be applied for a wing with both flap up and flap down (i.e. deflected). In the following, the steps to calculate the lift distribution along the span plus total wing lift coefficient will be presented. Since a wing has a symmetric geometry, we only need to consider one half of the wing. The technique can later be extended to both left and right wing-half. The application of the technique will be demonstrated at the end of this chapter.
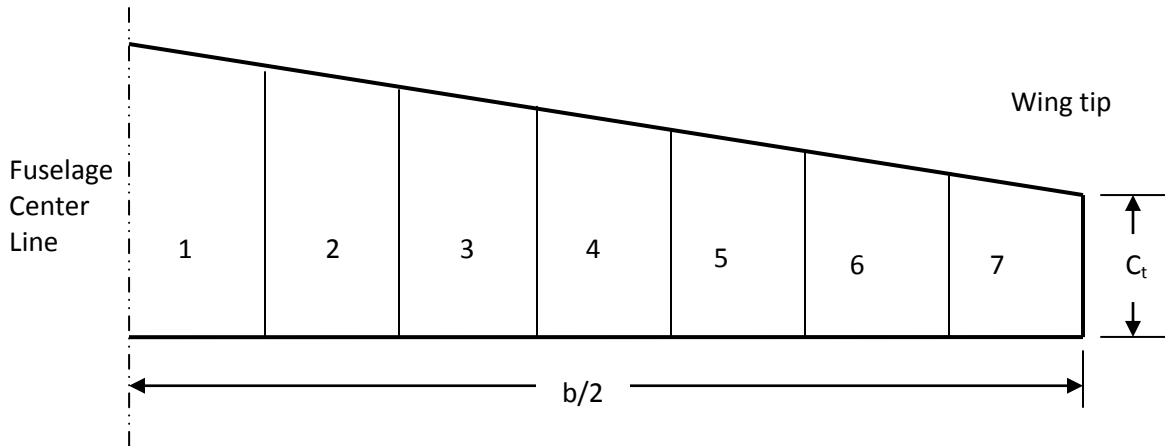

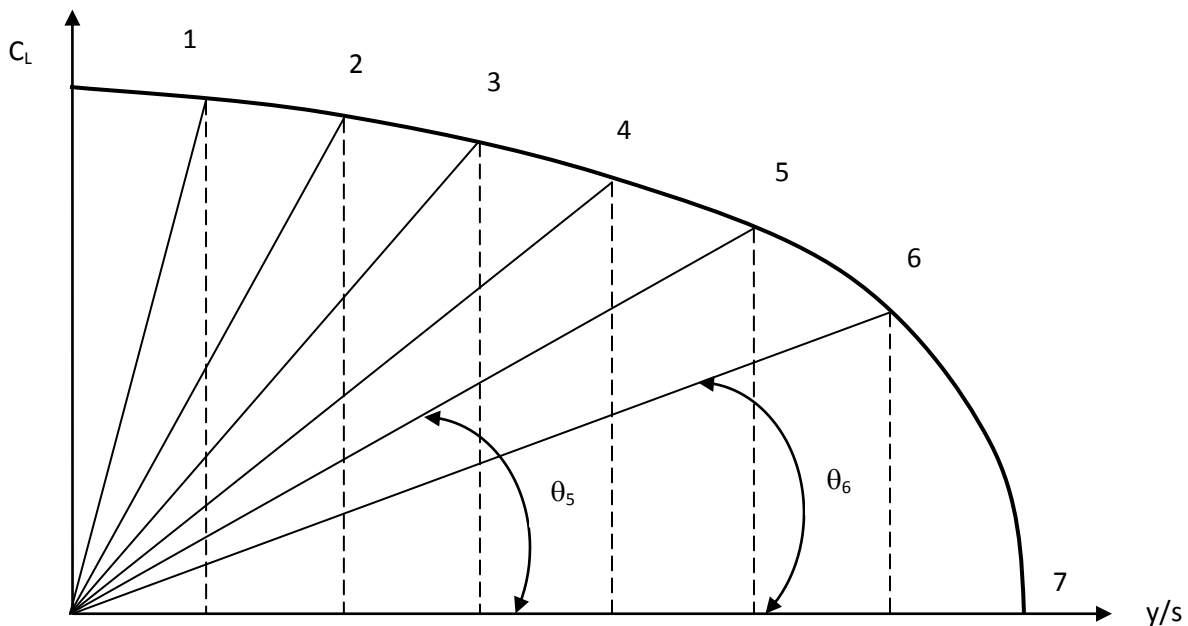
*Figure 5.57. Dividing a wing into several sections*



*Figure 5.58. Angles corresponding to each segment in lifting-line theory*

**Step 1.** Divide one half of the wing (semispan) into several (say N) segments. The segments along the semispan could have equal span, but it is recommended to have smaller segments in

the regions closer to the wing tip. The higher number of segments (N) is desired, since it yields a higher accuracy. As an example, in figure 5.57, a wing is shown that is divided into seven equal segments. As noted each segment has a unique chord and may have a unique span. You have the option to consider a unique airfoil section for each segment as well (recall the aerodynamic twist). Then, identify the geometry (e.g. chord and span) and aerodynamic properties (e.g. $\alpha$, $\alpha_o$, $C_{l\alpha}$) of each segment for future application.

**Step 2.** Calculate the corresponding angle ($\theta$) to each section. These angles are functions of lift distribution along the semispan as depicted in figure 5.58. Each angle ($\theta$) is defined as the angle between the horizontal axis and the intersection between lift distribution curve and the segment line. In fact, we originally assume that the lift distribution along the semispan is elliptical. This assumption will be corrected later.

The angle $\theta$ varies between 0 for the last segment; to a number close to 90 degrees for the first segment. The value of angle $\theta$ for other segments may be determined from corresponding triangle as shown in figure 5.58. For instance in figure 5.58, the angle $\theta_6$ is the angle corresponding to the segment 6.

**Step 3.** Solve the following group of equations to find $A_1$ to $A_n$:

$$\mu(\alpha_o - \alpha) = \sum_{n=1}^{N} A_n \sin(n\theta)\left(1 + \frac{\mu n}{\sin(\theta)}\right) \tag{5.40}$$

This equation is the heart of the theory and is referred to as the *lifting-line* equation or *monoplane* equation. The equation initially developed by Prandtl. In this equation, N denotes number of segments; $\alpha$ segment's angle of attack; $\alpha_o$ segment's zero-lift angle of attack; and coefficients $A_n$ are the intermediate unknowns. The parameter $\mu$ is defined as follows:

$$\mu = \frac{\overline{C}_i \cdot C_{l_\alpha}}{4b} \tag{5.41}$$

where $\overline{C}_i$ denotes the segment's mean geometric chord, $C_{l\alpha}$ segment's lift curve slope in 1/rad; and "b" is the wing span. If the wing has a twist ($\alpha_t$)., the twist angle must be applied to all segments linearly. Thus, the angle of attack for each segment is reduced by deducting the corresponding twist angle from wing setting angle. If the theory is applied to a wing in a take-off operation, where flap is deflected, the inboard segments have larger zero-lift angle of attack ($\alpha_o$) than outboard segments.

**Step 4.** Determine each segment's lift coefficient using the following equation:

$$C_{L_i} = \frac{4b}{\overline{C}_i}\sum A_n \sin(n\theta) \tag{5.42}$$

Now you can plot the variation of segment's lift coefficient ($C_L$) versus semispan (i.e. lift distribution).

**Step 5.** Determine wing total lift coefficient using the following equation:

$$C_{L_i} = \pi \cdot AR \cdot A_1 \tag{5.43}$$

where AR is the wing aspect ratio.

Please note that the lifting-line theory has other useful features, but they are not covered and used here.

## Examples 5.5

Determine and plot the lift distribution for a wing with the following characteristics. Divide the half wing into 10 sections.

$S = 25$ m$^2$, AR = 8, $\lambda = 0.6$, $i_w = 2$ deg, $\alpha_t = -1$ deg, airfoil section: NACA 63-209

If the aircraft is flying at the altitude of 5,000 m ($\rho = 0.736$ kg/m$^3$) with a speed of 180 knot, how much lift is produced?

**Solution:**

By using the Reference 2, we can find the airfoil section's features. A copy of the airfoil graphs are shown in figure 5.22. Based on the $C_l$-$\alpha$ graph, we have the following data:

$$\alpha_o = -1.5 \text{ degrees}, C_{l\alpha} = 6.3 \text{ 1/rad}$$

The application of the lifting-line theory is formulated through the following MATLAB m-file.

```
clc
clear
N = 9; % (number of segments - 1)
S = 25; % m^2
AR = 8; % Aspect ratio
lambda = 0.6; % Taper ratio
alpha_twist = -1; % Twist angle (deg)
i_w = 2; % wing setting angle (deg)
a_2d = 6.3; % lift curve slope (1/rad)
alpha_0 = -1.5; % zero-lift angle of attack (deg)
b = sqrt(AR*S); % wing span (m)
MAC = S/b; % Mean Aerodynamic Chord (m)
Croot = (1.5*(1+lambda)*MAC)/(1+lambda+lambda^2); % root chord (m)
theta = pi/(2*N):pi/(2*N):pi/2;
alpha=i_w+alpha_twist:-alpha_twist/(N-1):i_w; % segment's angle of attack
z = (b/2)*cos(theta);
c = Croot * (1 - (1-lambda)*cos(theta)); % Mean Aerodynamics Chord at each
segment (m)
mu = c * a_2d / (4 * b);
LHS = mu .* (alpha-alpha_0)/57.3; % Left Hand Side
% Solving N equations to find coefficients A(i):
for i=1:N
    for j=1:N
```

```
    B(i,j) =  sin((2*j-1) * theta(i)) * (1 + (mu(i) * (2*j-1)) /
sin(theta(i)));
    end
end
A=B\transpose(LHS);
for i = 1:N
    sum1(i) = 0;
    sum2(i) = 0;
    for j = 1 : N
        sum1(i) = sum1(i) + (2*j-1) * A(j)*sin((2*j-1)*theta(i));
        sum2(i) = sum2(i) + A(j)*sin((2*j-1)*theta(i));
    end
  end
CL = 4*b*sum2 ./ c;
CL1=[0 CL(1) CL(2) CL(3) CL(4) CL(5) CL(6) CL(7) CL(8) CL(9)];
y_s=[b/2 z(1) z(2) z(3) z(4) z(5) z(6) z(7) z(8) z(9)];
plot(y_s,CL1,'-o')
 grid
title('Lift distribution')
xlabel('Semi-span location (m)')
ylabel ('Lift coefficient')
CL_wing = pi * AR * A(1)
```

Figure 5.59 shows the lift distribution of the example wing as an output of the m-file.
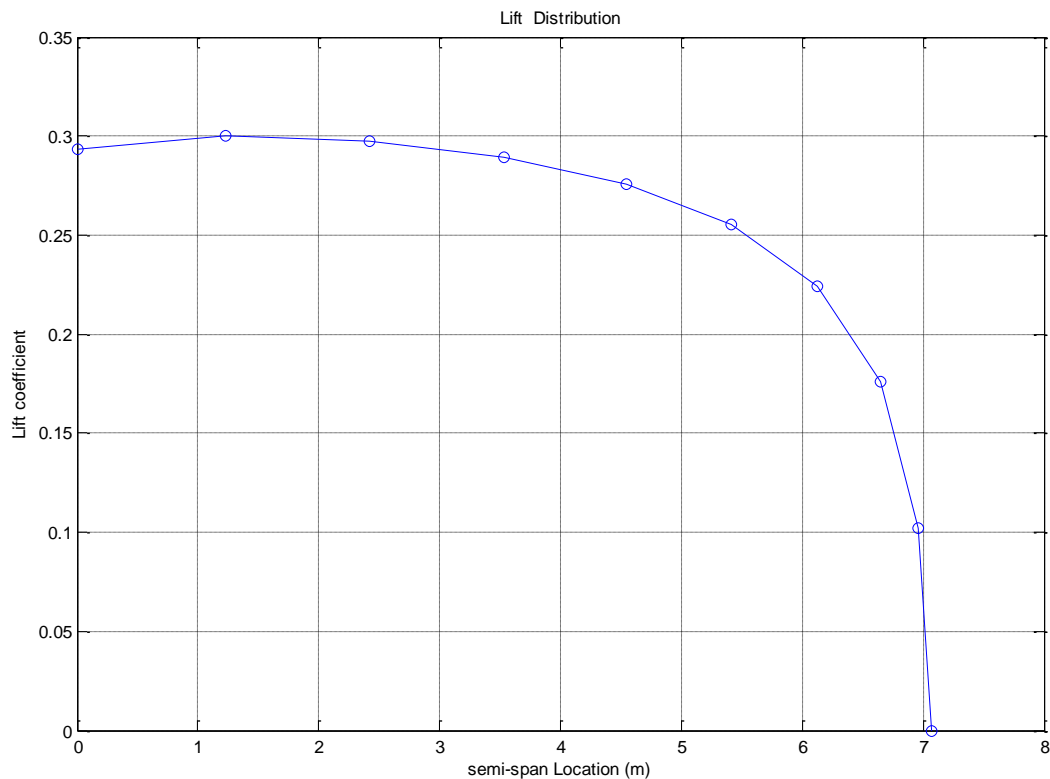


*Figure 5.59. The lift distribution of the wing in example 5.5*

As noted, the distribution in this wing is not elliptical, so it is not ideal. The wing needs some modification (such as increasing wing twist) to produce an acceptable output. The total lift coefficient of the wing is $C_L = 0.268$. The lift generated by this wing is as follows:

$$L = \frac{1}{2}\rho V^2 S C_L = \frac{1}{2} \times 0.736 \times (180 \times 0.5144)^2 \times 25 \times 0.268 = 21{,}169.2 \quad N \qquad (5.1)$$

To check the accuracy of lifting line theory, several aircraft are selected (from Ref. 4) to compare their real cruise lift coefficients with calculated lift coefficients based on this theory. The characteristics of these aircraft are given in table 5.17. For instance, the cruising lift coefficient for the *Bellance* aircraft based on the lift equation (Equation 5.10) is 0.2193, while the theoretical lift coefficient based on the lifting line theory would be 0.229. The difference between these two lift coefficients is only 4.5 percent. Thus, it can be concluded that the lifting line theory is fairly accurate for the low speed aircraft and can be utilized in the initial wing design process.

| Aircraft | $S$ (m$^2$) | $\lambda$ | AR | $\alpha_t$ (deg) | NACA | $\alpha_o$ (deg) | $C_{dmin}$ | $C_{lmin}$ | $i_w$ (deg) | mass (kg) | $V_c$ (knot) |
|---|---|---|---|---|---|---|---|---|---|---|---|
| Cessna 304A | 17.1 | 0.7 | 7.2 | 5.9 | 23018-23015 | - | - | - | 2° 3' | 2717 | 233 @ 24500 ft @ %75 power |
| Brandli | 8.5 | 0.77 | 5.7 | - | 747A415 | -2 | 0.0043 | 0.5 | 3 | 550 | - |
| Aerocare IMP | 10.4 | 1 | 7 | - | 4415 | -4 | 0.0065 | 0.3 | 0 | 703 | 130 |
| Cojetkovic CA61-61R | 11.75 | 1 | 6 | 0 | 4415 | -4 | 0.0065 | 0.3 | 0 | 430 | 104 |
| Scottish Aviation SA-3-120 | 12.52 | 0.59 | 8.4 | 0 | 63$_2$-615 | -4 | 0.005 | 0.4 | 1.15 | 1066 | 120 @ 1200 m @ %75 power |
| Bellanca 19-25 | 16.92 | 0.7 | 6.7 | 0 | 63$_2$-215 | -1 | 0.0047 | 0.2 | 2 | 1860 | 262 @ 7300 m @ %75 power |

*Table 5.17. Characteristics of several aircraft to check the accuracy of lifting line theory*

## 5.15. Accessories
Depending upon the aircraft type and flight conditions, the wing may have a few accessories to improve the flow over the wing. The accessories such as wingtip, fence, vortex generator, stall stripes, and strake are employed to increase the wing efficiency. In this section, few practical considerations will be introduced.

### 5.15.1. Strake
A strake (also known as a leading edge extension) is an aerodynamic surface generally mounted on the fuselage of an aircraft to fine-tune the airflow and to control the vortex over the wing. In order to increase lift and improve directional stability and maneuverability at high angles of

attack, highly swept strakes along fuselage forebody may be employed to join the wing sections. Aircraft designers choose the location, angle and shape of the strake to produce the desired interaction. Fighter aircraft F-16 and F-18 have employed strakes to improve the wing efficiency at high angles of attack. The design of the strake needs a high fidelity CFD software and is beyond the scope of this book.

## 5.15.2. Fence

Stall fences are used in swept wings to prevent the boundary layer drifting outboard toward the wing tips. Boundary layers on swept wings tend to drift because of the spanwise pressure gradient of a swept wing. Swept wing often have a leading edge fence of some sort, usually at about 35 percent of the span from fuselage centerline as shown in figure 5.60. The cross-flow creates a side lift on the fence that produces a strong trailing vortex. This vortex is carried over the top surface of the wing, mixing fresh air into the boundary layer and sweeping the boundary layer off the wing and into the outside flow. The result is a reduction in the amount of boundary layer air flowing outboard at the rear of the wing. This improves the outer panel maximum lift coefficient.
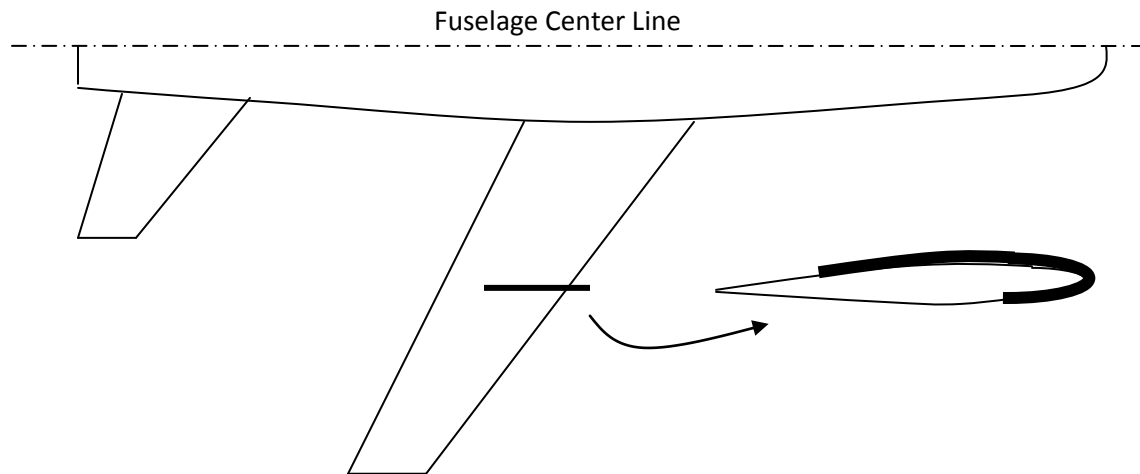


***a.*** *Fence over the wing*



b. *Fence over the canard of Beech Starship*

*Figure 5.60. Example of a stall fence*

Similar results can be achieved with a leading edge snag. Such snags tend to create a vortex which acts like a boundary layer fence. The ideal device is the under-wing fence, referred to as *vertilon*. Pylons supporting the engines under the wing, in practice, serve the purpose of the leading edge fences. Several high subsonic transport aircraft such as DC-9 and Beech Starship have utilized fence on their swept lifting surfaces. The design of the fence needs a high fidelity CFD software and is beyond the scope of this book.

### 5.15.3. Vortex generator

Vortex generators are very small, low aspect ratio wings placed vertically at some local angle of attack on the wing, fuselage or tail surfaces of aircraft. The span of the vortex generator is typically selected such that they are just outside the local edge of the boundary layer. Since they are some types of lifting surfaces, they will produce lift and therefore tip vortices near the edge of the boundary layer. Then these vortices will mix with the high energy air to raise the kinetic energy level of the flow inside the boundary layer. Hence, this process allows the boundary layer to advance further into an adverse pressure gradient before separating. Vortex generators are employed in many different sizes and shapes.

Most of today's high subsonic jet transport aircraft have large number of vortex generators on wings, tails and even nacelles. Even though vortex generators are beneficial in delaying local wing stall, but they can generate considerable increase in aircraft drag. The precise number and orientation of vortex generators are often determined in a series of sequential flight tests. For this reason, they are sometimes referred to as "aerodynamic afterthoughts". Vortex generators are usually added to an aircraft after test has indicated certain flow separations. In Northrop Grumman B-2A strategic penetration bomber utilizes small, drop-down spoiler panels ahead of weapon bay doors to generate vortexes to ensure clean weapon release. Figure 5.61 illustrates the Hawker Beechcraft Beech King 1900D twin turboprop regional airliner that equipped with small horizontal vortex generator on fuselage ahead of wing roots.



Figure 5. 61. The Hawker Beechcraft Beech King 1900D (note on winglets)
(Photo courtesy of Prestwick 99)

### 5.15.4. Winglet

Since there is a considerable pressure difference between lower and upper surfaces of a wing, tip vortices are produced at the wingtips. These tip vortices will then roll up and get around the local edges of a wing. This phenomenon will reduce the lift at the wingtip station, so they can be represented as a reduction in effective wing span. Experiments have shown that wings with

square or sharp edges have the widest effective span. To compensate this loss, three solutions are tip-tank; extra wing span; and winglet. Winglets are small, nearly vertical lifting surfaces, mounted rearward and/or downward relative to the wing tips.

The aerodynamic analysis of a winglet (e.g. lift, drag, local flow circulation) may be performed by classical aerodynamic techniques. The necessity of wingtips depends on the mission and the configuration of an aircraft, since they will add to the aircraft weight. Several small and large transport aircraft such as Pilatus PC-12, Boeing 747-400, McDonnell Douglas C-17A Globemaster III, and Airbus 340-300 have winglets. Figure 5.61 illustrates the Hawker Beechcraft Beech King 1900D twin turboprop regional airliner that equipped with winglets in order to improve hot and high performance.

## 5.16. Wing Design Steps

At this stage, we are in a position to summarize the chapter. In this section, the practical steps in a wing design process are introduced (see figure 5.1) as follows:

**Primary function:** Generation of the lift

1. Select number of wings (e.g. monoplane, bi-plane). See section 5.2.
2. Select wing vertical location (e.g. high, mid, low). See section 5.3.
3. Select wing configuration (e.g. straight, swept, tapered, delta).
4. Calculate average aircraft weight at cruise:

$$W_{ave} = \frac{1}{2}\left(W_i + W_f\right) \tag{5.44}$$

where $W_i$ is the aircraft at the beginning of cruise and $W_f$ is the aircraft at the end of cruising flight.

5. Calculate required aircraft cruise lift coefficient (with average weight):

$$C_{Lc} = \frac{2W_{ave}}{\rho V_c^2 S} \tag{5.45}$$

6. Calculate the required aircraft take-off lift coefficient:

$$C_{L_{TO}} = 0.85\frac{2W_{TO}}{\rho V_{TO}^2 S} \tag{5.46}$$

The coefficient 0.85 originates from the fact that during a take-off, the aircraft has the take-off angle (say about 10 degrees). Thus about 15 percent of the lift is maintained by the vertical component (sin (10)) of the engine thrust.

7. Select the high lift device (HLD) type and its location on the wing. See section 5.12.
8. Determine high lift device geometry (span, chord, and maximum deflection). See section 5.12.

9. Select/Design airfoil (you can select different airfoil for tip and root). The procedure was introduced in Section 5.4.
10. Determine wing incidence or setting angle ($i_w$). It is corresponding to airfoil ideal lift coefficient; $C_{li}$ (where airfoil drag coefficient is at minimum). See section 5.5.
11. Select sweep angle ($\Lambda_{0.5C}$) and dihedral angles ($\Gamma$). See sections 5.9 and 5.11.
12. Select other wing parameter such as aspect ratio (AR), taper ratio ($\lambda$) and wing twist angle ($\alpha_{twist}$). See sections 5.6, 5.7, and 5.10.
13. Calculate lift distribution at cruise (without flap, or flap up). Use tools such as lifting line theory (See section 5.14), and Computational Fluid Dynamics).
14. Check the lift distribution at cruise that must be elliptic. Otherwise, return to step 13 and change few parameters.
15. Calculate wing lift at cruise ($C_{Lw}$). Do not employ HLD at cruise.
16. The wing lift coefficient at cruise ($C_{Lw}$) must be equal to the required cruise lift coefficient (step 5). If not, return to step 10 and change wing setting angle.
17. Calculate wing lift coefficient at take-off ($C_{L\_w\_TO}$). Employ flap at take-off with the deflection of $\delta_f$ and wing angle of attack of: $\alpha_w = \alpha_{sTO} - 1$. Note that $\alpha_s$ at take-off is usually smaller than $\alpha_s$ at cruise. Please note that the minus one (-1) is for safety.
18. The wing lift coefficient at take-off ($C_{L\_w\_TO}$) must be equal to take-off lift coefficient (step 6). If not, first, play with flap deflection ($\delta_f$), and geometry ($C_f$, $b_f$); otherwise, return to step 7 and select another HLD. You can have more than one for more safety.
19. Calculate wing drag ($D_w$).
20. Play with wing parameters to minimize the wing drag.
21. Calculate wing pitching moment ($M_{ow}$). This moment will be used in the tail design process.
22. Optimize the wing to minimize wing drag and wing pitching moment

A fully solved example will demonstrate the application of these steps in the next section.

## 5.17. Wing Design Example
In this section, a major wing design example with the full solution is presented. To avoid lengthening the section, few details are not described and left to the reader to discover. These details are very much similar to the solutions that are explained in other examples of this section.

## Example 5.6

Design a wing for a normal category General Aviation aircraft with the following features:

$$S = 18.1 \text{ m}^2, \text{ m} = 1,800 \text{ kg}, V_C = 130 \text{ knot (@ sea level)}, V_S = 60 \text{ knot}$$

Assume the aircraft has a monoplane high wing and employs the split flap.

**Solution:**

The number of wings and wing vertical position are stated by the problem statement, so we do not need to investigate these two parameters.

### 1. Dihedral angle

Since the aircraft is a high wing, low subsonic, mono-wing aircraft, based on table 5.8, a "-5" degrees of anhedral is selected. This value will be revised and optimized when other aircraft components are designed during lateral stability analysis.

### 2. Sweep angle

The aircraft is a low subsonic prop-driven normal category aircraft. To keep the cost low in the manufacturing process, we select no sweep angle at 50 percent of wing chord. However, we may need to taper the wing; hence the leading edge and trailing edge may have sweep angles.

### 3. Airfoil

To be fast in the wing design, we select an airfoil from NACA selections. The design of an airfoil is out of the scope of this text book. The selection process of an airfoil for the wing requires some calculations as follows:

- Section's ideal lift coefficient:

$$C_{L_C} = \frac{2W_{ave}}{\rho V_c^2 S} = \frac{2 \times 1800 \times 9.81}{1.225 \times (130 \times 0.514)^2 \times 18.1} = 0.356 \tag{5.10}$$

$$C_{L_{C_w}} = \frac{C_{L_C}}{0.95} = \frac{0.356}{0.95} = 0.375 \tag{5.11}$$

$$C_{l_i} = \frac{C_{L_{C_w}}}{0.9} = \frac{0.375}{0.9} = 0.416 \tag{5.12}$$

- Section's maximum lift coefficient:

$$C_{L_{max}} = \frac{2W_{TO}}{\rho_o V_s^2 S} = \frac{2 \times 1800 \times 9.81}{1.225 \times (60 \times 0.514)^2 \times 18.1} = 1.672 \tag{5.13}$$

$$C_{L_{max_w}} = \frac{C_{L_{max}}}{0.95} = \frac{1.672}{0.95} = 1.76 \tag{5.14}$$

$$C_{l_{max_{gross}}} = \frac{C_{L_{max_w}}}{0.9} = \frac{1.76}{0.9} = 1.95 \tag{5.15}$$

The aircraft has a split flap, and the split flap generates an $\Delta C_L$ of 0.55 when deflected 30 degrees. Thus:

$$C_{l_{max}} = C_{l_{max_{gross}}} - \Delta C_{l_{max_{HLD}}} = 1.95 - 0.45 = 1.5 \qquad (5.16)$$

Thus, we need to look for NACA airfoil sections that yield an ideal lift coefficient of 0.4 and a net maximum lift coefficient of 1.5.

$$C_{l_i} = 0.416 \approx 0.4$$

$$C_{l_{max}} = 1.95 \qquad\qquad\qquad\qquad \textbf{(Flap down)}$$

$$C_{l_{max}} = 1.5 \qquad\qquad\qquad\qquad \textbf{(Flap up)}$$

By referring to Reference 2 and figure 5.23, we find the following seven airfoil sections whose characteristics match with or is close to our design requirements (all have $C_{li} = 0.4$, $C_{lmax} \approx 1.5$):

<div align="center">

**$63_1$-412, $63_2$-415, $64_1$-412, $64_2$-415, $66_2$-415**

</div>

Now we need to compare these airfoil sections to see which one is the best. The Table 5.18 compares the characteristics of the seven candidates. The best airfoil is the airfoil whose $C_{mo}$ is the lowest, the $C_{dmin}$ is the lowest, the $\alpha_s$ is the highest, the $(C_l/C_d)_{max}$ is the highest, and the stall quality is docile. By comparing the numbers in the above table, we can conclude the followings:

1- The NACA airfoil section $66_2$-415 yields the highest maximum speed, since it has the lowest $C_{dmin}$ (i.e. 0.0044).
2- The NACA airfoil section $64_2$-415 yields the lowest stall speed, since it has the highest maximum lift coefficient (i.e. 2.1).
3- The NACA airfoil section $66_2$-415 yields the highest endurance, since it has the highest $(C_l/C_d)_{max}$ (i.e. 150).
4- The NACA $63_2$-415 and $64_2$-415 yield the safest flight, due to its docile stall quality.
5- The NACA airfoil section $64_2$-415 delivers the lowest longitudinal control effort in flight, due to the lowest $C_{mo}$ (i.e. -0.056).

| No | NACA | $C_{dmin}$ | $C_{mo}$ | $\alpha_s$ (deg) Flap up | $\alpha_o$ (deg) $\delta_f = 60^o$ | $(C_l/C_d)_{max}$ | $C_l$ | $C_{lmax}$ $\delta_f = 30^o$ | Stall quality |
|----|------|-----------|----------|---------|---------|-----------------|-------|---------|-------|
| 1 | $63_1$-412 | 0.0049 | -0.075 | 11 | -13.8 | 120 | 0.4 | 2 | Moderate |
| 2 | $63_2$-415 | 0.0049 | -0.063 | 12 | -13.8 | 120 | 0.4 | 1.8 | Docile |
| 3 | $64_1$-412 | 0.005 | -0.074 | 12 | -14 | 111 | 0.4 | 1.8 | Sharp |
| 4 | $64_2$-415 | 0.005 | -0.056 | 12 | -13.9 | 120 | 0.4 | 2.1 | Docile |
| 5 | $66_2$-415 | 0.0044 | -0.068 | 17.6 | -9 | 150 | 0.4 | 1.9 | Moderate |
| 6 | 4412 | 0.006 | -0.1 | 14 | -15 | 133 | 0.4 | 2 | Moderate |
| 7 | 4418 | 0.007 | -0.085 | 14 | -16 | 100 | 0.4 | 2 | Moderate |

*Table 5.18. A comparison between seven airfoil candidates for the wing in example 5.6*

Since the aircraft is a non-maneuverable GA aircraft, the stall quality cannot be sharp; hence NACA $64_1$-412 is not acceptable. If the safety is the highest requirement, the best airfoil is

NACA $64_2$-415 due to its high $C_{lmax}$. When the maximum endurance is the highest priority, NACA airfoil section $66_2$-415 is the best, due to its high $(C_l/C_d)_{max}$. On the other hand, if the low cost is the most important requirement, NACA $66_2$-415 with the lowest $C_{dmin}$ is the best. However, if the aircraft stall speed, stall quality and lowest longitudinal control power are of greatest important design requirement, the NACA airfoil section $64_2$-415 is the best. This may be performed by using a comparison table incorporating the weighted design requirements.

Due to the fact that NACA airfoil section $64_2$-415 is the best in terms of three criteria, we select it as the most suitable airfoil section for this wing. Figure 5.62 illustrates the characteristics graphs of this airfoil.
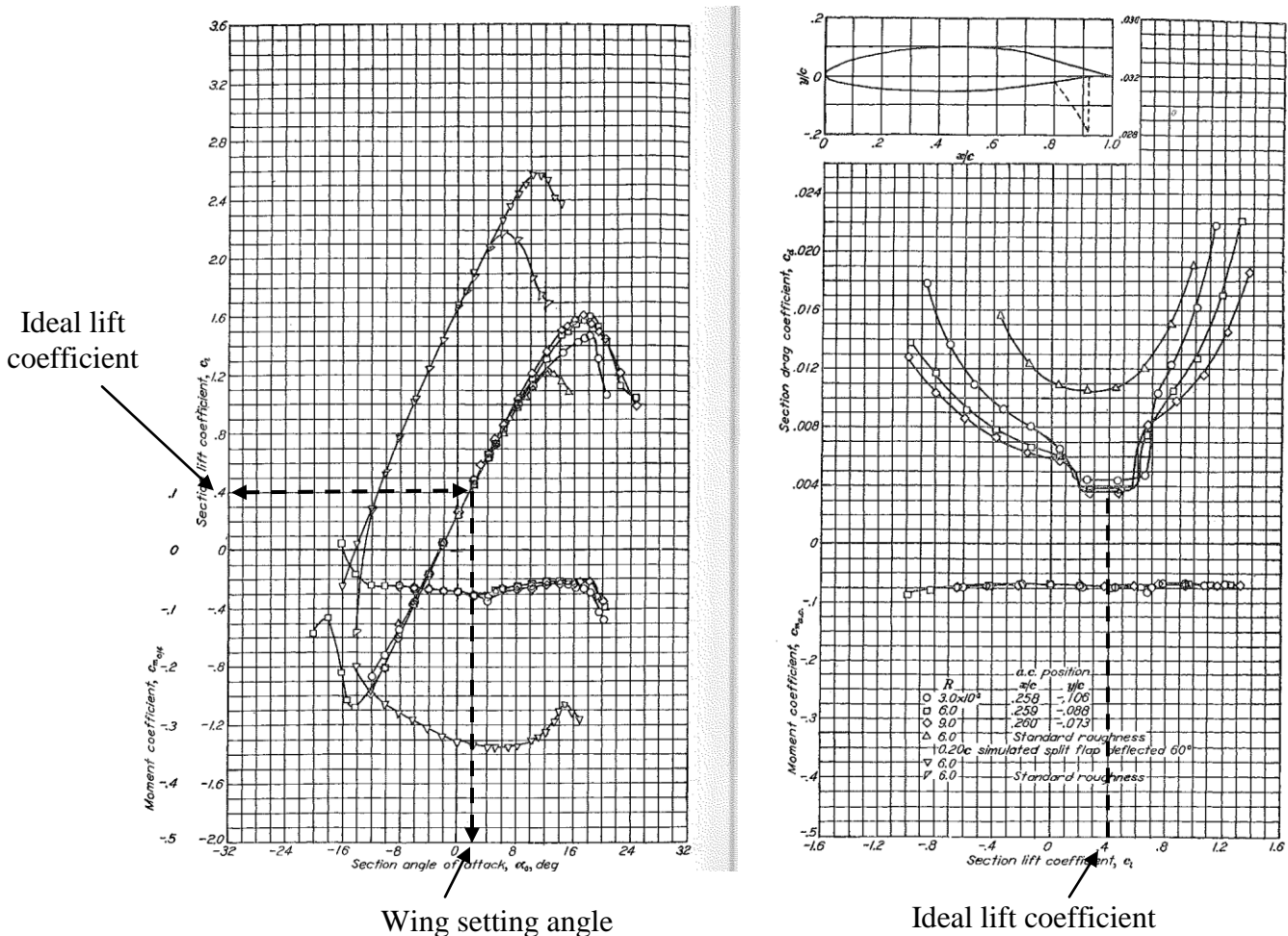


*Figure 5.62. Airfoil section NACA $66_2$-415*

### 4. Wing setting angle

Wing setting angle is initially determined to be the corresponding angle to the airfoil ideal lift coefficient. Since the airfoil ideal lift coefficient is 0.416, figure 5.62 (left figure) reads the corresponding angle to be 2 degrees. The value ($i_w$ = 2 deg) may need to be revised based on the calculation to satisfy the design requirements later.

### 5. Aspect ratio, Taper ratio, and Twist angle

Three parameters of aspect ratio, taper ratio, and twist angle are determined concurrently, since they are all influential for the lift distribution. Several combinations of these three parameters might yield the desirable lift distribution which is elliptical. Based on the table 5.6, the aspect ratio is selected to be 7 (AR = 7). No twist is assumed ($\alpha_t$ = 0) at this time to keep the manufacturing cost low and easier to build. The taper ratio is tentatively considered 0.3 ($\lambda$ = 3). Now we need to find out 1. if the lift distribution is elliptical; 2. if the lift created by this wing at cruise is equal to the aircraft weight. The lifting line theory is employed to determine lift distribution and wing lift coefficient.
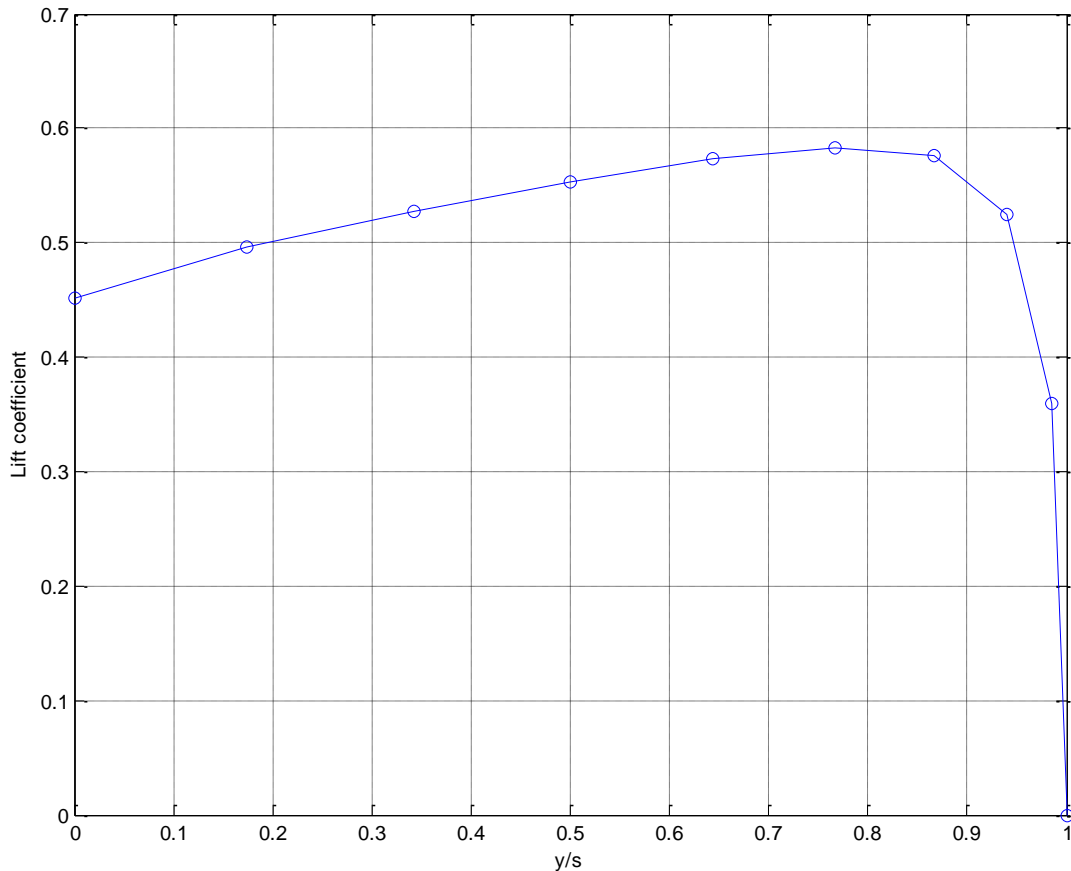


*Figure 5.63. The lift distribution of the wing (AR = 7, $\lambda$ = 0.3, $\alpha_t$ =0, $i_w$ =2 deg)*

A MATLAB m-file is developed similar to what is shown in example 5.5. The application of the lifting-line theory is formulated through this m-file. Figure 5.63 shows the lift distribution of the wing as an output of the m-file. The m-file also yields the lift coefficient to be:

$C_L$ = 0.4557

Two observations can be made from the results: 1. The lift coefficient is slightly higher than what is needed (0.4557 > 0.356); 2. The lift distribution is not elliptical. Therefore, some wing features must be changed to correct both outcomes.

After several trial and errors, the following wing specifications are found to satisfy the design requirements:

$$AR = 7, \lambda = 0.8, \alpha_t = \text{-1.5 deg}, i_w = 1.86 \text{ deg}$$

By using the same m-file and these new parameters, the following results are obtained:

- $C_L = 0.359$

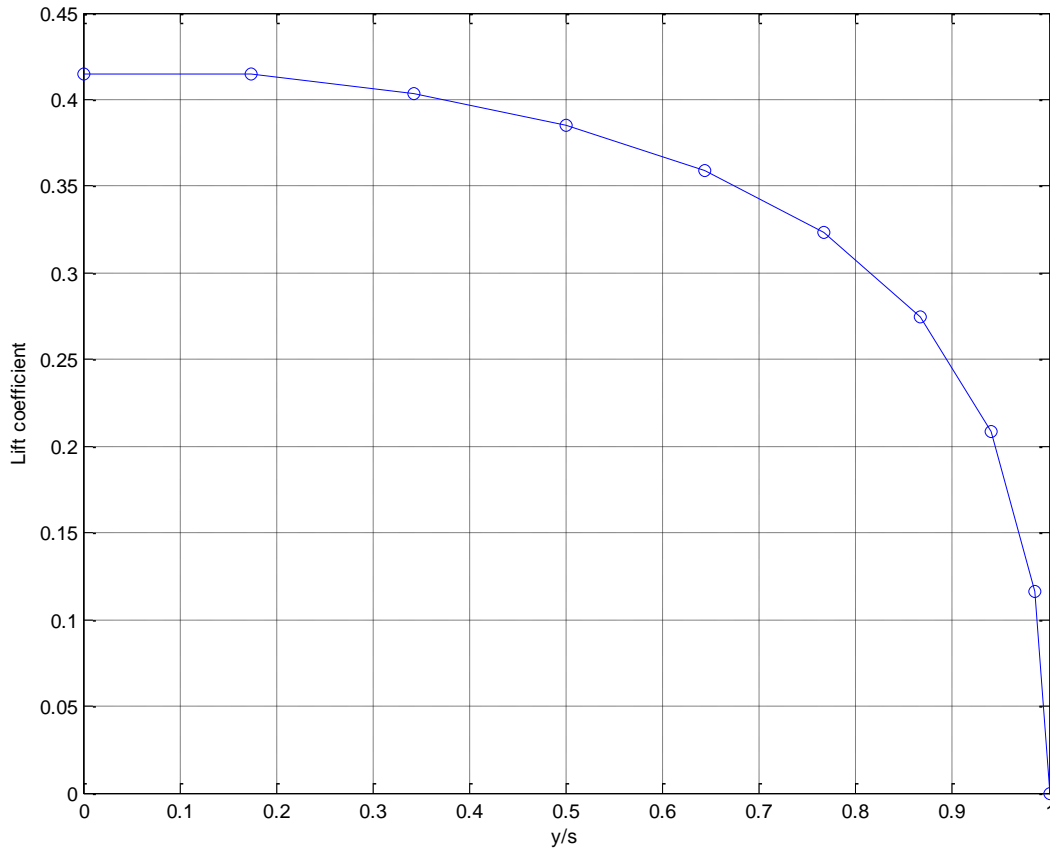- Elliptical lift distribution as shown in figure 5.64.



*Figure 5.64. The lift distribution of the wing (AR = 7, λ = 0.8, $\alpha_t$ =-1.5, $i_w$ =1.86 deg)*

Hence, this wing with the above parameters satisfies the aircraft cruise requirements. Now, we need to proceed to design the flap and to determine the flap parameters to satisfy the take-off requirements.

## 6. Flap parameters

Flap is usually employed during take-off and landing operations. We design the flap based on the take-off requirements and shall adjust it for the landing requirements. The take-off speed for a GA aircraft is about 20 percent faster than stall speed:

$$V_{TO} = 1.2 \cdot V_S = 1.2 \times 60 = 72 \quad knot = 37 \quad \frac{m}{\sec} \tag{5.38}$$

Hence, the wing; while flap is deflected; must generate the following lift coefficient during take-off:

$$C_{L_{TO}} = \frac{2W_{TO}}{\rho_o V_{TO}^2 S} = \frac{2 \times 1800 \times 9.81}{1.225 \times (37)^2 \times 18.1} = 1.161 \tag{5.46}$$

As the problem statement indicates, the wing employs a split flap. We need to determine the flap chord, flap span and flap deflection during take-off and landing. The flap chord is tentatively set to be 20 percent of wing chord. The flap span is tentatively set to be 60 percent of wing span. This is to leave about 30 percent of the wing span for aileron in future design applications. The flap deflection for take-off operation is tentatively set to be 20 degrees. The reasons for these three selections are found in the section 5.12. The wing angle of attack during take-off operation also needs to be decided. This angle is assumed to be as high as possible. Based on the figure 5.57, the airfoil stall angle is about 12 degrees when the flap is deflected 20 degrees (using an interpolation). For the sake of safety, we use only 10 degrees of angle of attack for wing during take-off operation, which is two degrees less than stall angle of attack. Thus, the initial flap parameters are as follows:

$$b_f/b = 0.6; \; C_f/C = 0.2, \; \alpha_{TO\_wing} = 10 \text{ degrees}, \; \delta_f = 20 \text{ degrees}$$

The lifting line theory is utilized again to determine the wing lift coefficient at take-off by the above high lift device specifications. A similar m-file is prepared as we did in previous section. The major change is to apply a new zero-lift angle of attack for the inboard (flap) section. The change in the zero-lift angle of attack for the inboard (flap) section is:

$$\Delta\alpha_o \approx -10 \cdot \Delta C_L \tag{5.39}$$

Based on the figure 5.62, the split flap increases the section's lift coefficient by 0.3 when deflected 20 degrees. Thus:

$$\Delta\alpha_o \approx -10 \cdot (0.3) = -3 \quad \text{deg} \tag{5.39}$$

This number will be entered in the lifting line program as input. This means that the inboard section (60 percent of the wing span) will have zero lift angle of attack of -6 (i.e. (-3) + (-3) = -6) due to flap deflection. The following is the *matlab* m-file to calculate the wing lift coefficient while the flap is deflected down during the take-off operation:

```
clc
clear
N = 9; % (number of segments-1)
S = 18.1; % m^2
AR = 7; % Aspect ratio
lambda = 0.8; % Taper ratio
alpha_twist = -1.5; % Twist angle (deg)
i_w = 10; % wing setting angle (deg)
a_2d = 6.3; % lift curve slope (1/rad)
a_0 = -3; % flap up zero-lift angle of attack (deg)
a_0_fd = -6; % flap down zero-lift angle of attack (deg)
b = sqrt(AR*S); % wing span
bf_b=0.6; %flap-to-wing span ratio
```

```matlab
MAC = S/b; % Mean Aerodynamic Chord
Croot = (1.5*(1+lambda)*MAC)/(1+lambda+lambda^2); % root chord
theta = pi/(2*N):pi/(2*N):pi/2;
alpha=i_w+alpha_twist:-alpha_twist/(N-1):i_w; % segment's angle of attack
for i=1:N
if (i/N)>(1-bf_b)
        alpha_0(i)=a_0_fd; %flap down zero lift AOA
else
      alpha_0(i)=a_0; %flap up zero lift AOA
 end
end
z = (b/2)*cos(theta);
c = Croot * (1 - (1-lambda)*cos(theta)); % MAC at each segment
mu = c * a_2d / (4 * b);
LHS = mu .* (alpha-alpha_0)/57.3; % Left Hand Side
% Solving N equations to find coefficients A(i):
for i=1:N
    for j=1:N
    B(i,j) =  sin((2*j-1) * theta(i)) * (1 + (mu(i) * (2*j-1)) /
sin(theta(i)));
    end
end
A=B\transpose(LHS);
for i = 1:N
    sum1(i) = 0;
    sum2(i) = 0;
    for j = 1 : N
        sum1(i) = sum1(i) + (2*j-1) * A(j)*sin((2*j-1)*theta(i));
        sum2(i) = sum2(i) + A(j)*sin((2*j-1)*theta(i));
    end
  end
CL_TO = pi * AR * A(1)
```

In take-off, the lift distribution is not a concern, since the flap increases the wing inboard lift coefficient. The m-file yields the following results:

$$C_{L_{TO}} = 1.254$$

Since the wing generated take-off lift coefficient is slightly higher than the required take-off lift coefficient, one or more of the wing or flap parameters must be changed. The easiest change is to reduce the wing angle of attack during take-off. Other options are to reduce the size of flap and to reduce the flap deflection. By a trial and error, it is determined that by reducing the wing angle of attack to 8.88 degrees, the wing will generate the required lift coefficient of 1.16.

$$C_{L_{TO}} = 1.16$$

Since the wing has a setting angle of 1.86 degrees, the fuselage will be pitched up 7 degrees during take-off, since 8.88 - 1.86 = 7.02. Thus:

$$i_w = 1.86 \text{ deg}, \ \alpha_{TO\_wing} = 8.88 \text{ deg}, \ \alpha_{TO\_fus} = 7.02 \text{ deg}, \ \delta_{f\_TO} = 20 \text{ deg}$$

At this moment, it is noted that the wing satisfies the design requirements both at cruise and at take-off.

## 7. Other Wing Parameters

To determine other wing parameters (i.e. wing span (b), root chord (Cr), tip chord (Ct), and Mean Aerodynamic Chord (MAC), we have to solve the following four equations simultaneously:

$$S = b \cdot \overline{C} \tag{5.17}$$

$$AR = \frac{b^2}{S} \tag{5.18}$$

$$\lambda = \frac{C_t}{C_r} \tag{5.24}$$

$$\overline{C} = \frac{2}{3}C_r\left(\frac{1+\lambda+\lambda^2}{1+\lambda}\right) \tag{5.26}$$

Solution of these equations simultaneously yields the following results:

$$b = 11.256 \ m; \quad MAC = 1.608 \ m; \quad C_r = 1.78 \ m; \quad C_t = 1.42 \ m$$

Consequently, other flap parameters are determined as follows:

$$\frac{b_f}{b} = 0.6 \Rightarrow b_f = 0.6 \times 11.256 = 6.75 \ m$$

$$\frac{C_f}{C} = 0.2 \Rightarrow C_f = 0.2 \times 1.608 = 0.32 \ m$$

Figure 5.65 illustrates the right half wing with the wing and flap parameters of example 5.6.

The next step in the wing design process is to optimize the wing parameters such that the wing drag and pitching moment are minimized. This step is not shown in this example to reduce the length of the chapter.
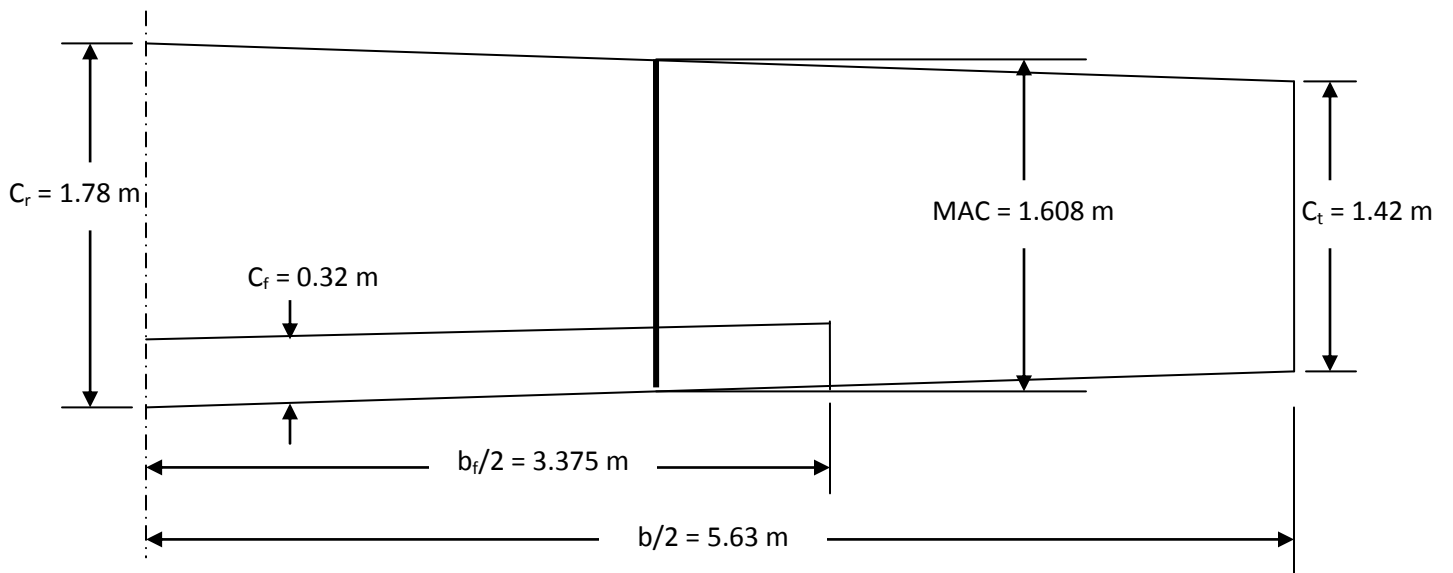
*a . Top view of the right half wing*
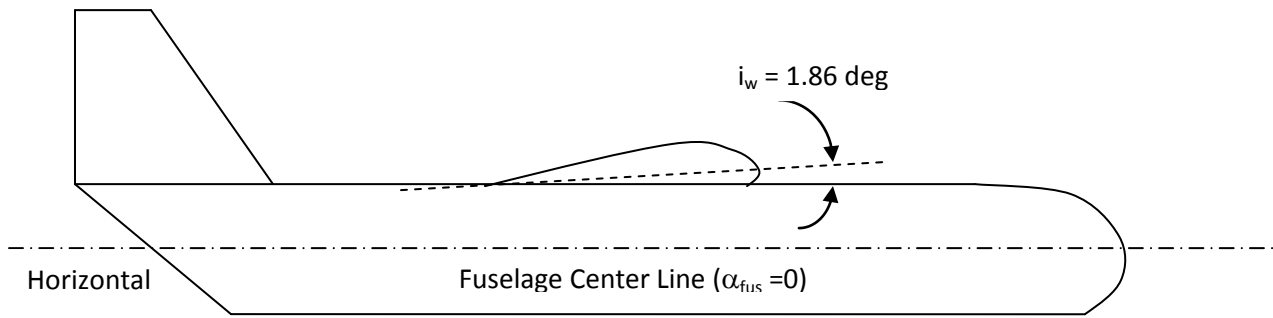


*b. Side view of the aircraft in cruising flight*
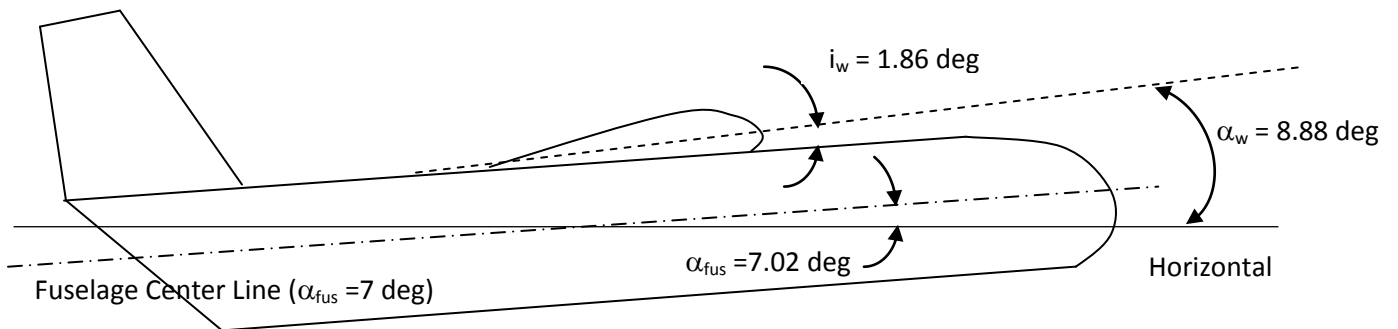


*c. Side view of the aircraft in take-off*

*Figure 5.65. Wing parameters of Example 5.6*

# Problems

**5.1.** Identify $C_{li}$, $C_{dmin}$, $C_m$, $(C_l/C_d)_{max}$, $\alpha_o$ (deg), $\alpha_s$ (deg), $C_{lmax}$, $a_o$ (1/rad), $(t/c)_{max}$ of the NACA 2412 airfoil section (flap-up). You need to indicate the locations of all parameters on the airfoil graphs as shown in figure 5.66.
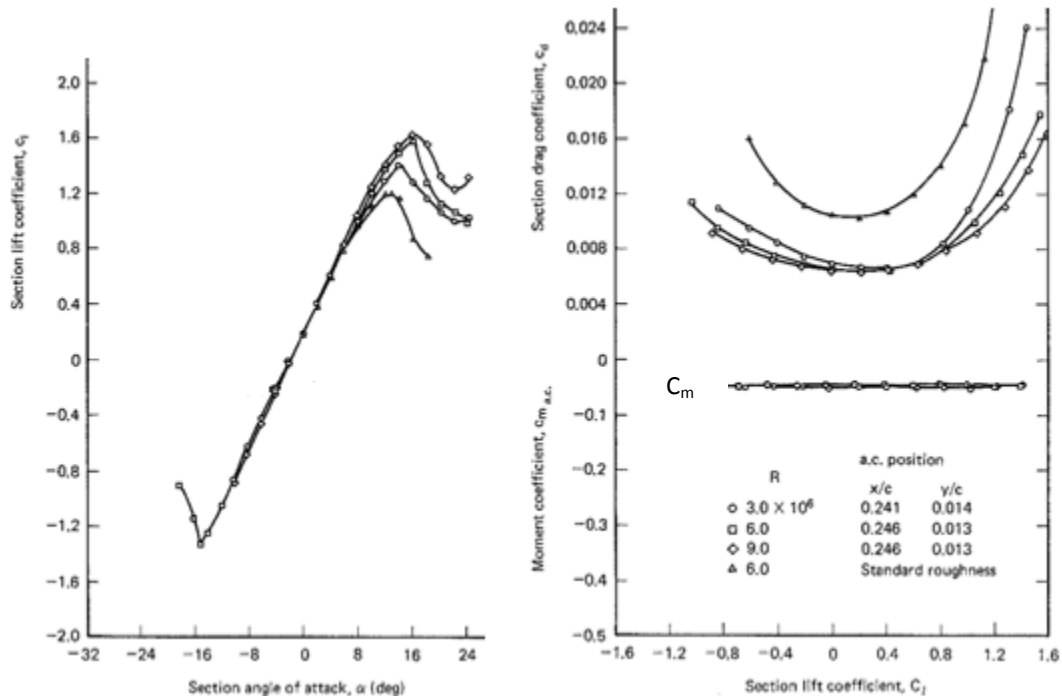


*Figure 5.66. Airfoil section NACA 2415*

**5.2.** Identify $C_{li}$, $C_{dmin}$, $C_m$, $(C_l/C_d)_{max}$, $\alpha_o$ (deg), $\alpha_s$ (deg), $C_{lmax}$, $a_o$ (1/rad), $(t/c)_{max}$ of the NACA $63_2$-615 airfoil section (flap-up). You need to indicate the locations of all parameters on the airfoil graphs as shown in figure 5.21.

**5.3.** A NACA airfoil has thickness-to-chord ratio of 18 percent. Estimate the lift curve slope for this airfoil in 1/rad.

**5.4.** Select a NACA airfoil section for the wing for a prop-driven normal category GA aircraft with the following characteristics:

$m_{TO}$ = 3,500 kg, S = 26 m$^2$, $V_c$ = 220 knot (at 4,000 m), $V_s$ = 68 knot (@ sea level)

The high lift device (plain flap) will provide $\Delta C_L$ = 0.4 when deflected.

**5.5.** Select a NACA airfoil section for the wing for a prop-driven transport aircraft with the following characteristics:

$m_{TO}$ = 23,000 kg, S = 56 m$^2$, $V_c$ = 370 knot (at 25,000 ft), $V_s$ = 85 knot (@ sea level)

---

The high lift device (single slotted flap) will provide $\Delta C_L = 0.9$ when deflected.

**5.6.** Select a NACA airfoil section for the wing for a business jet aircraft with the following characteristics:

$m_{TO} = 4,800$ kg, $S = 22.3$ m$^2$, $V_c = 380$ knot (at 33,000 ft), $V_s = 81$ knot (@sea level)

The high lift device (double slotted flap) will provide $\Delta C_L = 1.1$ when deflected.

**5.7.** Select a NACA airfoil section for the wing for a jet transport aircraft with the following characteristics:

$m_{TO} = 136,000$ kg, $S = 428$ m$^2$, $V_c = 295$ m/sec (at 42,000 ft), $V_s = 118$ knot (@sea level)

The high lift device (triple slotted flap) will provide $\Delta C_L = 1.3$ when deflected.

**5.8.** Select a NACA airfoil section for the wing for a fighter jet aircraft with the following characteristics:

$m_{TO} = 30,000$ kg, $S = 47$ m$^2$, $V_c = 1,200$ knot (at 40,000 ft), $V_s = 95$ knot (@sea level)

The high lift device (plain flap) will provide $\Delta C_L = 0.8$ when deflected.

**5.9.** A designer has selected a NACA 2412 (figure 5.65) for an aircraft wing during a design process. Determine the wing setting angle.

**5.10.** The airfoil section of a wing with aspect ratio of 9 is NACA 2412 (figure 5.65). Determine the wing lift curve slope in terms of 1/rad.

**5.11.** Determine the Oswald span efficiency for a wing with aspect ratio of 12 and sweep angle of 15 degrees.

**5.12.** Determine the Oswald span efficiency for a wing with aspect ratio of 4.6 and sweep angle of 40 degrees.

**5.13.** A straight rectangular wing has a span of 25 m and MAC of 2.5 m. If the wing swept back by 30 degrees, determine the effective span of the wing.

**5.14.** A trainer aircraft has a wing area of $S = 32$ m$^2$, aspect ratio AR = 9.3, and taper ratio of $\lambda = 0.48$. It is required that the 50 percent chord line sweep angle be zero. Determine tip chord, root chord, mean aerodynamic chord, and span, as well as leading edge sweep, trailing edge sweep and quarter chord sweep angles.

**5.15.** A cargo aircraft has a wing area of $S = 256$ m$^2$, aspect ratio AR = 12.4, and taper ratio of $\lambda = 0.63$. It is required that the 50 percent chord line sweep angle be zero. Determine tip chord, root chord, mean aerodynamic chord, and span, as well as leading edge sweep, trailing edge sweep and quarter chord sweep angles.

**5.16.** A jet fighter aircraft has a wing area of $S = 47$ m$^2$, aspect ratio AR = 7, and taper ratio of $\lambda = 0.8$. It is required that the 50 percent chord line sweep angle be 42 degrees. Determine tip chord, root chord, mean aerodynamic chord, span, and effective span, as well as leading edge sweep, trailing edge sweep and quarter chord sweep angles.

**5.17.** A business jet aircraft has a wing area of $S = 120$ m$^2$, aspect ratio AR = 11.5, and taper ratio of $\lambda = 0.55$. It is required that the 50 percent chord line sweep angle be 37 degrees. Determine the tip chord, root chord, mean aerodynamic chord, span, and

effective span, as well as leading edge sweep, trailing edge sweep and quarter chord sweep angles.

**5.18.**     Sketch the wing for problem 5.16.

**5.19.**     Sketch the wing for problem 5.17.

**5.20.**     A fighter aircraft has a straight wing with a planform area of 50 m$^2$, aspect ratio of 4.2 and taper ratio of 0.6. Determine wing span, root chord, tip chord, and Mean Aerodynamic Chord. Then sketch the wing.

**5.21.**     A hang glider has a swept wing with a planform area of 12 m$^2$, aspect ratio of 7 and taper ratio of 0.3. Determine wing span, root chord, tip chord, and Mean Aerodynamic Chord. Then sketch the wing, if the sweep angle is 35 degrees.

**5.22.**     The planform area for a cargo aircraft is 182 m2. The wing has an anhedral of -8 degrees; determine the effective wing planform area of the aircraft.

**5.23.**     A jet transport aircraft has the following characteristics:

$m_{TO} = 140,000$ kg, S = 410 m$^2$, $V_s = 118$ knot (@sea level), AR = 12, $\lambda = 0.7$, $i_w = 3.4$ deg, $\alpha_t = -2$ deg, airfoil section: NACA 63$_2$-615 (figure 5.21), $b_{A\_in}/b = 0.7$

Design the high lift device (determine type, $b_f$, $C_f$, $\delta_f$) for this aircraft to be able to take-off with a speed of 102 knot while the fuselage is pitched up 10 degrees.

**5.24.**     A twin engine GA aircraft has the following characteristics:

$m_{TO} = 4,500$ kg, S = 24 m$^2$, AR = 8.3, $\lambda = 0.5$, $i_w = 2.8$ deg, $\alpha_t = -1$ deg, $b_{A\_in}/b = 0.6$ airfoil section: NACA 63$_2$-615 (figure 5.21)

Design the high lift device (determine type, $b_f$, $C_f$, $\delta_f$) for this aircraft to be able to take-off with a speed of 85 knot while the fuselage is pitched up 10 degrees.

**5.25.**     Determine and plot the lift distribution for a business aircraft with a wing with the following characteristics. Divide the half wing into 12 sections.

S = 28 m$^2$, AR = 9.2, $\lambda = 0.4$, $i_w = 3.5$ deg, $\alpha_t = -2$ deg, airfoil section: NACA 63-209

If the aircraft is flying at the altitude of 10,000 ft with a speed of 180 knot, how much lift is produced?

**5.26.**     Determine and plot the lift distribution for a cargo aircraft with a wing with the following characteristics. Divide the half wing into 12 sections.

S = 104 m$^2$, AR = 11.6, $\lambda = 0.72$, $i_w = 4.7$ deg, $\alpha_t = -1.4$ deg, NACA 4412, $a_{TO\text{-}wing} = 10$ deg

If the aircraft is flying at the altitude of 25,000 ft with a speed of 250 knot, how much lift is produced?

**5.27.**     Consider the aircraft in problem 5.25. Determine the lift coefficient at take-off when the following high lift device is employed.

Single slotted flap, $b_f/b = 0.65$, $C_f/C = 0.22$, $\delta_f = 15$ deg, $a_{TO\text{-}wing} = 9$ deg

**5.28.**     Consider the aircraft in problem 5.26. Determine the lift coefficient at take-off when the following high lift device is employed.

---

triple slotted flap, $b_f/b = 0.72$, $C_f/C = 0.24$, $\delta_f = 25$ degrees, $a_{TO\text{-}wing} = 12$ deg

**5.29.**     Consider the aircraft in problem 5.28. How much flap need to be deflected in landing, if the fuselage is allowed to pitch up only 7 degrees with a speed of 95 knot.

**5.30.**     Design a wing for an utility category General Aviation aircraft with the following features:

$S = 22$ m$^2$, m = 2,100 kg, $V_C = 152$ knot (@ 20,000 ft), $V_S = 67$ knot (@ sea level)

The aircraft has a monoplane low wing and employs the plain flap. Determine airfoil section, aspect ratio, taper ratio, tip chord, root, chord, MAC, span, twist angle, sweep angle, dihedral angle, incidence, high lifting device type, flap span, flap chord, flap deflection and wing angle of attack at take-off. Plot lift distribution at cruise and sketch the wing including dimensions.

**5.31.**     Design a wing for a jet cargo aircraft with the following features:

$S = 415$ m$^2$, m = 150,000 kg, $V_C = 520$ knot (@ 30,000 ft), $V_S = 125$ knot (@ sea level)

The aircraft has a monoplane high wing and employs a triple slotted flap. Determine airfoil section, aspect ratio, taper ratio, tip chord, root, chord, MAC, span, twist angle, sweep angle, dihedral angle, incidence, high lifting device type, flap span, flap chord, flap deflection and wing angle of attack at take-off. Plot lift distribution at cruise and sketch the wing including dimensions.

**5.32.**     Design a wing for a supersonic fighter aircraft with the following features:

$S = 62$ m$^2$, m = 33,000 kg, $V_C = 1,350$ knot (@ 45,000 ft), $V_S = 105$ knot (@ sea level)

The controllability and high performance are two high priorities in this aircraft. Determine wing vertical position, airfoil section, aspect ratio, taper ratio, tip chord, root, chord, MAC, span, twist angle, sweep angle, dihedral angle, incidence, high lifting device type, HLD span, HLD chord, HLD deflection and wing angle of attack at take-off. Plot lift distribution at cruise and sketch the wing including dimensions.

**5.33.**     Determine and plot the lift distribution for the aircraft Cessna 304A at cruising flight. The characteristics of this aircraft are given in table 5.17. Then determine the lift coefficient at cruise.

**5.34.**     Determine and plot the lift distribution for the aircraft Scottish Aviation SA-3-120 at cruising flight. The characteristics of this aircraft are given in table 5.17. Then determine the lift coefficient at cruise.

**5.35.**     Determine and plot the lift distribution for the aircraft Aerocare IMP at cruising flight. The characteristics of this aircraft are given in table 5.17. Then determine the lift coefficient at cruise.

# References

1. Eppler, Richard, **Airfoil Design and Data**, Springer-Verlag, Berlin, 1990
2. Abbott I. H. and Von Donehoff A. F., **Theory of Wing Sections**, Dover, 1959
3. Anderson J. D., **Fundamentals of Aerodynamics**, McGraw-Hill, Fifth edition, 2010
4. Jackson P., **Jane's All the World's Aircraft**, Jane's information group, Various years
5. Blanchard B. S. and Fabrycky W. J., **Systems Engineering and Analysis**, Prentice Hall, Third edition, 2006
6. Shevell R. S., **Fundamentals of Flight**, Prentice Hall, Second edition, 1989
7. Sadraey M., **Aircraft Performance Analysis**, VDM Verlag Dr. Müller, 2009
8. Anderson J. D., **Aircraft Performance and Design**, McGraw-Hill, 1999
9. Hibbeler R. C., **Engineering Mechanics, Dynamics**, 9th Edition, Prentice Hall, 2001
10. Stevens B. L. and Lewis F. L., **Aircraft Control and Simulation**, Second Edition, Wiley, 2003
11. Anderson John D., **Modern Compressible Flow**, Third Edition, McGraw-Hill, 2003
12. Lan E. C. T., Roskam J., **Airplane Aerodynamics and Performance**, DAR Corp, 2003
13. Roskam J., **Airplane Flight Dynamics and Automatic Flight Control,** Part I, 2007, DAR Corp
14. Cavallok, B., "**Subsonic Drag Estimation Methods**," US Naval Air Development Center, NADC-AW-6604, 1966
15. Etkin B., Reid L. D., **Dynamics of Flight, Stability and Control**, Third Edition, Wiley, 1996
16. Houghton E. L. and Carpenter P. W., **Aerodynamics for Engineering Students**, Fifth edition, Elsevier, 2003